To the Graduate Council:

I am submitting herewith a thesis written by Arthur Shek-Kin Kwong entitled "A Variable-Speed Constant-Frequency System Using Cycloconverter Principles". I recommend that it be accepted in partial fulfillment of the requirements for the degree of Master of Science, with major in Electrical Engineering.

J. M. Bailey, Major Professor

We have read this thesis
and recommend its acceptance:

Accepted for the Council:

Vice Chancellor
Graduate Studies and Research

A VARIABLE-SPEED CONSTANT-FREQUENCY SYSTEM USING CYCLOCONVERTER PRINCIPLES

A Thesis

Presented for the

Master of Science

Degree

The University of Tennessee, Knoxville

Arthur Shek-Kin Kwong

June 1981

3051724

ACKNOWLEDGMENTS

The author wishes to express his sincere appreciation to his advisor, Dr. J. M. Bailey, who suggested the topic and provided the necessary guidance and encouragement during the preparation of this thesis. Considerable literature exists on this topics [1]. The options available in cycloconverter design and control theory in the "Variable-speed Constant-frequency (VSCF) System" are numerous combinations of this appears to be viable both from the technical and economic view point for modern wind power development. All these aspects require further study and development.

The author would like to express gratitude to Dr. J. W. Waller, Dr. J. F. Pierce, and Dr. T. V. Blalock for their professional assistance on electronic design of this project.

Appreciation is extended to Dr. T. W. Reddock and Dr. J. W. Waller for serving on the author's committee. Thanks are also due Ms. Daisy Ma who did an excellent work in typing the last two chapters of my thesis.

Dedicated to my grandmother for her encouragement.

ABSTRACT

This thesis develops a general theory that explains and describes the principles of operation and control of the solid-state thyristor cycloconverter as a forced commutated frequency changer. It is one of the elements of a variable-speed constant-frequency (VSCF) power-generating system for ac to ac frequency conversion.

The power source in this system is an induction generator with capacitive excitation. Performance characteristics of this machine in a VSCF power-generating system are also developed.

The frequency changer in the VSCF system utilizes bidirectional switches (TRIACs) to control the output frequency and input displacement factor.

PREFACE

To obtain constant frequency power from a generator running at variable speeds, a solid-state switching frequency changer can be utilized that converts polyphase ac power of a given frequency to single or polyphase power of a chosen frequency.

With the introduction of three or multi-layer solid-state devices such as thyristors or silicon controlled rectifiers (SCR), power switching electronic technolgy has developed at a phenomenal rate. Such devices are particularly applicable to these types of frequency changers which must perform such tasks as high power rectification, switching regulation etc. Features of the SCR include small size, rugged construction, low voltage drop and the ability to control the conduction period by means of simple solid-state logic. These factors make the solid-state frequency changer a viable candidate for use in modern static frequency conversion systems, e.g. for electric aircraft power generation and modern wind power conversion.

The intent of this thesis is to develop the theory necessary to analyze the operation of a capacitor-excited induction generator and a controllable displacement factor frequency changer (CDFFC) in a VSCF power-generating system.

A brief overall review of the basic concept is given in Chapter 1. The generic system discussed is a capacitor-excited induction generator and a CDFFC in a static frequency conversion role.

Chapter 2 deals the development of a general mathematical theory, with the analysis of output waveform and input current waveform, based on the basic positive-type waveform and negative-type waveform. Different construction of positive-type and negative-type waveform lead to the synthesis of composite waveform.

Chapter 3 describes the typical operating principles of a CDFFC. The mathematical analysis on the output voltage and input current of a CDFFC are given. Some important design data and the performance characteristics for a CDFFC are established.

In some VSCF system, particularly for high-speed application, an induction machine is suited by reason of operating conditions and reliability requirements. Specifically, the squirrel-cage type induction machine with its rugged construction is well suited to high-speed application. The induction machine can be operated as an independent generator without the necessity for an external supply, at a predetermined voltage and frequency, if excitation is provided by means of capacitors. The machine performance is introduced in Chapter 4.

Chapter 5 covers the application of a CDDFC in a VSCF power-generating system with an induction generator as the power source. The CDFFC provides a reactive power instead of an external capacitor for machine excitation, and the practical control circuit for a CDFFC is introduced. In such a system, the input phase angle and output voltage of the frequency changer are controlled independently.

TABLE OF CONTENTS

CHAPTER		PAGE
1.	INTRODUCTION	1
	1-1 Thyristor Cycloconverter	2
	1-2 An Induction Generator	35
	1-3 A VSCF System	41
2.	THEORETICAL ANALYSIS OF A STATIC FREQUENCY CHANGER	48
	2-1 General Concept of the Output Voltage Wave and Input Current Wave	49
	2-2 Waveform Fabrication of CDFFC	62
3.	CONTROLLABLE DISPLACEMENT FACTOR FREQUENCY CHANGER	89
	3-1 Voltage Characteristics of a CDFFC	90
	3-2 Input Current Characteristics of a CDFFC	100
	3-3 Input and Output Power Characteristics of CDFFC	121
	3-4 Summary	124
4.	PRINCIPLE OF CAPACITOR-EXCITED INDUCTION GENERATOR	131
	4-1 Performance from Magnetization Curve	132
	4-2 Slip and Load Relationship	141
	4-3 Voltage Regulation	145
	4-4 External Load Characteristics	147
	4-5 Conclusion	159
5.	APPLICATION IN A VSCF SYSTEM	162
	5-1 Construction of a VSCF System	162
	5-2 Control System of a CDFFC	166
	5-3 Conclusion	180
LIST OF REFERENCES		188
APPENDIX		191
VITA		210

LIST OF TABLES

TABLE PAGE

1.1. Input and Output Characteristics of a General Frequency Changer 6

1.2. Operating Range of a CDFFC 46

3.1. Conditions Determine Input Displacement Angle : Leading or Lagging 127

3.2. Summary of the Characteristics of a Six-pulse CDFFC 130

4.1. Test Parameters of the Induction Machine 134

A.1. Dominant Terms of the Amplitude $A_{6k,2n}$ in Equation (2-36) with Frequencies of $6kf_I \pm 2nf_O$ ($k = 1,2$; $n = 0,1,...$) 192

A.2. Dominant Terms of the Amplitude $B_{[3(2k-1)],(2n+1)}$ in Equation (2-36) with Frequencies $3(2k-1)f_I \pm (2n+1)f_O$ ($k = 1,2$; $n = 0,1,2,.....6$) 193

A.3. Numerical Values of a and b in the Cofficient Terms of the Harmonic Series from Equation (2-45) through (2-50) 194

A.4. Numerical Values of the Amplitude of the Dominant Components in Equation (3-1) 197

A.5. Numerical Values of the Amplitude of Unwanted Components in the Output Voltage of the CDFFC with Sinusoidal Mean Voltage 198

A.6. Numerical Values of the Amplitude of Extrabasal Components in the Input Current of the CDFFC with Sinusoidal Mean Voltage 202

B.1. Induction Generator 208

LIST OF FIGURES

FIGURE		PAGE
1-1.	An Ideal Cycloconverter	5
1-2.	Single-phase to Single-phase Two-pulse Cycloconverter	7
1-3.	Three-phase to Single-phase Three-pulse Cycloconverter	12
1-4.	Three-phase to Three-phase Three-pulse Cycloconverter	13
1-5.	Six-phase to Three-phase Cycloconverter	16
1-6.	Six-pulse Cycloconverter, and associated waveforms	19
1-7.	Cycloconverter with Intergroup Reactor to Reduce Circulating Current	20
1-8.	Positive-type and Negative-type Waveform Construction	22
1-9.	Effect of output to Input Frequency Ratio and the Pulse Number of a Cycloconverer on the Output Waveform Distortion	24
1-10.	Commutation Overlap	26
1-11.	Commutation Overlap, Three-pulse Midpoint Converter with Finite Commutating Reactance	28
1-12.	Phase Diagram of a Cycloconverter	29
1-13.	A Practical Bridge-type Cycloconverter with Single-phase Output	32
1-14.	Circle Diagram of in Induction Machine	37
1-15.	Single-phase Equivalent Circuit of the Capacitor-excited Induction Generator	40
1-16.	A VSCF Power-generating System	43
1-17.	Input to Output Equivalent Circuit	45

FIGURE PAGE

2-1. Diagrammatic Representation of a Simple q to p Phase Frequency Changer 50

2-2. Typical Three-phase Cycloconverter 53

2-3. A Consecutive Composite Waveform 63

2-4. Two Complementary Waveform Generated by the Triangular Modulating Function 66

2-5. Two Periodic Existence Functions Control the Output Waveform Fabrication 69

2-6. A Consecutive Composite Waveform with Different Modulating Angles 76

2-7. Cosine Wave Crossing Control Method Applied to a Cycloconverter 78

2-8. Curves Showing the Approximate Variation of the Coefficients with the Output Voltage Ratio r . . 82

3-1. Typical Consecutive Composite Output Waveforms of a CDFFC, with Different Modulating Angle at $f_I = 3f_o$ 95

3-2. Distribution of the Unwanted Components in the Output Voltage Waveform of a CDFFC 97

3-3. Distribution of the Predominant Unwanted Components in the Output of the Three-pulse CDFFC, with Amplitudes at Maximum Output Voltage and Unity Load Displacement Factor . . . 99

3-4. Amplitude of the Unwanted Component in the Output Voltage of the Three-, Six-, and Twelve-pulse Cycloconverter, with Maximum Output Voltage Ratio (r=1) 101

3-5. Distribution of the Extrabasal Components in the Input Current Waveform of a CDFFC 109

3-6. Per Unit Quadrature Component of Input Current of the CDFFC as a Function of the Output Displacement Angle ϕ_o and Output Voltage Ratio r 111

FIGURE PAGE

3-7. Relationship Between Per Unit Quadrature Component of Input Current, Output Displacement Angle and Output Voltage Ratio, for CDFFC with $\sigma = \phi_o$ and $\sigma = \pi + \phi_o$. 112

3-8. Relationship Between the Load Phase Angle, Control Angle and Input Phase Angle, with Maximum Output Voltage Ratio 114

3-9. Relationship Between the Control Angle for Different Output Voltage Ratios and Two Load Phase Angles 115

3-10. Relationship Between Load Phase Angle and Control Range of Input Phase Angle for CDFFC 116

3-11. Phase Relationship Between the Output or Input Voltage and Current of the CDFFC 125

3-12. Construction Method of the Output Voltage Waveform Affects the Input Displacement Angle . . 128

4-1. Build-up Characteristics of the Capacitor-excited Induction Generator 135

4-2. Improved the Build-up Characteristic of the Capacitor-excited Induction Generator with External Reactor 139

4-3. Capacitor-excited Induction Generator with External Reactor and Resistive Load 142

4-4. Per Phase Equivalent Circuit of the Capacitor-excited Induction Generator with Modified Internal Machine Parameters 146

4-5. Reactor Operating in Parallel with Wye and Delta in Three-phase System 148

4-6. External Performance of the Induction Generator with a Unity Power Factor Load 151

4-7. External Performance of the Induction Generator by Inserting Series Capacitor with Load 153

4-8. Terminal Voltage and Load Voltage Versus Output Power of the Induction Generator 155

4-9. Slip Versus Output Power of the Induction Generator 156

FIGURE PAGE

4-10. Power Factor Versus Output Power of the Induction Generator 157

4-11. Efficiency Versus Output Power of the Induction Generator 158

5-1. Block Diagram of the VSCF Power-generating System 163

5-2. Control System of a CDFFC 167

5-3. Phase Control Circuit of a CDFFC 169

5-4. Firing Pulse Generator Using Integral Control Principle 171

5-5. An Integral Control for a CDFFC 173

5-6. The Associated Waveforms of a Six-pulse CDFFC, with Integral Control Method 175

5-7. Extended Output Firing Pulses for a Three-pulse Circuit 178

5-8. Six-pulse Frequency Changer 179

5-9. Associated Output Waveforms of a Six-pulse CDFFC in the VSCF Power-generating System 181

5-10. Complete Schematic Diagram for VSCF Power-generating System Utilizes Induction Generator and a Six-pulse CDFFC 187

CHAPTER 1

INTRODUCTION

In recent years, thyristors or silicon control rectifiers (SCR) have assumed a dominant position among high-power switching devices. They can be employed for static frequency conversion of ac power from a variable input frequency to a constant or controllable output frequency feeding to the system load. This type of application is classified as a variable-speed constant-frequency (VSCF) power-generating system.

The term "Thyristors" means a bistable semi-conductor device comprising three or more junctions that can be switched from the "Off" state to the "On" state or vice versa, such switching occurring within at least one quadrant of the principal voltage-current output characteristics. The theory of ac to ac frequency conversion in this thesis requires the solid-state switching devices operation based on a four-quadrant (360 degrees) operating range. This type of circuit, which employs thyristors to control output frequency and typically is used in a VSCF power conversion system such as an electric aircraft power generator. It is particularly suitable for more modern applications such as wind power conversion and is termed a "Thyristor Cycloconverter". This chapter introduces the

characteristics of the thyristor cycloconverter. It gives an overview of ideal, single-phase and poly-phase standard circuit, and explains how they are operated and how the output waveforms are constructed. Some voltage control and harmonic reduction techniques are introduced. Operation of an induction machine in the generator mode, with negative slip, will be discussed. The analysis of the "Biuld-up" voltage characteristics of a self-excited induction generator is introduced. Some machine equations are given. Finally both a thyristor cycloconverter and an induction generator applied in a variable-speed constant-frequency (VSCF) system are introduced. The system block diagram is presented, the input and output equivalent circuits are illustrated, and some important system equations are derived.

1-1 THE THYRISTOR CYCLOCONVERTER

A cycloconverter is used to convert ac power of one frequency to ac of a variable lower frequency. This ac to ac conversion without an intermediate dc link converter has been used in place of a static frequency changer. The basic technique involved in static power frequency conversion were established in the 1930s. The frequency converters developed were in the classical cycloconverter configuration ultilized with a grid-controlled mercury arc rectifier to convert standard three-phase to single-phase ac power from

50Hz to 15Hz, 16-2/3Hz or 25Hz for the operation of ac commutator locomotive drive motors on the railway in Europe. However with the discovery and fast industrial development of the thyristor, the cycloconverter has reemerged as a viable frequency changer.

The cycloconverter can operate in one of two modes, "Envelope Converter" or "Phase-Controlled Converter". The phase-control converter is the most common method in use and will be used here to illustrate the fundamental properties of cycloconverters. The following are the major advantages of using the static cycloconverter :

(1) Improvement of overall efficiency and power factor voltage by the elimination of the dc link.

(2) Simple and small control circuitry for control voltage within the converter.

(3) Natural line commutation without forced commutation control circuitry.

(4) Low maintenance cost with complete solid-state control circuitry.

(5) Small size and light weight.

1-1-1 An Ideal Cycloconverter

The ideal cycloconverter is assumed to be without voltage drop; thus real power at the input terminal must be equal to the real power at the output terminal, insuring power flow in either direction. The ideal functional

cycloconverter is shown in Figure 1-1. It is assumed to have a pure sinusoidal voltage and current at the terminals and has the ability to independently transform this frequency, amplitude and phase angle to some different frequency, amplitude, and phase angle. The input and output variables of an ideal cyloconverter are summarized in Table 1.1. Such an ideal power converter could be considered as a general transformer with the capability of both independently transforming the frequency and amplitude of a given input voltage and of transforming the phase angle of the load to some different input phase angle.

1-1-2 Single-phase Cycloconverter

The principle of operation of a single-phase cycloconverter is illustrated in Figure 1-2. It is a two-phase midpoint phase-controlled cycloconverter. The load voltage is supplied from all the voltages of the supply through two groups of controlled rectifier elements, positive (P) and negative (N). When one group is conducting, the other is blocked. The positive group delivers positive half-cycle of the load current, negative group the negative half-cycle.

The operation of the phase-controlled cycloconverter can be explained by reference to the waveform given in Figure 1-2(B). When an input ac voltage is applied to a circuit [Figure 1-2(A)], it forms an unfiltered and

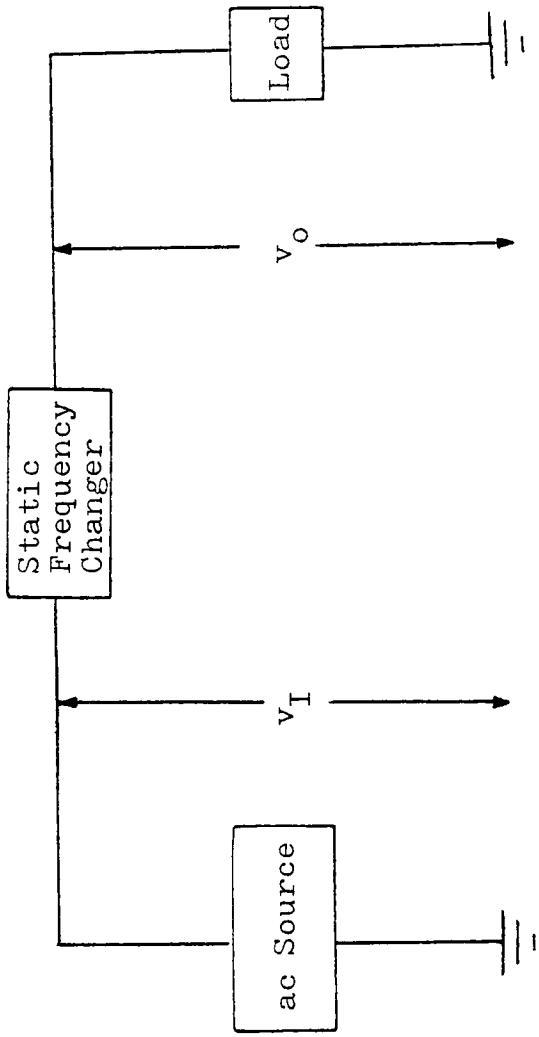
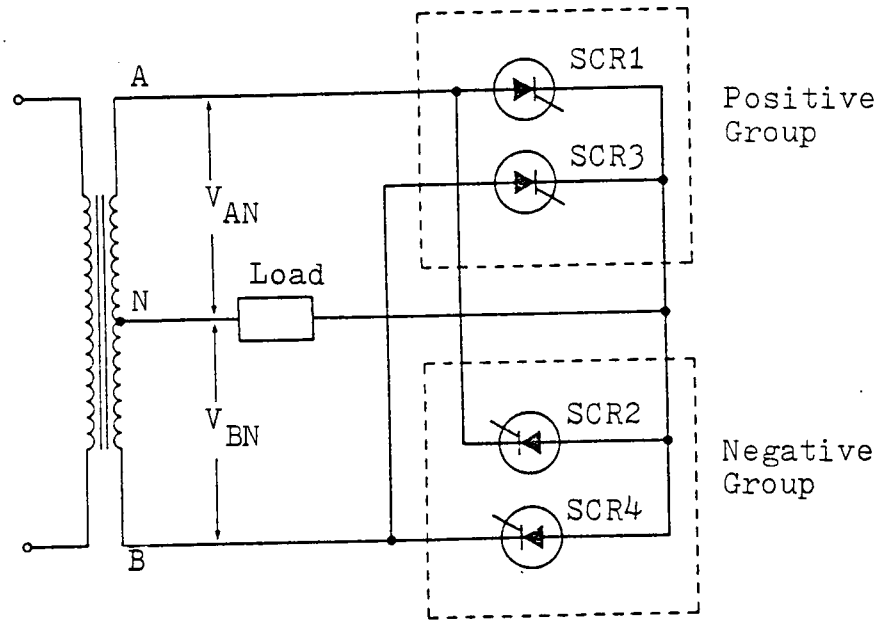


Figure 1-1. An ideal cycloconverter.

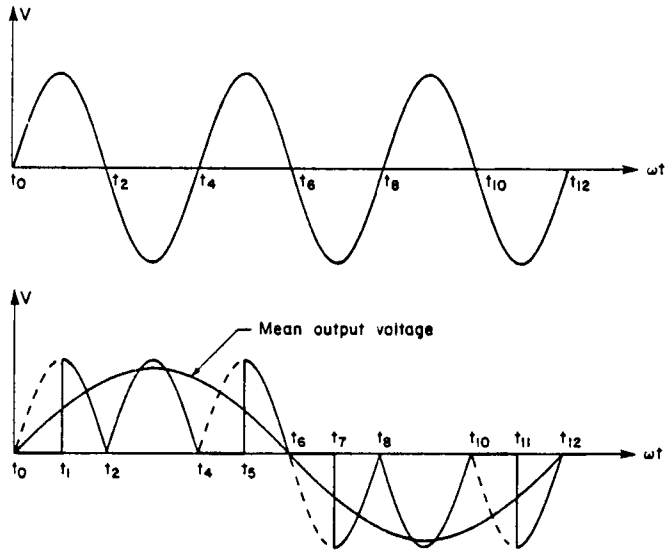
Table 1.1. Input and output characteristics of a general frequency changer.

VARIABLES	INPUT	OUTPUT
Excitation	$v_I = V_I \sin \omega_I t$	$v_o = V_o \sin \omega_o t$
Response	$i_I = I_I \sin(\omega_I t + \phi_I)$	$i_o = I_o \sin(\omega_o t + \phi_o)$
Given	V_I, ω_I	Z_o, ϕ_o
Control	Z_I, ϕ_I	V_o, ω_o
Restrictions	$P_I = P_o = V_I I_I \cos \phi_o$	$P_o = P_I = V_o I_o \cos \phi_o$

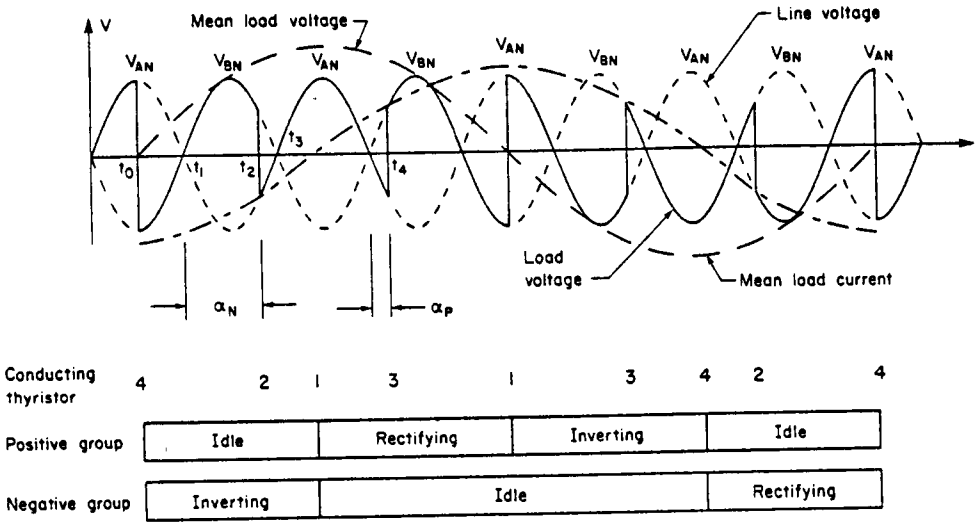


A. Basic Circuit

Figure 1-2. Single-phase to single-phase two-pulse cycloconverter.



B. Input Waveform and Resistive Load Waveform



C. Inductive Load Waveform

Figure 1-2. (Continued)

pulsating dc waveform at the output load which consists of a "Pure Resistance". During the first cycle of input voltage, SCR1 conducts when the top (point A) of the transformer secondary is positive; SCR3 conducts when the bottom (point B) of the transformer secondary is positive. The anode current of both SCR1 and SCR3 flow in the same direction through the load between $t_0 - t_6$, producing unidirectional pulses of load current and voltage. SCR1 and SCR3 continue to conduct for a number of input voltage cycles which depends upon the frequency desired at the output. When a time interval equal to the duration of one half-cycle at the desired output frequency has elapsed, triggering of SCR1 and SCR3 stops at t_6, and SCR2 and SCR4 are alternately triggered starting at t_7. Unidirectional current pulses now flow through the resistive load. SCR2 and SCR4 continue to conduct alternately for a time interval equal to the duration of one half-cycle at the desired output frequency. The successive conduction periods of the paired SCR's are varied by timing the trigger pulse in such a way that the average current rises from half-cycle to half-cycle. The result is that the average current in the load varies like a sine wave. When the output is filtered, a sine wave much lower in frequency than the input signal is obtained.

Figure 1-2(C), illustrates the waveform for an "Inductive Load". During the intervals at $t_0 - t_1$, $t_2 - t_3$ and $t_4 - t_5$ the load voltage and current are conducting in

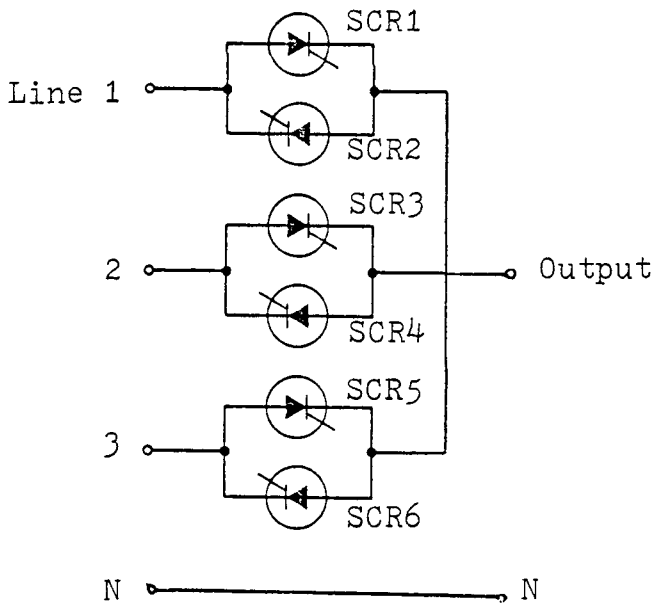
the positive half-cycle, there is a flow of power from the supply to the load. But when voltage and current are in an opposite sense there is regeneration from the load to the supply because of the stored energy in the inductive load.

The conduction period is varied and therefore the power supplied to the load, by varying the trigger angle in the same proportion of each half-cycle. In Figure 1-2(C) α_P and α_N represent the minimum and maximum delay angles for the positive groups and the negative groups of the cycloconverter, respectively. For a firing delay angle $\alpha_P = 0^\circ$, it has a maximum output voltage during the positive half-cycle; and similarly for a firing angle $\alpha_N = 0^\circ$, for the negative half-cycle. Therefore the amplitude and frequency of the mean dc voltage may be controlled by the firing delay angles α_P and α_N. In order to increase the mean output voltage of the positive/negative converter, α_P/α_N is reduced, and α_N/α_P is increased. It is clear, each converter operates both in its rectifying and inverting region, during the course of a given half-cycle of load current. If the control is such that the firing pulses are applied simultaneously to both converters, the firing delay angles are related by $\alpha_P + \alpha_N = 180^\circ$.

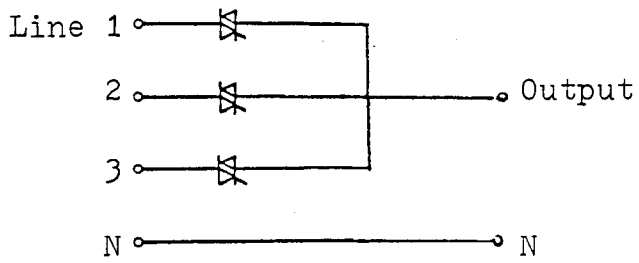
1-1-3 Three-phase Cycloconverter

The single-phase circuit described in Figure 1-1 can be modified for three-phase application. There are many circuit configurations which can be used for single-phase output or polyphase output. The simplest configuration is that of a three-pulse midpoint circuit with a sigle-phase output as illustrated in Figure 1-3. Figure 1-3(A) illustrates the dual converter configuration. Six SCRs are utilized; three forming the positive group and the other three forming the negative group. The configuration is inverse-parallel in a three-phase three-pulse thyristor circuit. The configuration of Figure 1-3(B) utilizes three TRAICs (bidirectional switches) instead of six SCRs to form the dual converter.

The cycloconverter consisting of three group of switches can be triggered by three-pulses at different instants. The firing circuit requirements are that the SCRs/TRIACs must be fired in pairs/alone. Therefore the gate signals must be spaced 120 degrees apart and be of sufficient duration to achieve a latching current. A single-phase output cycloconverter is rarely used in practice. Therefore the corresponding cycloconverter is modified [Figure 1-4] for three-phase three-pulse output. Each phase contains two separated groups (positive and negative) of circuits for an unidirectional converter

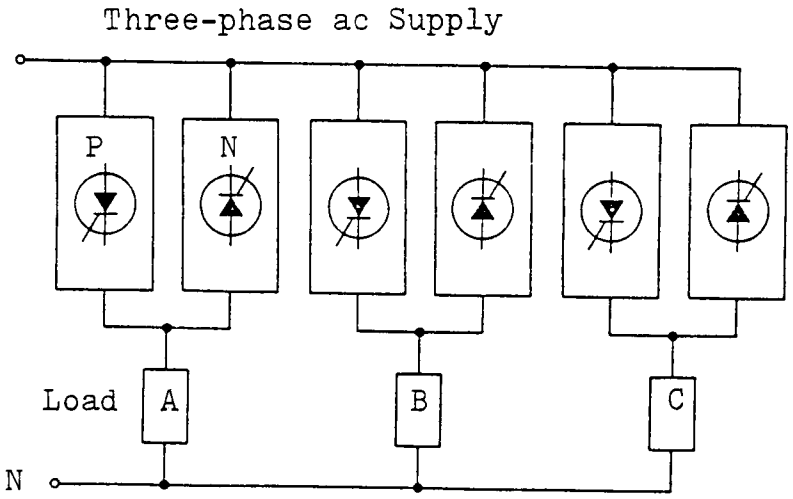


A. SCR Connection

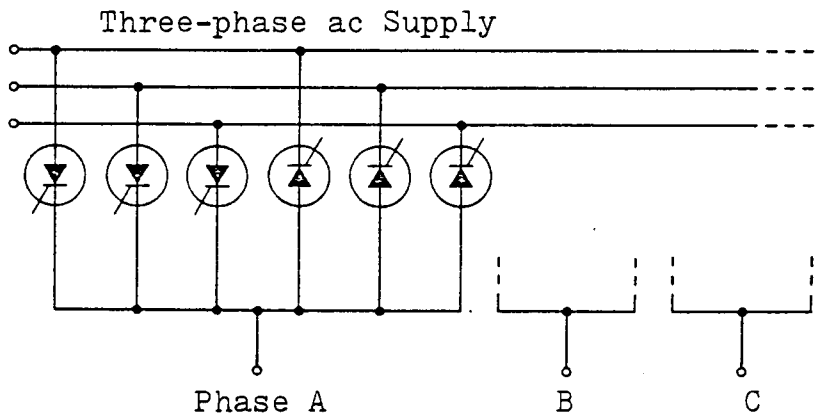


B. TRIAC Connection

Figure 1-3. Three-phase to single-phase three-pulse cycloconverter.

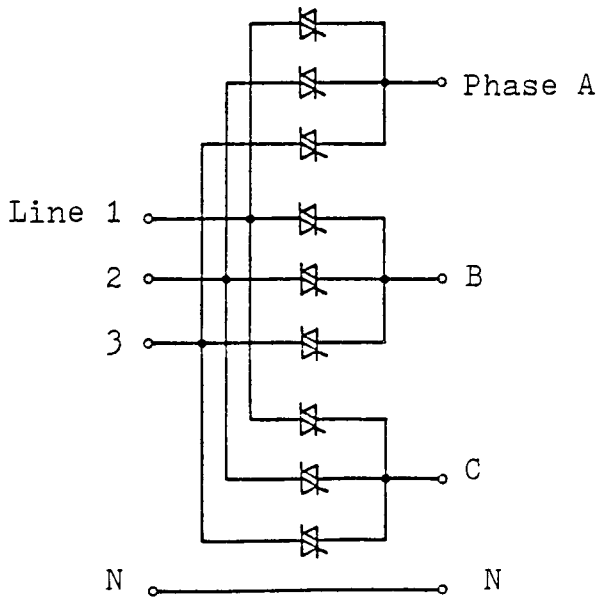


A. Schematic Diagram



B. SCR Connection

Figure 1-4. Three-phase to three-phase three-pulse cycloconverter.



C. TRIAC Connection

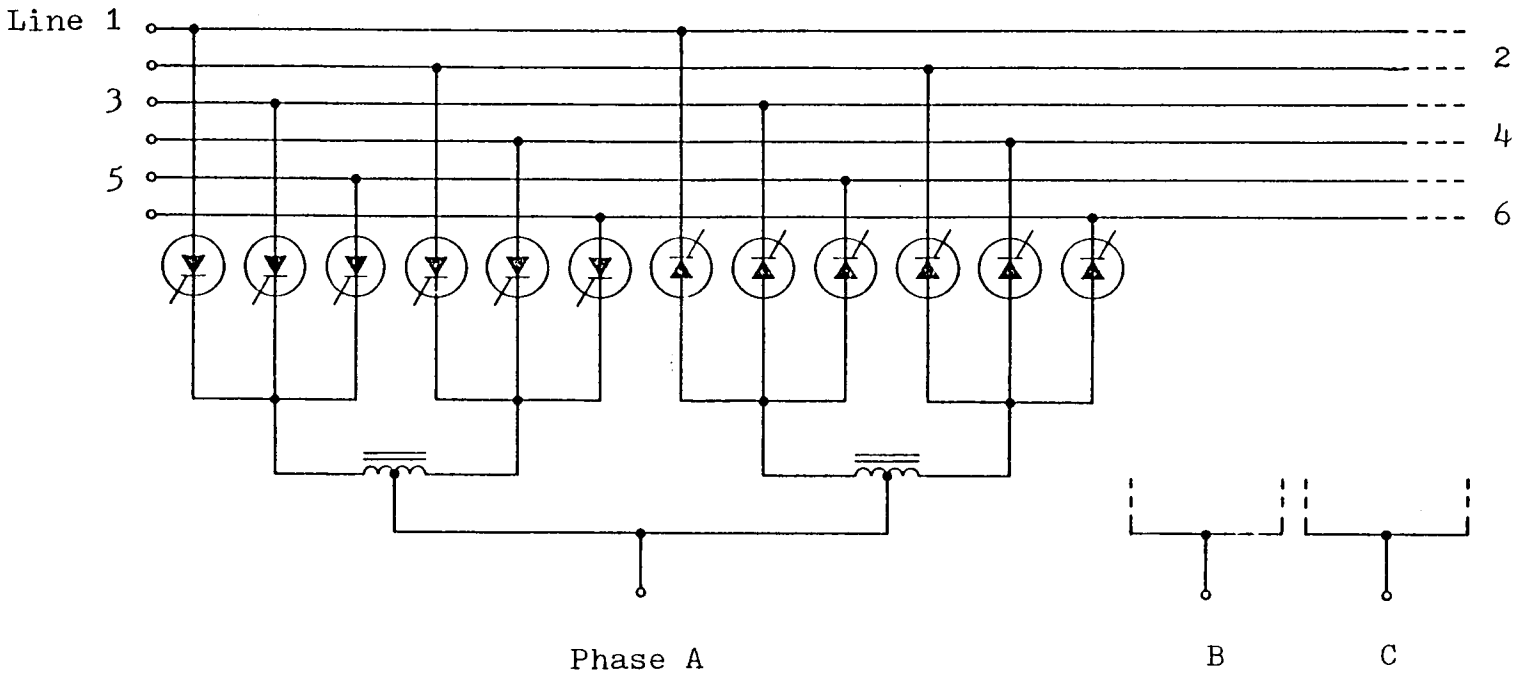
Figure 1-4. (Continued)

[Figure 1-4(A) and (B)] or one group for a bidirectional converter [Figure 1-4(C)].

The pulse numbers (corresponding to the cycloconverter circuit) directly affects the level of distortion [Refer to Figure 1-9(A)]. Increasing the pulse number of a frequency changer reduces the harmonic content (low frequency ripple) of the output voltage wave. Other factors affecting the load harmonics, are directly dependent on the pulse number of the converter. These factors include the ratio of input to output frequency, the level of the output voltage, the load power factor and the techniques used to control the load voltage. An increase in the pulse number can be obtained in a number of ways. One technique ulitizes twelve six-pulse midpoint converters with an interphase transformer as shown in Figure 1-5(A), to form six dual converters with a three-phase output. In Figure 1-5(B), six TRIACs are used to form six dual converters.

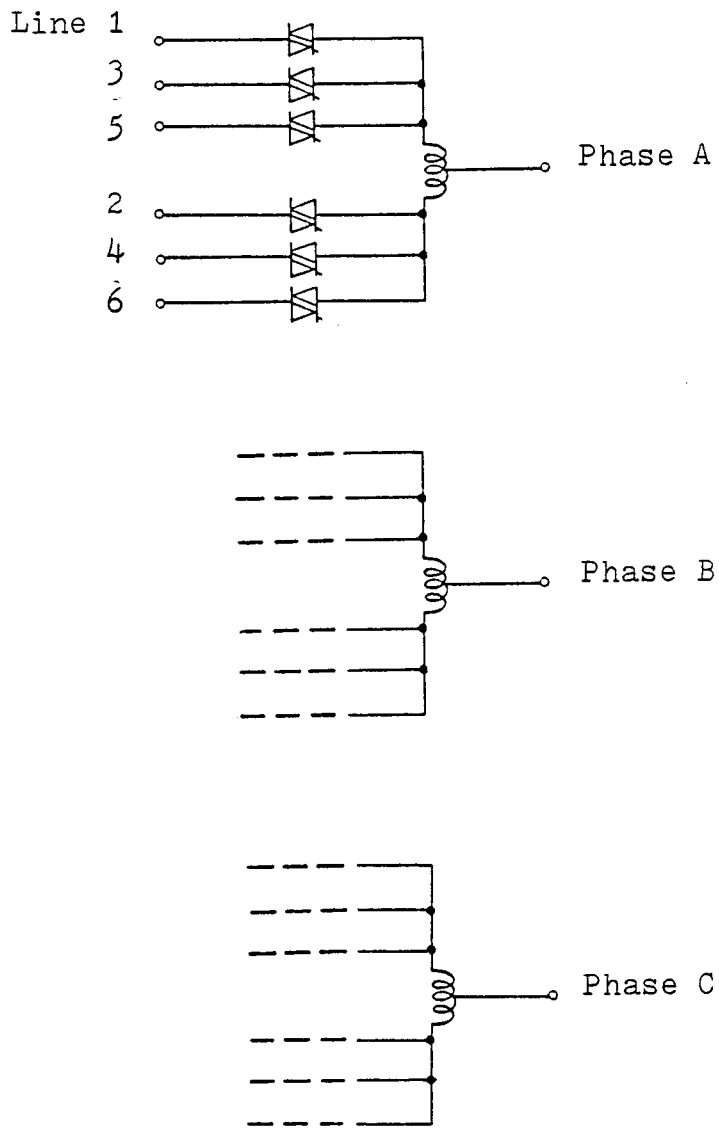
1-1-4 Circulating Current

The operation of a phase-controlled cycloconverter has been previously discussed with reference to a simple system as in Figure 1-2. The output frequency is controlled by the rate of change of the load voltage for a firing delay angles α_P and α_N. By suitably varying the firing delays with relationship of $\alpha_P + \alpha_N = 180^\circ$ on each half-cycle, any desired output waveforms may be made. For an ideal case the



A. SCR connection

Figure 1-5. Six-phase to three-phase cycloconverter.



B. TRIAC Connection

Figure 1-5. (Continued)

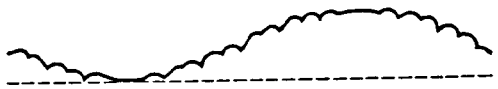
difference between the instantaneous voltage of the positive group and negative group are expected to be equal [Refer to Figure 1-6(A) and (B), with six-pulse cycloconverter], there is no net transfer of power in the system. In practice, the two instantaneous voltages are not equal [Figure 1-6(C)]. Therefore the output current waveform inevitably has large harmonic ripple components superimposed upon it. For this reason a large circulating current circulates between the converters and it will increase the thyristor loading. In order to limit the amplitude of the circulating ripple current but to support the circulating ripple voltage, it is necessary to connect a current-limiting reactor between the two converters shown in Figure 1-7. The preferred method of eliminating the circulating current utilizes current detectors in each phase to detect the instantaneous circulating currents and a logic control circuit to blank the triggering pulses to the inactive converter at the appropriate times. However this requires a much more complex firing control circuit.

1-1-5 Output Waveform Construction

The output voltage waveform of a converter is generated by the method of connecting, in turn, each input voltage to the output for a prescribed time interval. The output voltage is thus composed of segments of the input voltage waves, and the time duration of each segment is determined



A. Positive Group Output Voltage



B. Negative Group Output Voltage



C. Instantaneous Difference Between Positive Group And Negative Group

Figure 1-6. Six-pulse cycloconverter, and associated waveforms.

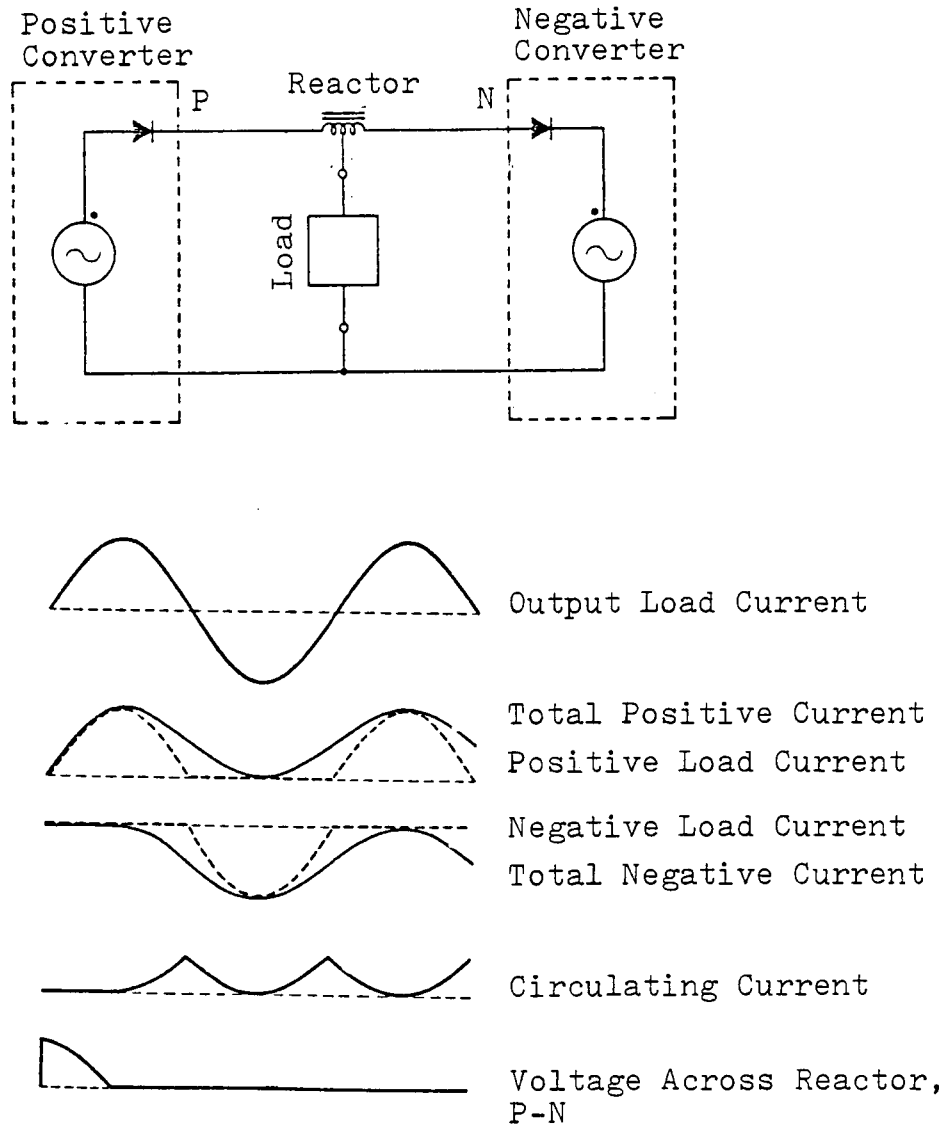
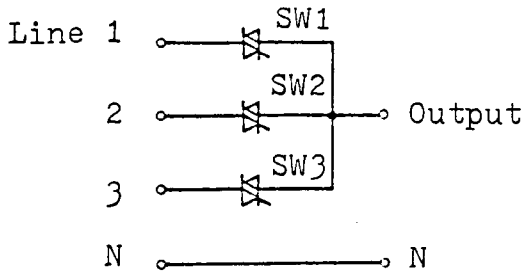


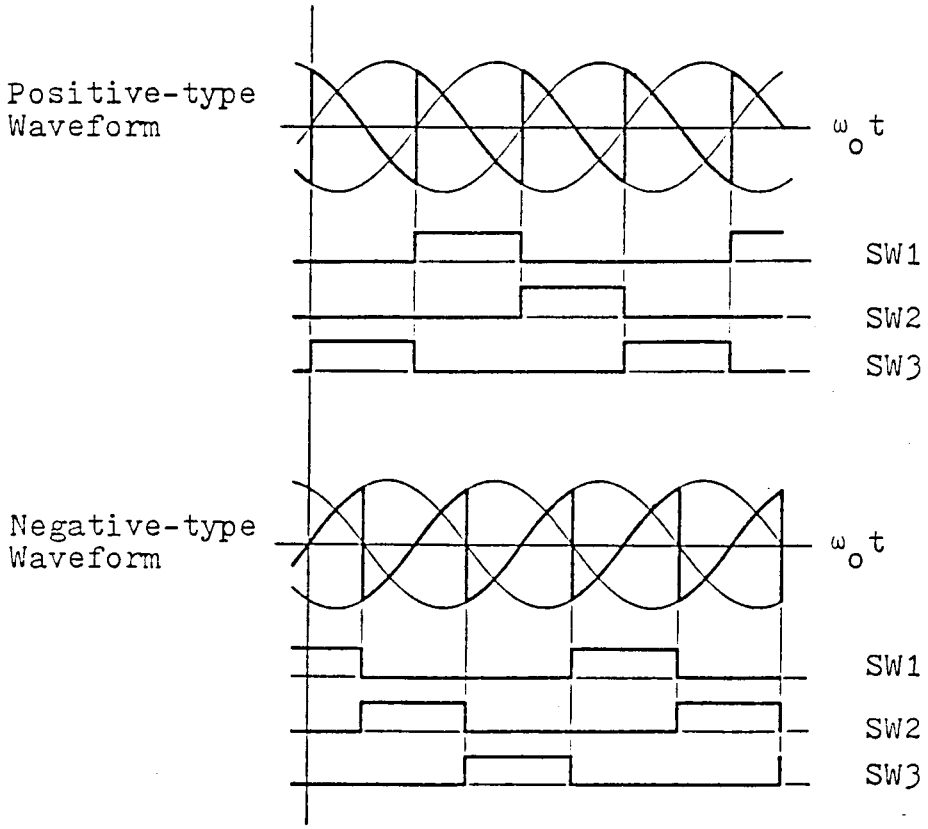
Figure 1-7. Cycloconverter with intergroup reactor to reduce circulating current

by the corresponding switch closure. Refer to Figure 1-6(A) and (B), the voltage waveforms are shown for six-pulse cycloconverter, which illustrate the "Positive" and "Negative" type output waveforms. The basic technique of the waveform construction will be discussed in this section.

To investigate the basic characteristics of different ac to ac converters, it is enough to consider a single-phase three-pulse converter circuit. There are two basic complementary output waves shown in Figure 1-8(B), which are produced by the three-pulse frequency changer. The positive-type and negative-type output voltage waveforms are defined as "Zero Mean" voltage according to Figure 1-8. The reason is that they have the average values of the identical segments of the input voltages waves to generate the final voltage wave. In order to understand the basic construction of the waveform, the positive-type and negative-type waveform are introduced in Figure 1-8. The two complementary waves considered are the familar waveshapes used to construct the final output waveform of the cycloconverter. Basically the repetition rate duration of switch closures are the important variables in obtaining the desired output waveform. By manipulation of these switching variables (SW1, SW2,...etc) we may obtain any desired waveshape.



A. Basic Circuit With TRIAC Connection



B. Basic Positive-type and Negative-type Waveform with Zero Mean Output Voltage

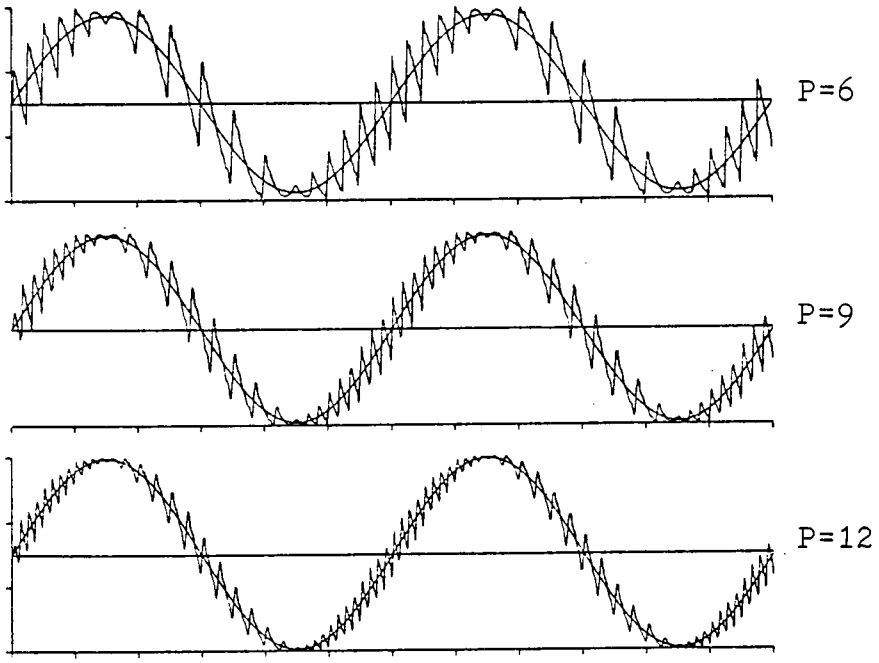
Figure 1-8. Positive-type and negative-type waveform construction.

1-1-6 Factors that Effect the Output Distortion

There are a number of factors that affect the harmonic content of the output waveform. These factors include the pulse number, the input to output frequency ratio of the converter, the source reactance of the generator and the circulating current in the corresponding circuit.

The higher the pulse number, the greater the reduction of the harmonic content of the output wave. This problem has been previously discussed in Section 1-1-3. In Figure 1-9(A) and (B) the output waveforms including positive-type and negative-type, are illustrated. Different frequency ratios (high input to low output) and different pulse numbers are shown to compare the output distortion level. In order to keep the harmonic content of the output waveforms within acceptable limits, the output frequency f_o must be less than the supply frequency f_I (i.e. $f_o << f_I$). Typically, the maximum usable output frequency is somewhere between 1/3 and 2/3 of the input frequency. For example, a 60Hz input frequency is used to produce 20Hz or less output frequency. The variation of operating range of frequency changer is dependent upon the particular cycloconverter circuits.

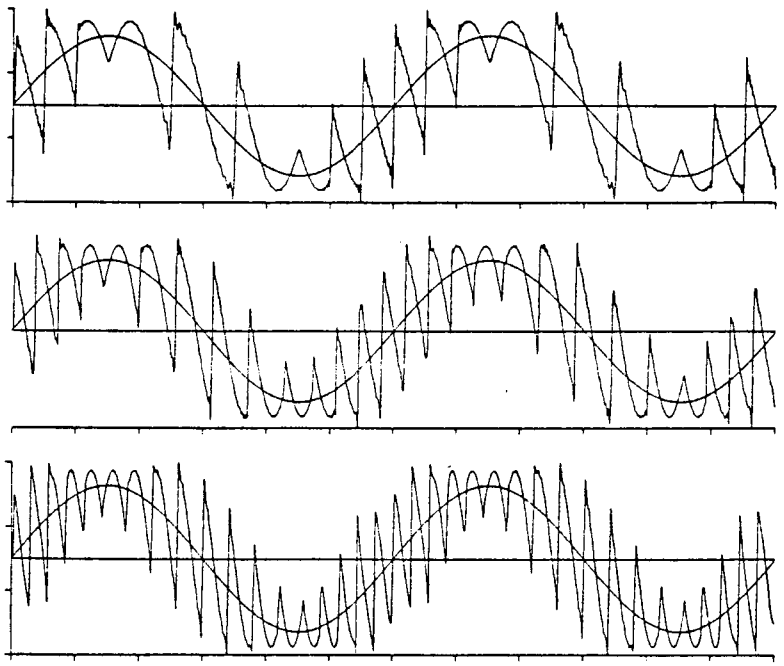
Sometimes the load voltage waveform from a cycloconverter is affected by commutation overlap caused by source reactance [Refer to Figure 1-10]. The illustration



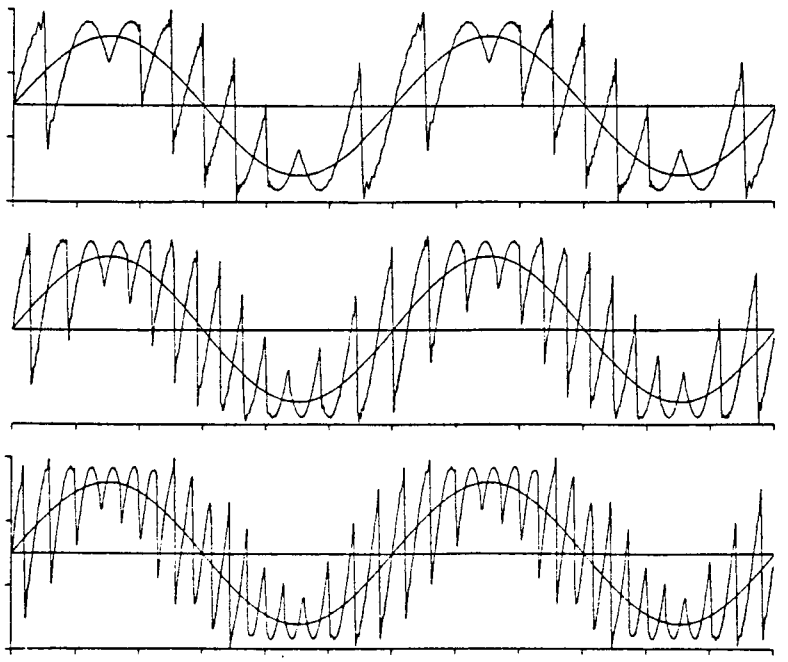
A. Different Pulse Number at $f_o=3f_I$

Figure 1-9. Effect of output to input frequency ratio and the pulse number of a cycloconverter on the output waveform distortion.

Positive-type Waveform

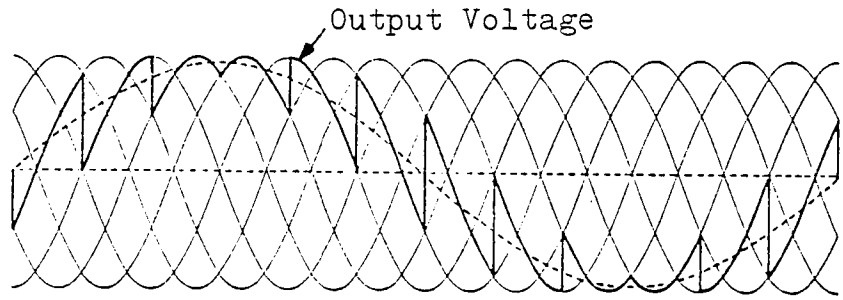


Negative-type Waveform

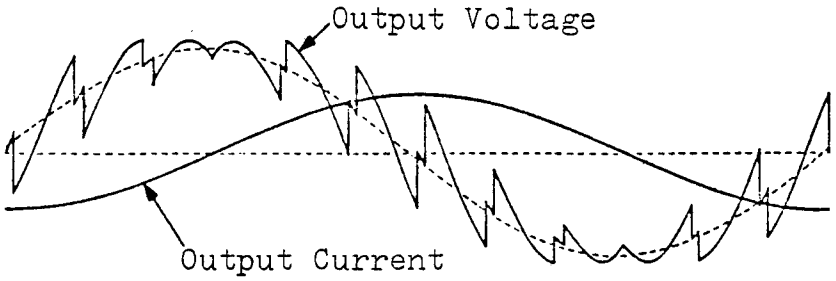


B. Various Output to Input Frequency Ratio

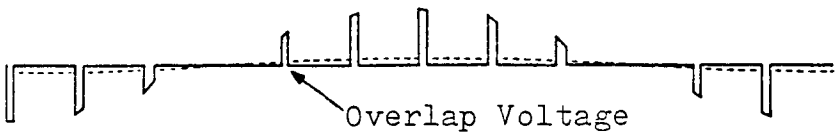
Figure 1-9. (Continued)



A. With Zero Source Reactance



B. With Finite Source Reactance

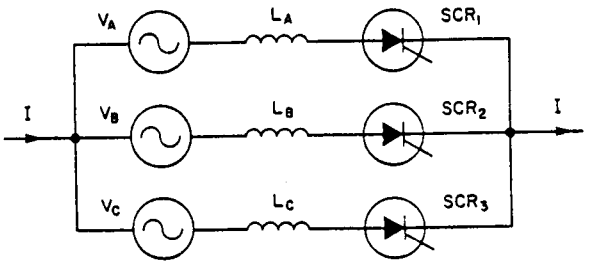


C. Notch Voltage Wave

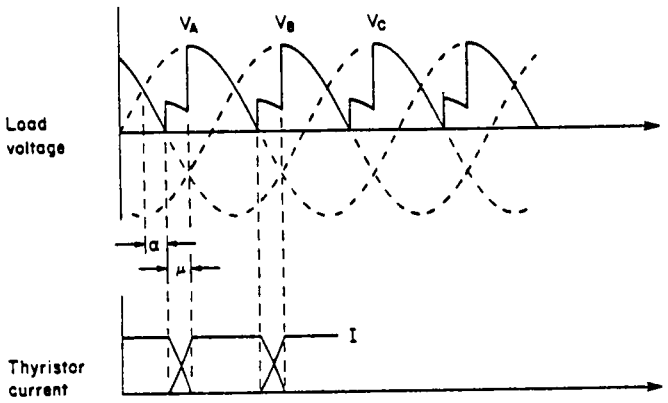
Figure 1-10. Commutation overlap

in Figure 1-11 shows a shift in the load voltage harmonic content where μ is the overlap angle and α is the decay angle. When overlap is present, the harmonic content of the mean voltage will be increased. It affects the time necessary to commutate inside the frequency changer. In order to avoid the overlap, the firing decay angle α and overlap angle μ must be adjusted. Increasing the firing angle α, the overlap angle μ decreases. The mean output voltage and peak load current are reduced, therefore the regeneration period will be shortened.

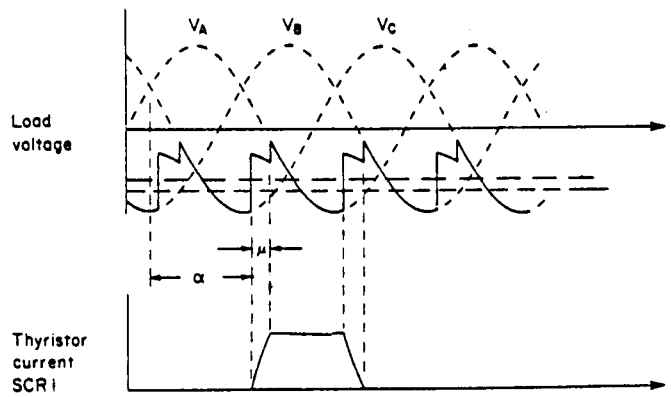
The equivalent circuit [Figure 1-13(B)] of a phase-controlled rectifier can be adapted to suit the case of a cycloconverter explains the output frequency response. However a "Correction Factor" for the case of the high frequency ratio f_O/f_I must be derived. As the frequency ratio of a cycloconverter increases, the quality of the output waveform deteriorates due to the frequency response of thyristors and other reactance components (e.g. filter and intergroup reactor) in that circuit. Therefore the analysis begins with a quantitative measure of the quality of the output waveform developed by means of a vector diagram [Refer to Figure 1-12]. The vector diagram shows that the "Resulting Frequency Ratio Correction Factor" can be used to improve the calculation of the net output voltage. The equivalent circuit has the pseudo-instantaneous voltage v_O at any instant and is



A. Basic Circuit

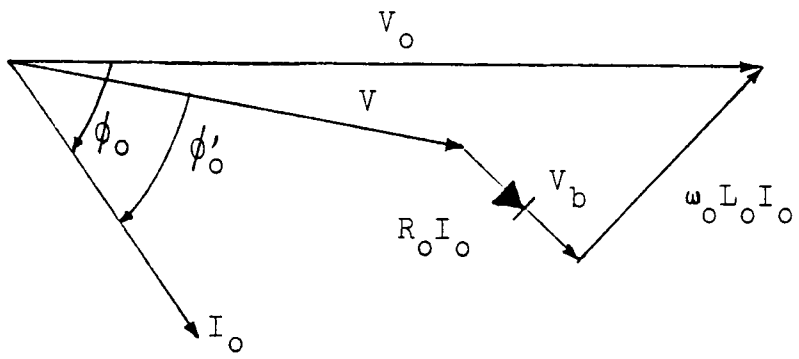


B. Voltage and Current Waveforms, Rectifying

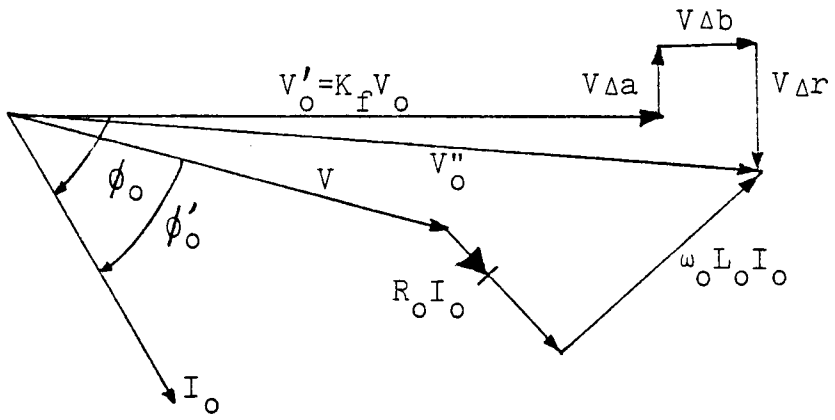


C. Voltage and Current Waveforms, Inverting

Figure 1-11. Commutation overlap, three-pulse midpoint converter with finite commutating reactance.

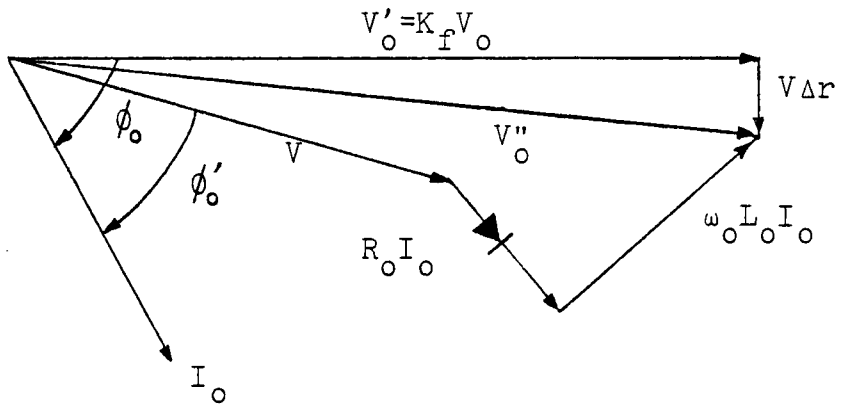


A. Phase Diagram



B. Phase Diagram including High Frequency Ratio

Figure 1-12. Phase diagram of a cycloconverter.



C. Phase Diagram including Frequency Correction Factor

Figure 1-12. (Continued)

sinusoidal at the output, if the operating frequency ratio in the system is set high enough. The equivalent effective output resistance R_o shown in Figure 1-13 at any instant is

$$R_o = S \times R_c \qquad (1-1)$$

where R_c is a real source resistance, S is a number of commutating groups in series or cascade connection. For example, the three-phase bridge circuit is effectively a cascade connection of two three-phase commutating groups, for which S = 2 .

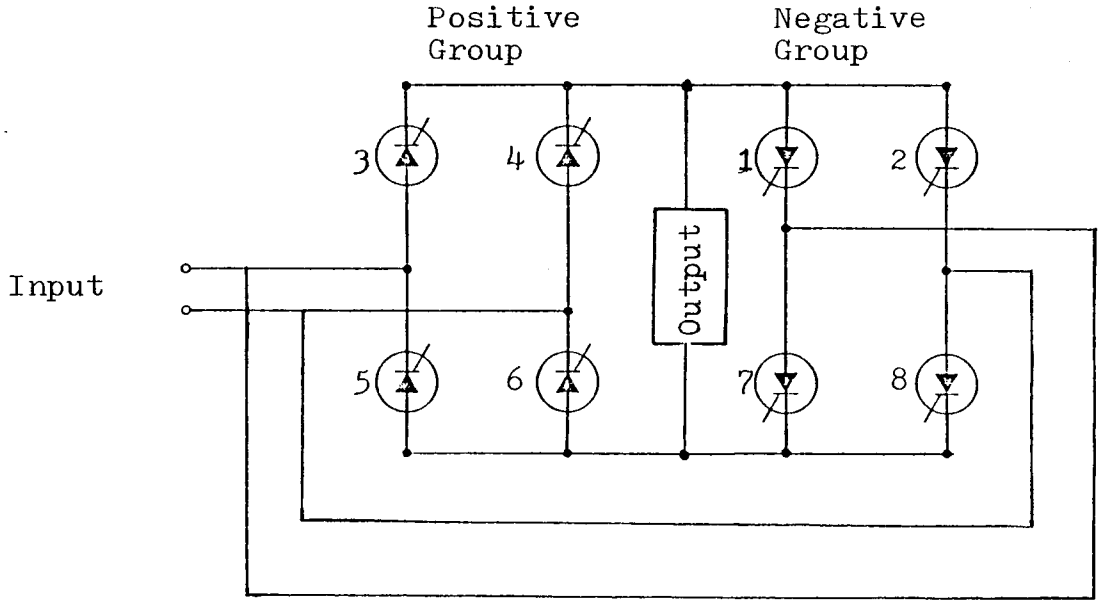
The total effective loop inductive L_o at any instance is

$$L_o = S(L_c + L_g) + L_f \qquad (1-2)$$

where L_g is an intergroup inductance, L_c is a commutating inductance, and L_f is the output filter inductance in the equivalent circuit for the cycloconverter.

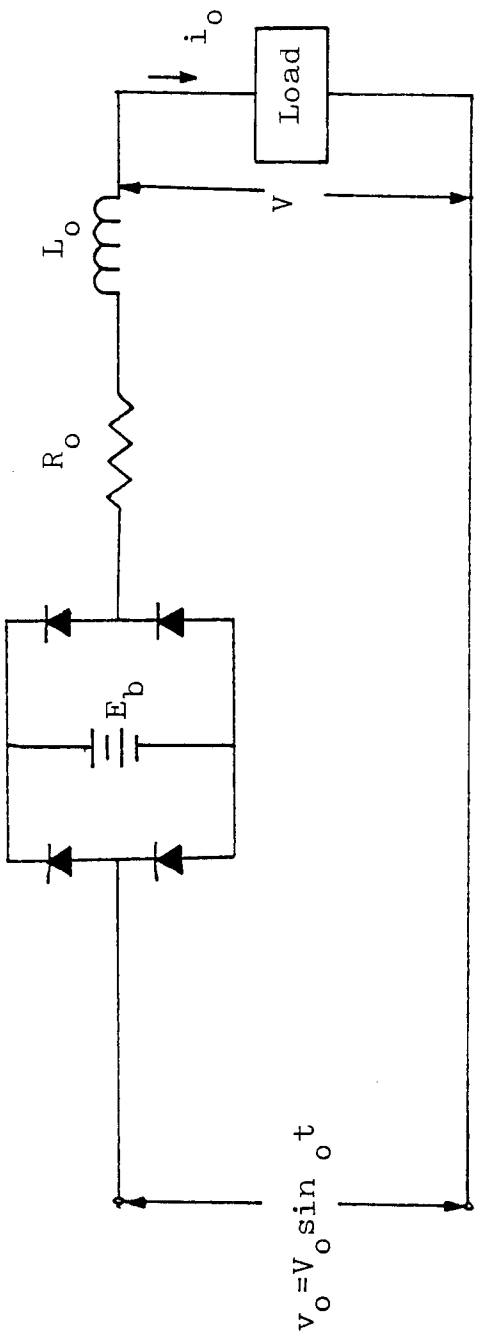
The fundamental component of a back emf V_b in the equivalent circuit is a constant-drop term that causes loss of voltage in a rectifier circuit. The pseudo-instantaneous load voltage v can be written as follows:

$$v = V_o \sin \omega_o t - E_b \mathrm{sgn}(i_o) - R_o i_o - L_o (di_o / dt) \qquad (1-3)$$



A. Bridge-type Circuit

Figure 1-13. A practical bridge-type cycloconverter with single-phase output.



B. Output Equivalent Circuit

Figure 1-13. (Continued)

where signum function (sgn) is presented as a function of load current i_o. Equation (1-3) can be transformed in rms phasor notation, if output voltage and current are sinusoidal

$$V = V_o - V_b\underline{|\phi_o} - R_oI_o\underline{|\phi_o} - \omega_oL_oI_o\underline{|\phi_o - 90^\circ} \qquad (1\text{-}4)$$

where angle ϕ_o of load current is assumed lagging with respect to control voltage V_o, and angle ϕ_o' of load current is also assumed lagging with respect to load terminal voltage V_o. Figure 1-12(A) shows a phasor diagram for a practical cycloconverter which is based on Equation (1-4).

As the frequency ratio f_o/f_I of a cycloconverter decreases, the quality of the output waveform improves. The effect of a high frequency ratio can be approximated by reducing the voltage V_o by a factor K_f and introducing current-dependent voltage phasors $V\Delta a$, $V\Delta b$, and $V\Delta r$ where $V\Delta a$ is a component of distortion voltage that leads V_o by 90 degrees, $V\Delta b$ is a component of distortion voltage in phase with V_o, and $V\Delta r$ a component of distortion voltage caused by variation of equivalent resistance, lags V_o by 90 degrees. Assuming $\phi_o = \phi_o'$, the phasor diagram of a cycloconverter, including the effect of high frequency is shown in Figure 1-12(B) where V_o' is the value of V_o including a "Reduction Factor", and V_o'' is the output emf corrected including a "Reduction and Distortion Factor". In order to correct the

level of distortion in a cycloconverter caused by the high frequency ratio, a saturating reactor [Figure 1-7], a bridge circuit [Figure 1-13(A)], delta-connected load (circulating current around the delta) or line capacitor may be used for neutral the distortion components. As a result it is possible to reduce the harmonic currents circulating in the circuit. After correction, the current-dependent components of distortion voltage $V_{\Delta a}$ and $V_{\Delta b}$ disappear. The phasor diagram including the frequency ratio correction factor is shown in Figure 1-12(C). A more detailed description of a frequency changer using cycloconverter principles will be developed in Chapter 2 and 3.

1-2 AN INDUCTION GENERATOR

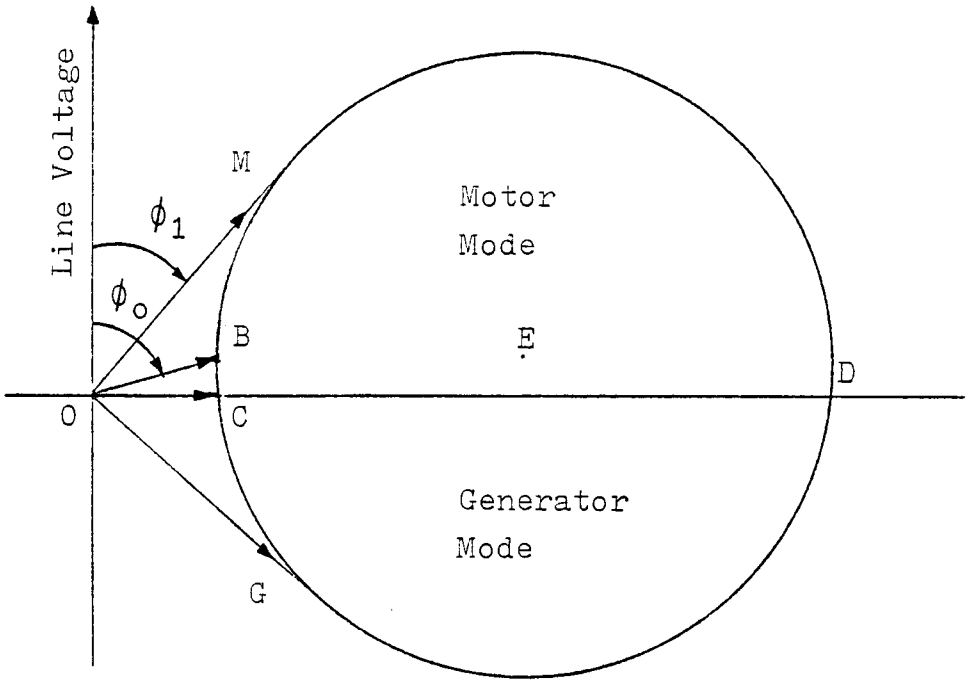
Typically a high-speed application in a power system demands the use of a generator rotor without winding. A squirrel-cage induction machine is mechanically well suited for this type of application. The induction generator is a simple and robust machine cheaper more efficient and easier to operate, control and maintain than the synchronous generator. It is suitable for small-capacity independent power sources (normally carrying leading currents, or where such leading current components can readily be supplied) to supply a high power factor load.

1-2-1 Circle Diagram

An induction motor can be served as an induction generator if it is driven to a speed slightly above its synchronous speed. The performance characteristics of an induction generator is usually determined in a graphical form by the circle diagram as shown in Figure 1-14. The generator mode corresponds to the lower half circle. The admittance (generating) vector OG in Figure 1-14 leads the line voltage. Thus the generator draws all its excitation from the system and must absorb a definite amount of lagging current for an applied voltage and load current [Refer to Table B.1 in the Appendix]. The induction generator then requires a source of reactive current for excitation, as does the induction motor. To make the induction motor serve as a generator, the reactive power (vector OC in Figure 1-14) must be supplied by external source such as over-excited synchronous machines or by means of a static capacitance. In this thesis, the power source requires the external excitation by means of capacitors.

1-2-2 Build-up of Terminal Voltage

The induction generator, with negative slip, requires a source of magnetizing current for excitation. By supplying the magnetizing (exciting) current from the static capacitors connected in shunt across the terminals of the machine, it can be operated as an independent generator.



OM = Stator current I_1 in Motor Mode.
OG = Stator current I_1 in Generator Mode.
OB = No-load current I_o at phase angle ϕ_o.
OC = Reactive component of no-load current I_o.
OD = $V_1/(X_1+X_2)$, the ideal short-circuit current, where V_1 is a per phase terminal voltage and X_1+X_2 are stator and rotor leakage reactance per phase referred to stator.
CB = Active component of no-load current I_o, associated with both stator core and mechanical losses per phase.
CD = Diameter of current locus circle, of center E.

Figure 1-14. Circle diagram of an induction machine.

The "Build-up" voltage characteristics of a squirrel-cage induction generator are similar to a dc shunt generator. Therefore its build-up voltage depends upon the residual magnetism in the iron of the magnetic current. The residual magnetizing current in the rotor first sets up a small alterating emf in the stator while starting; this emf is at a frequency which is proportional to the rotor speed. Applying this emf to the capacitor, it causes a lagging magnetizing current to flow in the stator winding and produces an armature reaction flux to help the original residual flux. By this process the induction machine receives its excitation from the capacitance, and produces electrical power feeding energy back into the lines.

The induced voltage of the induction generator does not build up unless the exciting capacitive reactance X_c is smaller than a certain critical value of machine magnetizing reactance X_m. If the capacitance is of the proper value, the current will be large enough to increase the flux existing in the air gap. An increase of the air gap flux will result in a higher voltage, larger existing current drawn by the capacitance, more air gap flux and so on until terminal voltage of the machine reaches its final limits by saturation. Since an induction machine is normally designed to operate at small slip, about five percent or less, rated output conditions as a generator is obtained at speed above five percent or less of the synchronous speed.

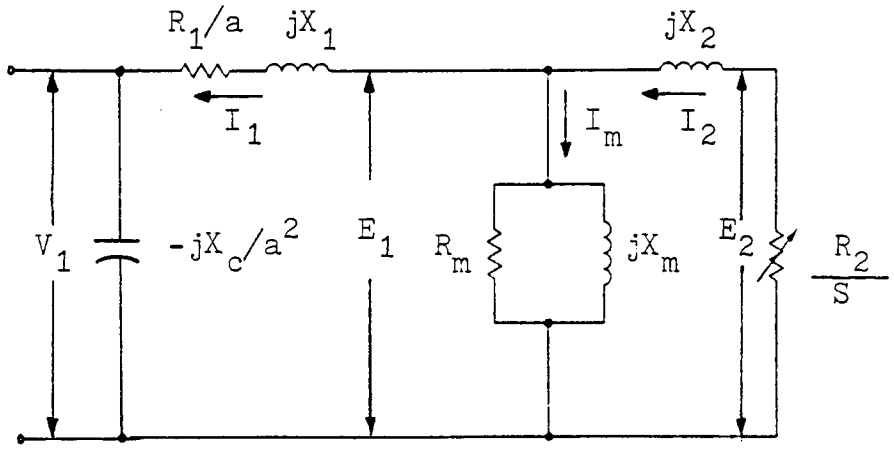
1-2-3 Single-phase Equivalent Circuit

The operating behaviour of the machine can be investigated in terms of the equivalent circuit shown in Figure 1-15. The steady-state equivalent circuit for any given self-excited frequency ω_e can be expressed in terms of the parameters R_1, R_2, X_1, X_2, R_m, X_m and X_c all referred to the nomal angular frequency ω_1 by using the factor $a = \omega_e/\omega_1$. If the shaft speed is expressed as the symbol N_s of normal synchronous speed, then $a\text{-}N_s = S$, where the slip S is negative. The capacitor in the equivalent circuit has been external excitated. The output voltage V_1 of the machine is

$$V_1 = E_1 - I_1(R_1/a + jX_1) \qquad (1\text{-}5)$$

The magnetic field produced by the rotor winding rotates at synchronous speed and the stator rotates at a slower speed. The ratio of the difference between the synchronous and the actual speed to the synchronous speed is Slip S. The frequency of the stator is $f_1 = Sf_2$, and the stator induced voltage is $E_1 = SE_2$ those are also dependent on the slip. Therefore the stator current I_1 and the rotor current I_2 of the machine may be written in terms of slip frequency. As there is no externally voltage, the mesh equation for current I_1 and I_2 are

$$I_1[R_1/a + j(X_1 - X_c/a^2)] + (I_1 - I_2)jX_m = 0 \qquad (1\text{-}6)$$



$a = \omega_e / \omega_1$

ω_e : self-excited frequency

ω_1 : normal angular frequency

Figure 1-15. Single-phase equivalent circuit of the capacitor-excited induction generator.

and

$$I_2[R_2/a + jX_2] + (I_2 - I_1)jX_m = 0 \qquad (1\text{-}7)$$

where $a = \omega_e/\omega_1 = S+N_s$.

An normal induction motor runs at a speed slightly less than its synchronous speed N_s. The output slip speed N_2 is equal to $(N_s - S)$ when the induction machine is operated as a motor. When the induction machine absorbs its rated power and becomes an induction generator, the output slip speed N_1 is equal to $(N_s + S)$. Actually the difference of $(N_s - S)$ to $(N_s + S)$ depends upon the rotor type and normal slip value of the motor or generator action. The performance of an induction machine is discussed in Chapter 4.

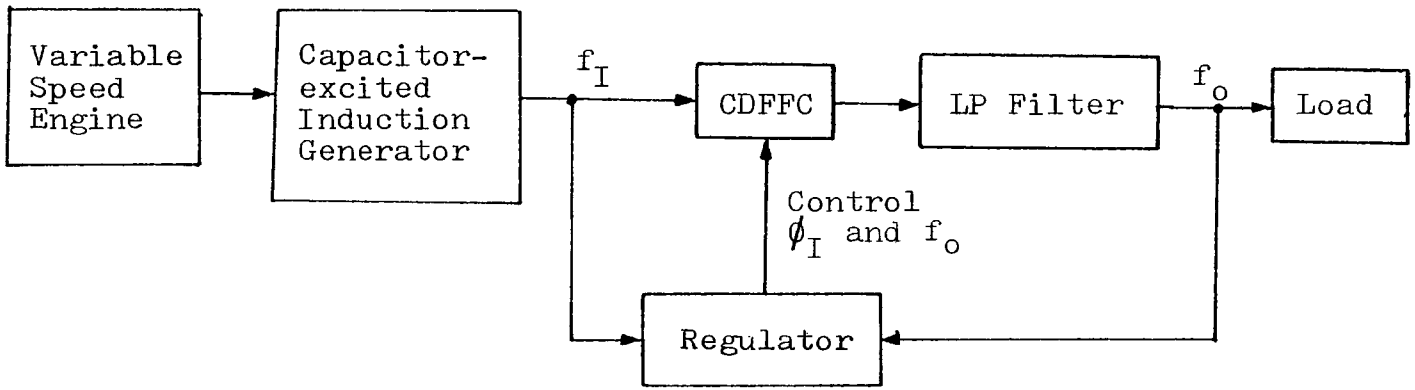
1-3 A VSCF SYSTEM

A VSCF power-generating system using a cycloconverter as a frequency changer converts ac power at one variable frequency to ac power at another constant frequency. Static power conversion systems using "TRAIC" in a VSCF system can very effectively replace hydromechanical constant-speed drive systems (with coupling device between the engine and the alternator) and other intermediate dc link converter system (rectifier-fed inverter).

1-3-1 System Block Diagram

A VSCF power conversion unit in an engine-driven generator system is shown in the block diagram in Figure 1-16. This closed-loop control unit shown the scheme how to control the input displacement factor and output frequency at any load power factor, and may convert a variable input frequency f_I to another desired constant output frequency f_o. This type of frequency changer is classified as a "Controllable Displacement Factor Frequency Changer (CDFFC)".

The control circuit of a frequency changer is very complex owing to the relatively involved logic functions (triggering signal) that have to be performed. The power source is a capacitor-excited induction generator producing a sine wave voltage, at a frequency depending upon engine speed. The output load voltage is synthesized into a desired lower frequency from the high frequency supply, is then filtered by a low pass filter to produce a sine wave at the output load. The regulator senses an error signal feedback from output and supplies logic functions to control the desired input phase angle ϕ_I and output frequency f_o of the cycloconverter under all output load conditions. After the cycloconverters correct its switching frequency and its input displacement, the feedback signal causes the reduction of an error signals from the regulator, and maintains



Input		Output	
V_I	= constant	V_o	= constant
f_I	= variable	f_o	= constant
ϕ_I	= controlled to maintain V_I	ϕ_o	= variable

Figure 1-16. A VSCF power-generating system.

stability of the system within desired limits. A low-pass filter is used to remove the desired high frequency ripple.

1-3-2 Equivalent Circuit of CDFFC and its Operating Ranges

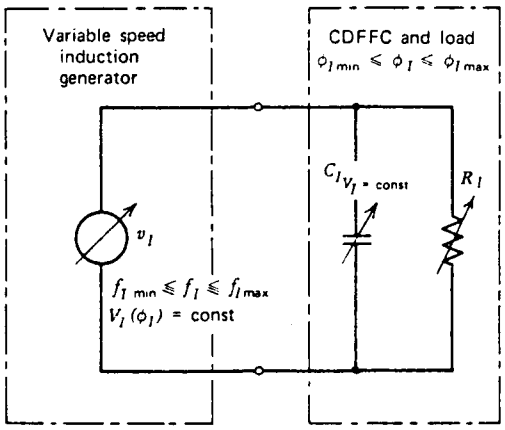
The input and output equivalent circuit of a CDFFC is shown in Figure 1-17. It is derived under the ideal condition of equal real input and output power. However this assumption may not be suitable for a complex output load. The basic operating characteristics of a CDFFC is summarized in Table 1.2.

A CDFFC with load can be considered as an impedance consisting of a parallel combination of a variable resistor and capacitor. The equation of the equivalent circuit input resistance R can be written in the form

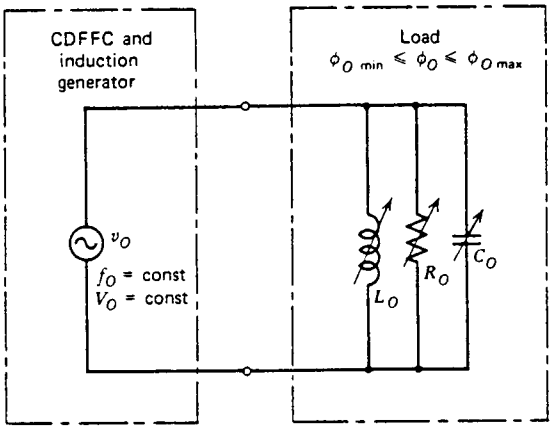
$$R_I = (V_I / V_o)^2 R_o \qquad (1\text{-}8)$$

where the real output power is equal to the real input power. The simple equivalent circuit can not be derived for the condition of complex output load. Since the reactive input power is not dependent on the output real and reactive power, the output admittance can be written as

$$Y_o = (1 / R_o) + (1 / j\omega_o L_o) + j\omega_o C_o \qquad (1\text{-}9)$$



A. Input Equivalent Circuit



B. Output Equivalent Circuit

Figure 1-17. Input and output equivalent circuit.

Table 1.2. Operating range of a CDFFC.

Output Frequency Range	$0 \leq f_o < f_I$
Output Voltage Range	$0 \leq V_o \leq \max V_o$
Input Displacement Angle Range	$-\min \phi_I \leq \phi_I \leq \max \phi_I$ $\max \phi_I = F(V_o, \phi_o)$

The input admittance can be transformed

$$Y_o = (1 / R_I) + j\omega_I C_I \qquad (1\text{-}10)$$

From Equation (1-8), (1-9) and (1-10) the input capacitor can be represented as

$$C_I = \left\{(I_I / V_I) - (1 / R_I)\right\} / j\omega_I \qquad (1\text{-}11a)$$

or

$$C_I = \left\{(I_I / V_I) - (I_o / V_o) + (1 / j\omega_o L_o) + j\omega_o C_o\right\} / j\omega_I \qquad (1\text{-}11b)$$

where $I_I = V_I Y_I$ and $I_o = V_o Y_o$. The detail operating description will be discussed in Chapter 5.

CHAPTER 2

THEORETICAL ANALYSIS OF A STATIC FREQUENCY CHANGER

Investigation of the power conversion process requires the development of a general mathematical theory to express the characteristics of output and input waveforms of a frequency changer. The cause and effect of the external performance characteristics including input current, input displacement and the power factor of a frequency changer directly influences the output voltage waveform. Determination of the relationships between the generated "Output Voltage" and "Input Current" waveforms are the main objective of this chapter.

Any composite waveforms can be synthesized from derivatives of the two basic positive-type and negative-type waves. Therefore all equations in this chapter are derived in terms of the positive-type and negative-type waves, respectively.

The system matrix equations introduce the mathematical concept for the waveform generation. Some corresponding existence functions and modulating funtion and there effect on waveforms are established and defined. The development of a consecutive composite waveform technique, corresponding to various practical modulating function, is presented. Some related performance indices are computed.

2-1 GENERAL CONCEPT OF THE OUTPUT VOLTAGE WAVE AND INPUT CURRENT WAVE

The output wave of a cycloconverter is composed of segments that are determined by the corresponding switch closures at precribed time intervals. To analyze the output and input waveform characteristics, two complementary waves (positive-type and negative-type) must be considered. Other factors that affect the structure of the output voltage waveform and input current waveform include the pulse number of the converter, the ratio between the output and input frequencies, the relative level of the output voltage, the output displacement angle of the load and the control technique of the firing instants.

2-1-1 General Output Voltage

The simple block diagram of a q-phase ac input source with frequency f_I and generating p-phase output power with a desired frequency f_o is shown in Figure 2-1. The general relationship between the input and the generated output voltage waveform $v_o(t)$ can be expressed by the matrix equation in Equation (2-1)

$$[v_o(t)] = [H(t)]\,[v_I(t)] \tag{2-1}$$

The terms $[v_o(t)]$, $[H(t)]$ and $[v_I(t)]$ reveal all the input and output characteristics of a frequency changer. Thus

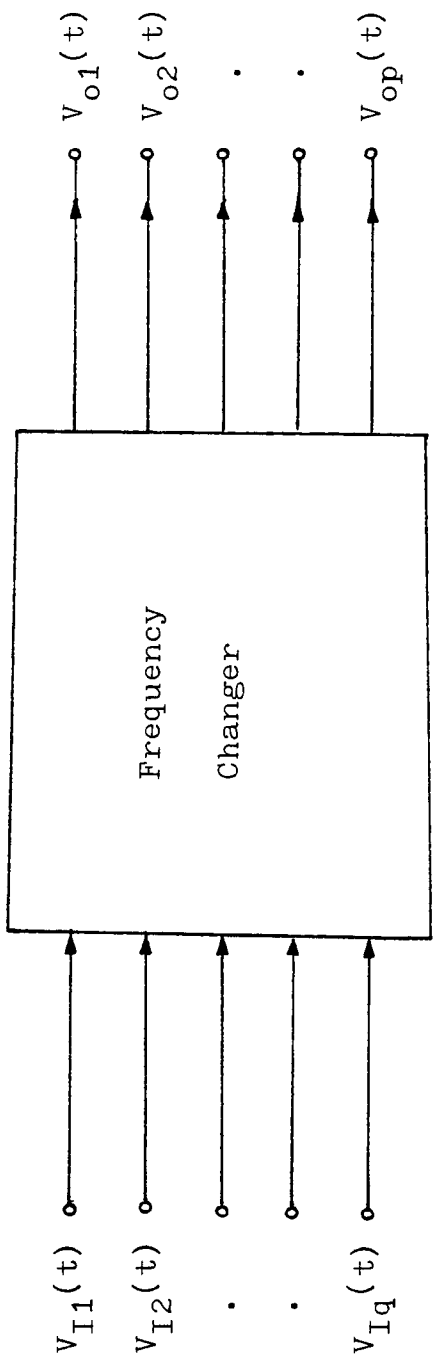


Figure 2-1. Diagrammatic representation of a simple q to p phase frequency changer.

$[v_o(t)]$ is the time-varying output voltage vector with a dimension of (p x 1), $[v_I(t)]$ is the time-varying input voltage vector with a dimension of (q x 1), and $[H(t)]$ is a (p x q) time-varying existence matrix representing an array of bilateral switches contain the relationship between input and output terminals. For a multi-phase network, Equation (2-1) may be generally written in the following matrix form:

1. For a general m-phase output with n-phase input

$$\begin{bmatrix} v_{o1}(t) \\ v_{o2}(t) \\ \cdot \\ \cdot \\ v_{op}(t) \\ \cdot \\ \cdot \\ v_{om}(t) \end{bmatrix} = \begin{bmatrix} h_{11}(t) & h_{12}(t) & \cdots & h_{1q}(t) & \cdots & h_{1n}(t) \\ h_{21}(t) & h_{22}(t) & \cdots & h_{2q}(t) & \cdots & h_{2n}(t) \\ \cdot & & & & & \\ \cdot & & & & & \\ h_{p1}(t) & h_{p2}(t) & \cdots & h_{pq}(t) & \cdots & h_{pn}(t) \\ \cdot & & & & & \\ \cdot & & & & & \\ h_{m1}(t) & h_{m2}(t) & \cdots & h_{mq}(t) & \cdots & h_{mn}(t) \end{bmatrix} \begin{bmatrix} v_{I1}(t) \\ v_{I2}(t) \\ \cdot \\ \cdot \\ v_{Iq}(t) \\ \cdot \\ \cdot \\ v_{In}(t) \end{bmatrix} \tag{2-2}$$

2. For a three-phase output with three-phase input

$$\begin{bmatrix} v_{o1}(t) \\ v_{o2}(t) \\ v_{o3}(t) \end{bmatrix} = \begin{bmatrix} h_{11}(t) & h_{12}(t) & h_{13}(t) \\ h_{21}(t) & h_{22}(t) & h_{23}(t) \\ h_{31}(t) & h_{32}(t) & h_{33}(t) \end{bmatrix} \begin{bmatrix} v_{I1}(t) \\ v_{I2}(t) \\ v_{I3}(t) \end{bmatrix} \tag{2-3}$$

3. For a single-phase output with three-phase input

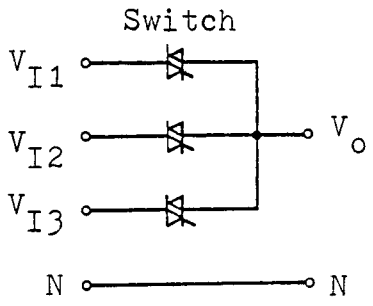
$$v_{o1}(t) = \begin{bmatrix} h_{11}(t) & h_{12}(t) & h_{13}(t) \end{bmatrix} \begin{bmatrix} v_{I1}(t) \\ v_{I2}(t) \\ v_{I3}(t) \end{bmatrix} \qquad (2\text{-}4)$$

where $v_{I1}(t)$ through $v_{In}(t)$ are time function of the input voltage waves, and $v_{01}(t)$ through $v_{0m}(t)$ are the output voltage waves. To investigate the characteristics of the output voltage, it is enough to consider a three-pulse converter circuit shown in Figure 2-2.

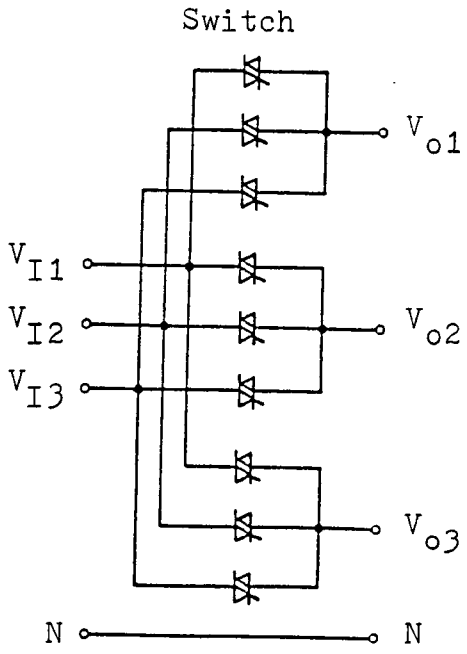
In the analysis of the output voltage waves, it is assumed that the multi- input voltages of a frequency changer are symmetrically displaced sinusoids, that is,

$$v_I(t) = V_I \begin{bmatrix} \sin\omega_I t \\ \sin(\omega_I t - 2\pi/n) \\ \cdot \\ \cdot \\ \sin(\omega_I t - (n-1)2\pi/n) \end{bmatrix} \qquad (2\text{-}5)$$

where $\omega_I = 2\pi f_I$ is the input angular velocity, and v_I is the amplitude of each of the input voltage.



A. Single-phase Output



B. Three-phase Output

Figure 2-2. Typical three-pulse cycloconverter.

Matrix [H(t)], a time-varying existence function, represents arrays of bilateral switches connecting the input terminal q-th to output terminal p-th in some ordered sequence. Each element of matrix [H(t)] therefore may be defined by a given switch h_{pq} (p = 1,2,3,...m; q = 1,2,3,...n) whose values are step functions either unity (h_{pq} = 1, switch closed) or zero (h_{pq} = 0, switch opened) at a given time.

$$h_{pq} = \sum_{k=0}^{\infty} \left(u(t_k) - u(t_{k+1}) \right) \tag{2-6}$$

where $u(t_k)$ and $u(t_{k+1})$ are unit step functions entering at time t_k and t_{k+1}, respectively. In some practical applications, each existence function in a frequency changer is actually required for the output waveform to have a prescribed frequency f_o and amplitude V_o. Therefore each existence function h_{pq} may be described as having precisely the duration of each constituent segment of the output waveform that is the function of input frequency f_I, output frequency f_o, and output to input voltage ratio V_o/V_I. The general expression is

$$h_{pq} = h_{pq}(f_I, f_o, V_o/V_I, t) \tag{2-7}$$

where p = 1,2,3,...m; q = 1,2,3,...n. For convenience the existence function is considered as a function of time. The

h's are rectangular pulse trains with modulated temporal parameters M(t) [see Section 2-2-1-1]. By controlling pulse position, width, and repetition rate, any desired waveforms with different modulating technique may be produced. Each generated pulse will trigger each power switch at the proper time. This may be described as the "On" and "Off" state of the power switches represented in Figure 2-2.

The output voltage is not a pure sinusoid as it is composed of different segments of input voltage waves. The resulting components of frequency and amplitude are freferred to as "Wanted" and "Unwanted". The component of the output voltage wave with desired frequency f_o will be considered a "Wanted Output Voltage". All other additional components will be considered "Unwanted" components. Generally each unwanted/wanted output voltage wave contains sinusoidal components having a frequency spectrum which is not/is integrally related.

It is convenient to write Equation (2-2) into the following form:

$$v_{op}(t) = \left[h_{p1}(t)\ h_{p2}(t)\ \ldots\ldots\ h_{pn}(t)\right] \begin{bmatrix} v_{I1}(t) \\ v_{I2}(t) \\ \cdot \\ v_{In}(t) \end{bmatrix}$$

$$= V_o \sin(\omega_o t - (p-1)2\pi/m) + \sum_{L=1}^{\infty} V_{UL} \sin(\omega_{UL} t - \phi_{UL}) \qquad (2\text{-}8)$$

where the first term of the above equation represents the wanted output voltage component, and the second term represents the unwanted output voltage components. Thus, V_{UL} is the amplitude of L-th unwanted components, $\omega_o = 2\pi f_o t$ is the wanted angular velocity, $\omega_{UL} = 2\pi f_{UL}$ is the unwanted angular velocity where f_{UL} is a frequency of the L-th unwanted components, and ϕ_{UL} is a phase angle of the L-th unwanted components. Due to the presence of these harmonics, more precise definitions expressing the ratio in frequency, amplitude and distortion factor at the output are required. The effects of the output voltage wave of a frequency changer on the supply may be characterized by the "Output Voltage Wave Indices" which is measured at the output terninals. The frequency ratio ν_{oL} of the significant unwanted components f_{UL} to the wanted output frequency f_o of a frequency changer is defined

$$\nu_{oL} \triangleq \left| f_{UL} / f_o \right| \qquad L = 1,2,\ldots \qquad (2\text{-}9)$$

The amplitude ratio γ_{oL} of the significant unwanted components V_{UL} to the desired output voltage V_o of a frequency changer is defined

$$\gamma_{oL} \triangleq \left| V_{UL} / V_o \right| \qquad L = 1,2,... \qquad (2\text{-}10)$$

The total rms output voltage distortion factor μ_o of a frequency changer is defined

$$\mu_o \triangleq \sqrt{\left(\sum_{L=1}^{\infty} V_{UL}^2 \right)} / V_o \qquad (2\text{-}11)$$

In order to approach the ideal output waveform, it must be possible to minimize γ_{oL} and μ_o and maximize ν_{oL}. In practice, a corrective feedback adjusts the firing instants, and thereby, suppresses the objectionable distortion terms. The above indices points out that the distortion is determined by $h_{pq}(f_I, f_o, V_o/V_I, t)$ which describes the operating state of the switches. The angle variation of an existence function is controlled by the modulating function which is designed to be operated by the power switches to form the desired output waveform.

2-1-2 General Input Current

The description of the output voltage can be written for the input current wave $i_I(t)$ in terms of output current, by transposing the existence matrix [H(t)] of the switches.

The expression is

$$\left[i_I(t)\right] = \left[H(t)\right]^T \left[i_o(t)\right] \qquad (2\text{-}12)$$

The above input current equation can be expressed for a multi-phase network, in the following matrix form:

1. From a general n-phase input to m-phase output

$$\begin{bmatrix} i_{I1}(t) \\ i_{I2}(t) \\ \cdot \\ \cdot \\ i_{Iq}(t) \\ \cdot \\ \cdot \\ i_{In}(t) \end{bmatrix} = \begin{bmatrix} h_{11}(t) & h_{21}(t) & \cdots & h_{p1}(t) & \cdots & h_{m1}(t) \\ h_{12}(t) & h_{22}(t) & \cdots & h_{p2}(t) & \cdots & h_{m2}(t) \\ \cdot & & & & & \\ \cdot & & & & & \\ h_{1q}(t) & h_{2q}(t) & \cdots & h_{pq}(t) & \cdots & h_{mq}(t) \\ \cdot & & & & & \\ \cdot & & & & & \\ h_{1n}(t) & h_{2n}(t) & \cdots & h_{pn}(t) & \cdots & h_{mn}(t) \end{bmatrix} \begin{bmatrix} i_{o1}(t) \\ i_{o2}(t) \\ \cdot \\ \cdot \\ i_{op}(t) \\ \cdot \\ \cdot \\ i_{om}(t) \end{bmatrix} \qquad (2\text{-}13)$$

2. From a three-phase input to three-phase ouput

$$\begin{bmatrix} i_{I1}(t) \\ i_{I2}(t) \\ i_{I3}(t) \end{bmatrix} = \begin{bmatrix} h_{11}(t) & h_{21}(t) & h_{31}(t) \\ h_{12}(t) & h_{22}(t) & h_{32}(t) \\ h_{13}(t) & h_{23}(t) & h_{33}(t) \end{bmatrix} \begin{bmatrix} i_{o1}(t) \\ i_{o2}(t) \\ i_{o3}(t) \end{bmatrix} \qquad (2\text{-}14)$$

3. From a single-phase input to n-phase output

$$i_{I1}(t) = \left[h_{1q}(t)\ h_{2q}(t)\ \ldots\ h_{nq}(t)\right] \begin{bmatrix} i_{o1}(t) \\ i_{o2}(t) \\ \cdot \\ i_{om}(t) \end{bmatrix} \qquad (2\text{-}15)$$

In the analysis of the input current waves, it is assumed that the multi- output currents of the frequency changer are symmetrically displaced sinusoidal, that is

$$\begin{bmatrix} i_{o1}(t) \\ i_{o2}(t) \\ \cdot \\ i_{op}(t) \\ \cdot \\ i_{om}(t) \end{bmatrix} = \begin{bmatrix} I_{o1} \sin(\omega_o t + \phi_{o1}) \\ I_{o2} \sin(\omega_o t - 2\pi/m + \phi_{o2}) \\ \cdot \\ I_{op} \sin(\omega_o t - (p-1)2\pi/m + \phi_{op}) \\ \cdot \\ I_{om} \sin(\omega_o t - (m-1)2\pi/m + \phi_{om}) \end{bmatrix} \qquad (2\text{-}16)$$

where $\omega_o = 2\pi f_o$ is the output angular velocity, I_{op} ($p = 1,2,\ldots m$) is the amplitude of each of the output current, and ϕ_{op} is a phase angle of the p-th output current wave.

The input current equation may be written in the following form:

$$i_{Iq}(t) = \left[h_{1q}(t)\ h_{2q}(t)\ \ldots\ldots\ h_{nq}(t)\right] \begin{bmatrix} i_{o1}(t) \\ i_{o2}(t) \\ . \\ i_{om}(t) \end{bmatrix}$$

$$= I_I \sin(\omega_I t - (q-1)2\pi/n + \phi_I) + \sum_{L=1}^{\infty} I_{EL} \sin(\omega_{EL} t + \phi_{EL}) \qquad (2\text{-}17)$$

where the first term of Equation (2-17) represents the "Fundamental Input Current" component which has the frequency of the ac source. The second term represents the "Extrabasal (unwanted) Input Current" components have frequencies that are not integrally related to the fundamental component. I_I and I_{EL} are the amplitudes of the fundamental and extrabasal current components, $\omega_{EL} = 2\pi f_{EL}$ and $\omega_I = 2\pi f_I$ are the angular velocity and ϕ_I and ϕ_{EL} are the phase angle. The quantities and performance of the input current waveform, measured at the input terminal, may be expressed by means of "Input Current Wave Indices". The frequency ratio ν_{EL} of the significant unwanted component f_{EL} to the wanted input component f_I of a frequency changer is defined as

$$\nu_{EL} \triangleq \left| f_{EL} / f_I \right| \qquad L = 1,2,\ldots \qquad (2\text{-}18)$$

The amplitude ratio γ_{EL} of the significant unwanted components I_{EL} to the desired input current I_I of a frequency changer is defined

$$\gamma_{EL} \triangleq \left| I_{EL} / I_I \right| \qquad L = 1,2,... \qquad (2\text{-}19)$$

The ratio μ_I of fundamental to total rms input current distortion factor of a frequency changer is defined as

$$\mu_I \triangleq I_I / \left(I_I^2 + \sum_{L=1}^{\infty} I_{EL}^2\right)^{\frac{1}{2}} \qquad (2\text{-}20)$$

which is a ratio masures the amount of harmonic currents flowing in the system. The input displacement factor δ_I of a frequency changer is defined

$$\delta_I \triangleq \cos \phi_I \qquad (2\text{-}21)$$

where δ_I is the ratio of the real input power, in watts, to the apparent power of the fundamental wave, in volt-ampers. It is a measure of the amount of the phase displacement between the system voltage and the fundamental of the current at the input. It shows the relationship between the real and reactive input power. Consequently the input displacement factor cos ϕ_I of a single-phase output frequency changer is substantially lower than the output load displacement factor.

The input power factor λ_I of a frequency changer is usually defined as the product of distortion factor and displacement factor as

$$\lambda_I \triangleq \mu_I \, \delta_I \tag{2-22}$$

where λ_I is the ratio of the real input power, in watt, to the apparent power, in rms volt-ampers (input phase voltage and the total rms input current). It shows the relationship between the real power and the reactive input power plus extrabasal input power. Referring to Equation (2-7), the performance of above input current indices are entirely dependent upon the elements (existence functions) of the existence matrix [H(t)].

2-2 WAVEFORM FABRICATION OF CDFFC

In the frequency changer, each output voltage wave is composed of segments of the input voltage waves and the time duration of each segment is completely determined by the corresponding two sets of complementary existence functions (h_{pq} and $h_{pq\pi}$). For a particular waveshape construction, the existence function allows a sinusoidal mean voltage to be generated in which the waveform is composed of half-cycle sections of complementary positive-type and negative-type voltage waves. This type of waveform fabrication referred to as "Consecutive Composite Waves", is illustrated in Figure 2-3.

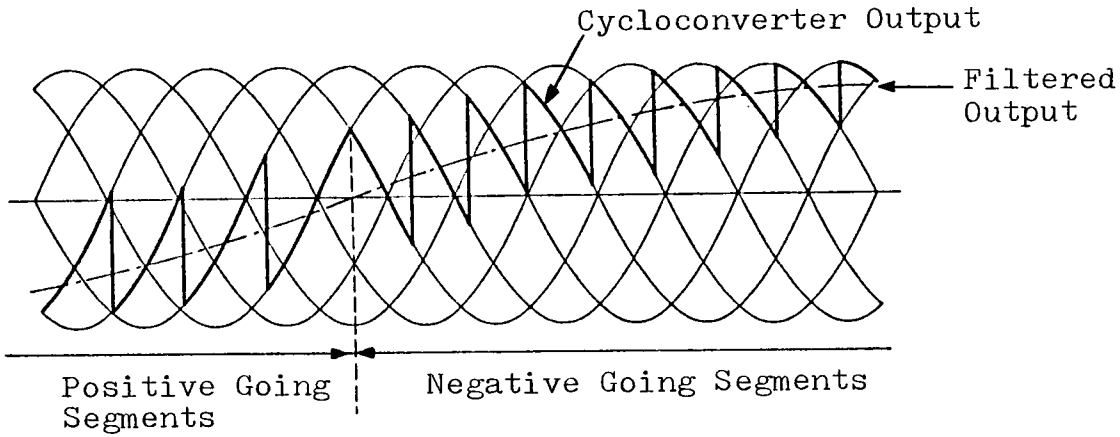


Figure 2-3. A consecutive composite waveform.

2-2-1 Build-up of Output Voltage Wave

The shape of the waveform shown in Figure 2-3 is obtained by piecing together the positive-type and negative-type waves. By shifting the points (not the phase angle) of change-over between positive going segments and negative going segments with respect to a reference point, the output waveform may be of any desired form. A consecutive composite waveform generally contains the subfrequency (unwanted) components with frequencies that are lower than the wanted output frequency [Refer to Figure 3-2]. The amplitude of the subfrequency components will become relatively low if the f_O/f_I ratio is small. For this reason, the allowed amplitude of the subfrequency component will limit the maximum output frequency f_O. For a P-pulse converter this limit is generally not higher than

$$\max\left(f_O \,/\, f_I\right) = (P - 2) \,/\, P \qquad (2\text{-}23)$$

where P is a pulse number. For example, in three-pulse circuit max $f_O = (1 \,/\, 3) f_I$.

The mathematical expression of different "Sinusoidal Mean" waveforms from the positive-type v_O and negative-type $v_{O\pi}$ complementary waveforms is a basic concept for understanding waveform fabrication and is shown in Figure

2-4. In Figure 2-4(A) and (B) the mathematical modulating function M(t) is now introduced to aid in describing the generation of a time-dependent function that forms the output wave. It describes the angular variation of the existence functions h(t) and $h_{\pi}(t)$ with respect to their quiescent angular position and defined the operation of the power switches in the frequency changer circuit. v_{ow} is the wanted filtered output voltage, and v_o is the cycloconverter output voltage. $\Omega(t)$ is just differentiate of M(t).

2-2-1-1 With Triangular Wave Modulating Function M(t)

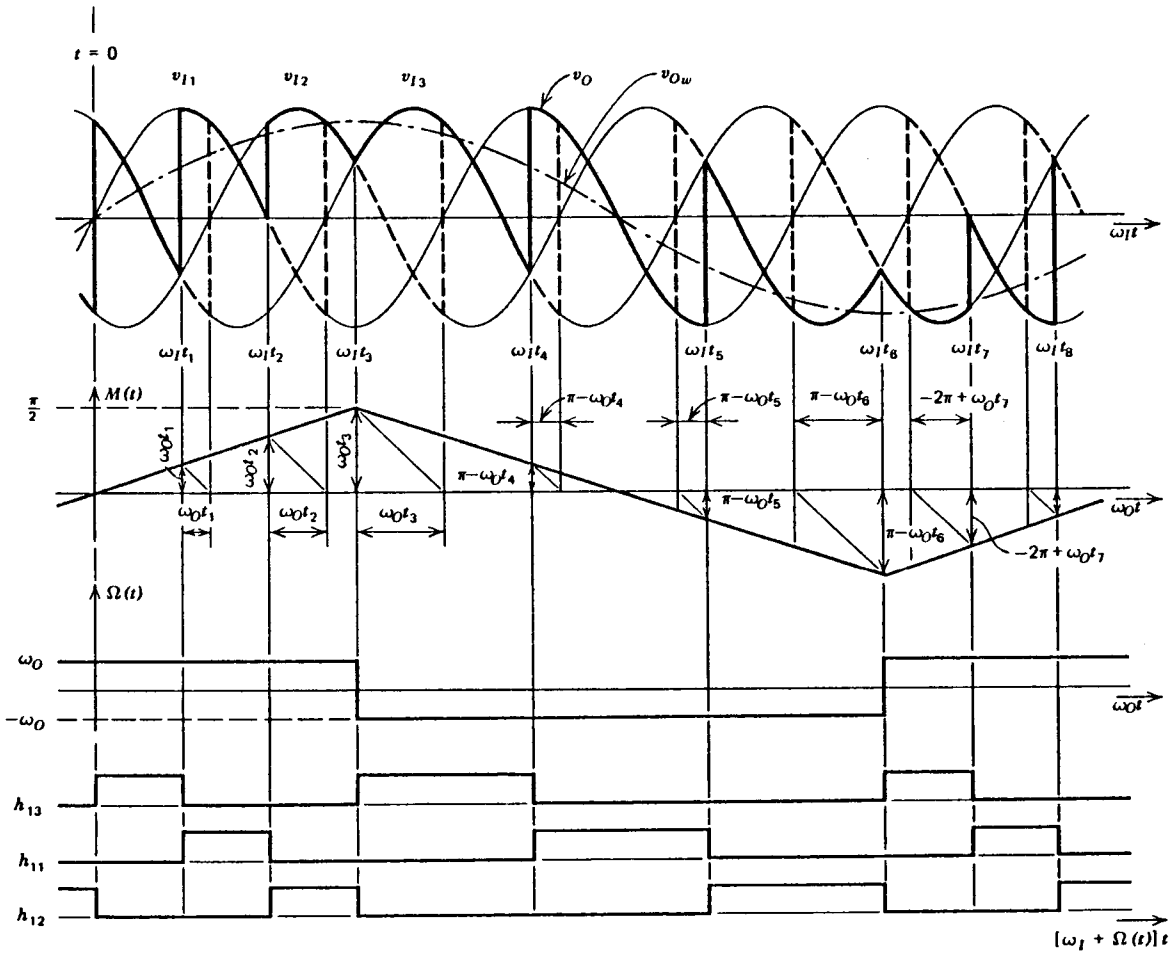
The phase shift of each existence functions are controlled by the cosine wave crossing control method [Refer to Figure 2-7] that is the basic concept of controlling the firing delay angle with related to the modulating function. The simplest form of the modulating function M(t) may be written as a triangular function of time,

$$M(t) = \omega_o t + \psi \qquad (2\text{-}24a)$$

or

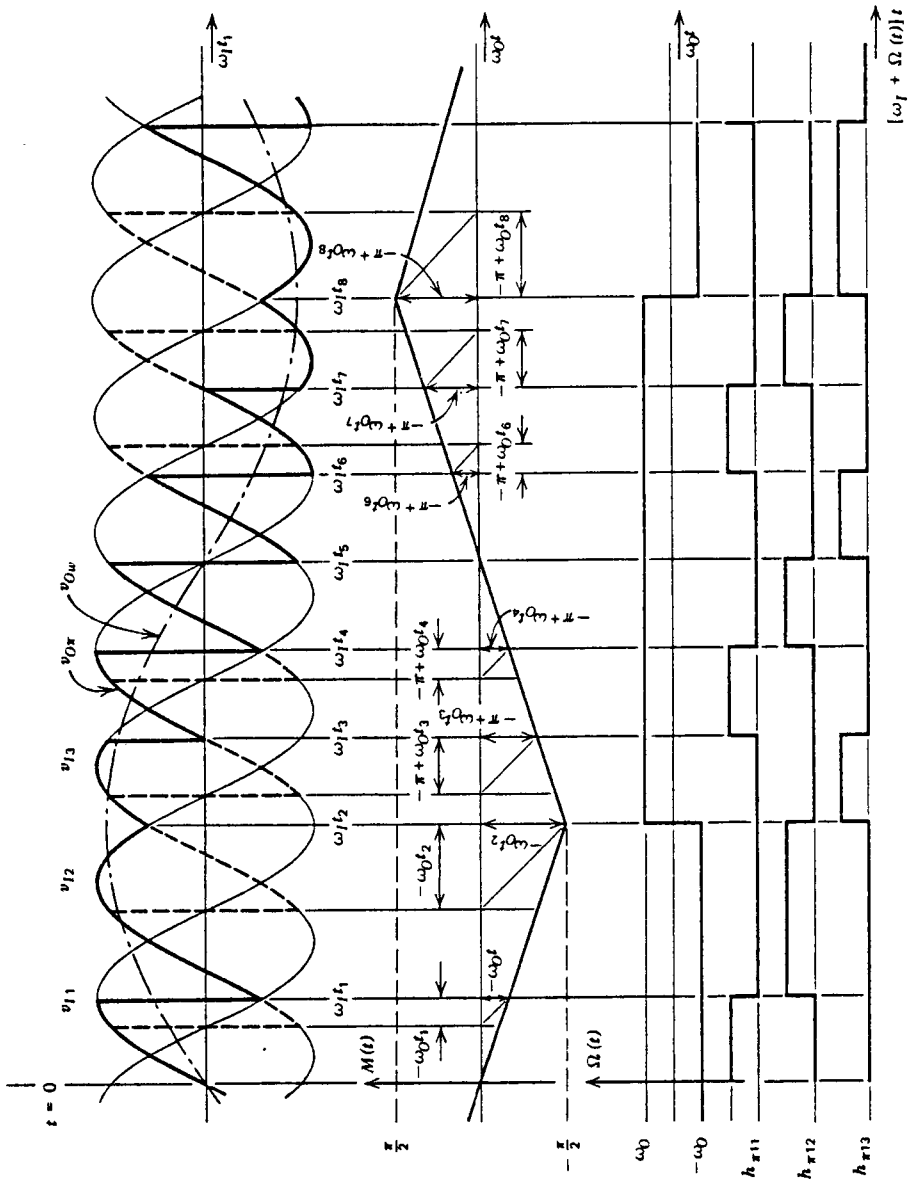
$$M(t) = \sin^{-1}(\sin(\omega_o t + \psi)) \qquad (2\text{-}24b)$$

where ω_o is a wanted output frequency and ψ is a constant of arbitrary phase [Referred to Figure 2-4, $\psi = 0$ with repect to the reference point]. The operating range is defined as



A. Positive-type Waveform

Figure 2-4. Two complementary waveform generated by the triangular modulating function.



B. Negative-type Waveform

Figure 2-4. (Continued)

$$-\pi/2 \leq \sin^{-1}(r \sin(\omega_o t + \psi)) \leq \pi/2 \qquad (2\text{-}25)$$

where r is the output ratio defined by $r = (V_o / \max V_o)$ where $0 \leqslant r \leqslant 1$. The instantaneous angular shifting of the consecutive composite waveform is controlled by diagonal existence matrices defined as $[E(\rho)]$ and $[E_\pi(\rho)]$ and are function of switching angle ρ. The operating range of the angle of modulating function M(t) is $-\pi \leqslant \rho \leqslant \pi$ which is measured by the angular frequency ω_o at the output. It is equivalent to varying the commencement and/or duration of the conduction interval of the corresponding power switches by h(t) and angle ρ in a frequency changer circuit. These two periodic existence functions $E(\rho)$ and $E_\pi(\rho)$ shown in Figure 2-5 are defined as follows:

$$E(\rho) = \begin{cases} 1 & -\rho < \omega_o t \leqslant \pi - \rho \\ 0 & \pi - \rho < \omega_o t \leqslant 2\pi - \rho \end{cases} \qquad (2\text{-}26)$$

and

$$E_\pi(\rho) = \begin{cases} 0 & -\rho < \omega_o t \leqslant \pi - \rho \\ 1 & \pi - \rho < \omega_o t \leqslant 2\pi - \rho \end{cases} \qquad (2\text{-}27)$$

Equation (2-26) and (2-27) are single valued periodic functions which may be represented by a Fourier series:

$$E(\rho) = \frac{1}{2} + \frac{2}{\pi} \sum_{m=1}^{\infty} \frac{1}{2m-1} \sin((2m-1)(\omega_o t + \rho)) \qquad (2\text{-}28)$$

and

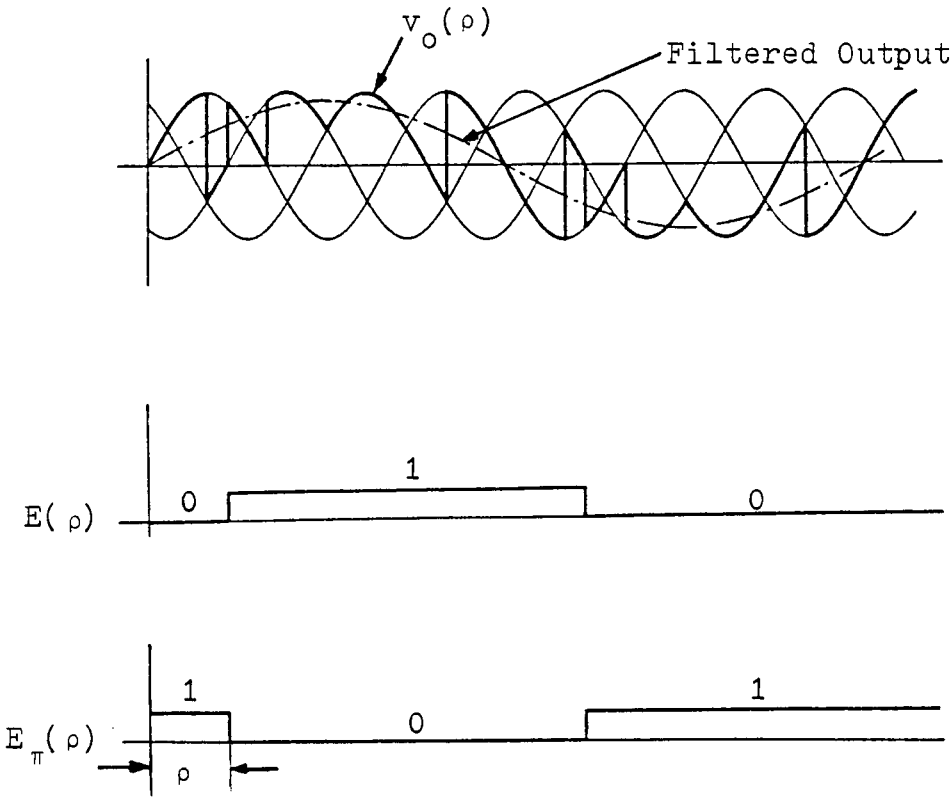


Figure 2-5. Two periodic existence functions control the output waveform fabrication.

$$E_{\pi}(\rho) = \frac{1}{2} - \frac{2}{\pi} \sum_{m=1}^{\infty} \frac{1}{2m-1} \sin((2m-1)(\omega_o t + \rho)) \qquad (2\text{-}29)$$

The output voltage wave $v_o(\rho)$ is the arithmetic mean of two complementary voltage waveforms v_o and $v_{o\pi}$ which can be shifted its wave angle by the corresponding given alternate periodic functions $E(\rho)$ and $E_{\pi}(\rho)$, that is,

$$v_o(\rho) = E(\rho)v_o + E_{\pi}(\rho)v_{o\pi} \qquad (2\text{-}30)$$

Substituting the above Equation (2-30) into (2-4), the following expression is given for single-phase three-pulse output.

$$[v_o(\rho)] = \left([E(\rho)][H] + [E_{\pi}(\rho)][H_{\pi}]\right) \begin{bmatrix} v_I \end{bmatrix} \qquad (2\text{-}31a)$$

or

$$v_o(\rho) = \Big(E(\rho)[h_{11}\ h_{12}\ h_{13}] + E_{\pi}(\rho)[h_{11\pi}\ h_{12\pi}\ h_{13\pi}]\Big) \begin{bmatrix} v_{I1} \\ v_{I2} \\ v_{I3} \end{bmatrix} \qquad (2\text{-}31b)$$

Thus $E(\rho)[H]$ and $E_{\pi}(\rho)[H_{\pi}]$ are the ideal control functions that express the "Shape" of the output wave and the "Position" of output phase angle. For a three-phase output, two periodic functions $E(\rho)$ and $E_{\pi}(\rho)$ may be written in the matrix form as follows:

$$E(\rho) = \begin{bmatrix} E_1(\rho) & 0 & 0 \\ 0 & E_2(\rho) & 0 \\ 0 & 0 & E_3(\rho) \end{bmatrix} \tag{2-32}$$

and

$$E_\pi(\rho) = \begin{bmatrix} E_{1\pi}(\rho) & 0 & 0 \\ 0 & E_{2\pi}(\rho) & 0 \\ 0 & 0 & E_{3\pi}(\rho) \end{bmatrix} \tag{2-33}$$

There are two components including wanted and unwanted frequencies appearing at the output waveform. The wanted component of the output wave is defined as its output component contains only the wanted frequency, and the unwanted components contain output components in addition to the wanted component. The maximum voltage of the wanted frequency component of the output voltage wave is given

$$\max v_o = S\ (3\sqrt{3}V_I\ /\ \pi) = \max v_d \tag{2-34}$$

It is dependent on the pulse group number S of the power converter. Max v_d is the maximum amplitude of a steady-state voltage that is equal to the maximum value of a wanted component voltage. S is the number of pulse groups in series or cascade connection in each output phase. For example a single-phase three-pulse circuit [Referred to Figure 2-2(A)] is effectively a series connection of one three-pulse group, for which S = 1. The unwanted frequency

components of the output wave has a frequency spectrum related to pulse number as

$$f_U = Pkf_I + (n - 1)f_o \qquad (2\text{-}35)$$

where P is any pulse number from one to infinity, k is any integer from one to infinity, for Pk odd n is any odd integer from one to infinity, and for Pk even n is any even integer from two to infinity [Refer to Figure 3-2]. Equation (2-36) is derived from Equation (2-30) relates the modulating function $M(t) = \sin^{-1}(r \sin\omega_o t)$, and the two complementary waves v_o and $v_{o\pi}$ in terms of the input and output frequencies as shown in [1] and [2].

$$
\begin{aligned}
\text{(a)}\quad & v_O(\rho) = \frac{3\sqrt{3}}{2\pi} V_I \left\{ \sin(\omega_O t + \psi) \right. \\
& + \sum_{k=1}^{\infty} \left(\frac{\sin\{[3k\omega_I + (3k \pm 1)\omega_O]t + (3k + 1)\psi\}}{2(3k \pm 1)} \right. \\
& \left. \left. - (-1)^{3k} \frac{\sin\{[3k\omega_I - (3k \pm 1)\omega_O]t - (3k \pm 1)\psi\}}{2(3k \pm 1)} \right) \right\}
\end{aligned}
$$

$$
\begin{aligned}
\text{(b)}\quad & - \frac{3\sqrt{3}}{\pi^2} V_I \sum_{k=1}^{\infty} \sum_{m=1}^{\infty} \frac{1}{2m - 1} \\
& \times \left\{ 2A_{6k,0}(\pm\cos\{[6k\omega_I \pm (2m - 1)\omega_O]t \pm (2m - 1)\rho\}) \right. \\
& + \sum_{n=1}^{\infty} \left(A_{6k,2n} \right. \\
& \quad \times (\pm\cos\{[6k\omega_I \pm \{2(n + m) - 1\}\omega_O]t \pm (2m - 1)\rho \pm 2n\psi\} \\
& \quad \mp \cos\{[6k\omega_I \pm \{2(n - m) + 1\}\omega_O]t \mp (2m - 1)\rho \pm 2n\psi\}) \\
& + B_{[3(2k-1)],(2n-1)} \\
& \quad \times (\cos\{[3(2k - 1)\omega_I \pm 2\{(n + m) - 1\}\omega_O]t \\
& \qquad \pm (2m - 1)\rho \pm (2n - 1)\psi\} \\
& \quad - \cos\{[3(2k - 1)\omega_I \pm 2(n - m)\omega_O]t \\
& \qquad \left. \left. \mp (2m - 1)\rho \pm (2n - 1)\psi\}) \right) \right\}
\end{aligned}
$$

(2-36)

where $A_{6k,0}$, $A_{6k,2n}$, and $B_{[3(2k-1)],(2n-1)}$, k = 1,2,3,..., n = 1,2,3,... are the numerical values of the general coefficients of the harmonic series. The dominant terms of the amplitudes $A_{6k,2n}$ and $B_{[3(2k-1)],(2n-1)}$ are summarized with numerical values in Table A.1 and A.2 in the Appendix. Part (a) in Equation (2-36) shows that two components are in phase with each other, but part (b) shows that they are out of phase. At appropriate values of integer n and m, some components may repeatedly have same frequencies and amplitudes but with different phase angles and either in phase or out of phase with each other at that instant. Therefore the resulting amplitudes at the frequencies of the output waveform are to sum up other components, including wanted and unwanted components together, become total component.

The resulting frequencies of the unwanted components can be divided into one of the two main groups called "Sum" and "Difference" frequencies.

$$\omega_{U1} = \begin{cases} 3k\omega_I + (3k \mp 1)\omega_o \\ 3k\omega_I - (3k \mp 1)\omega_o \end{cases} \qquad (2\text{-}37)$$

and

$$\omega_{U2} = \begin{cases} 3(2k - 1)\omega_I \pm (2L - 1)\omega_o \\ 6k\omega_I + 2L\omega_o \end{cases} \qquad (2\text{-}38)$$

where k = 1,2,3,..., n = 1,2,3,..., m = (n - 1) = 1,2,3,...

For each k in Equation (2-36) there are four corresponding ω_{U1}, and an infinite number of ω_{U2} components when L is varying. The frequencies of ω_{U1} are the sum of the spectra placed in part (a), and the frequencies of ω_{U2} are the difference of the spectra placed in (b). Therefore these two groups of components are independent of each other.

A consecutive composite waveform, with different modulating angles synthesized from Equation (2-36) are shown in Figure 2-6 at frequency ratio $f_o/f_I = 1/3$.

2-2-1-2 With Amplitude-Dependent Modulating Function

In the previous investigation the amplitude of the output waveform is entirely dependent upon the input wave. In order to control the amplitude of output waveform, another mathematical modulating function M(r,t) will now be introduced [compare to Equation (2-24)] which consists of two variables the "Frequency" and "Amplitude" of the sinusoidal mean output voltage. This amplitude-dependent frequency modulation function expressed in radians is given, for $0 \leqslant r \leqslant 1$

$$M(r,t) = \sin^{-1}(r \sin(\omega_o t + \psi)) \qquad (2\text{-}39)$$

where ψ is an arbitrary phase angle, assigned the value zero for convenience; t is the time, and r is the output voltage ratio defined as

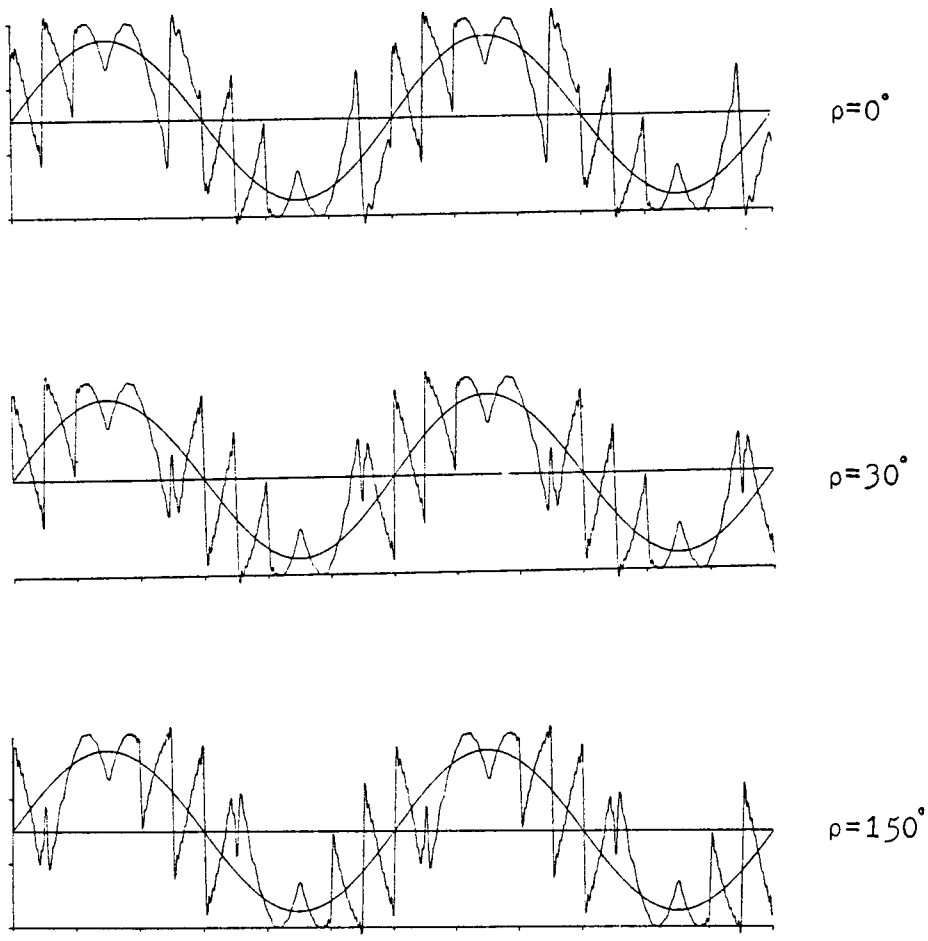
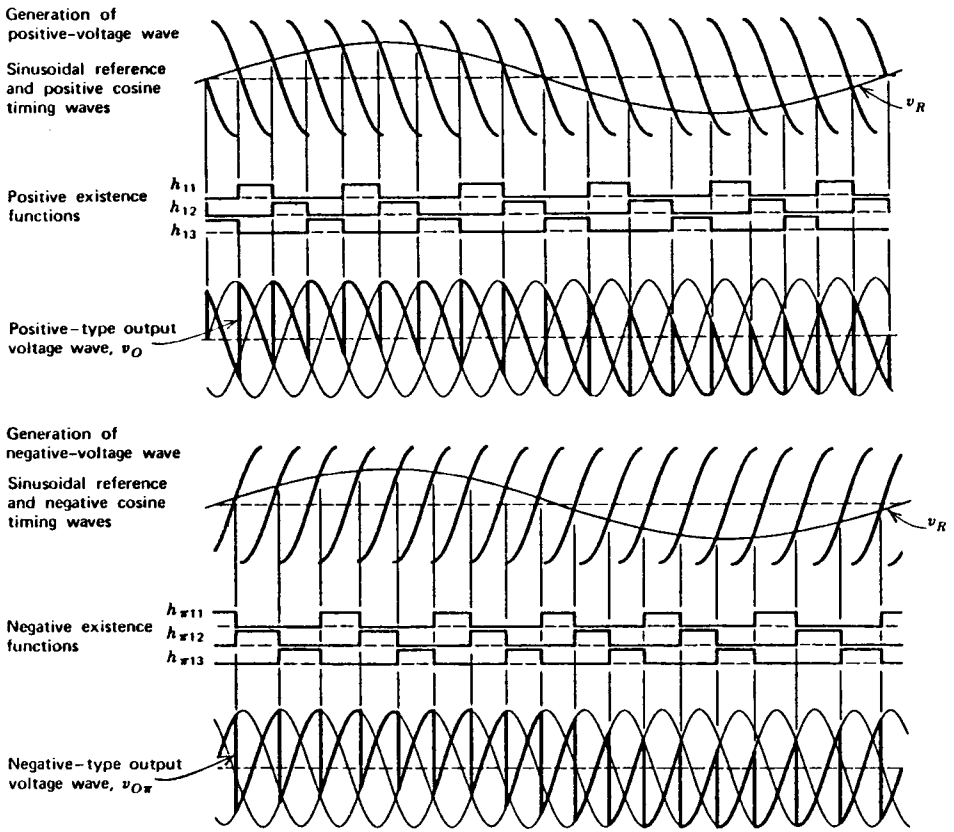


Figure 2-6. A consecutive composite waveform with different modulating angles.

$$r = V_o / \max V_o \qquad (2\text{-}40)$$

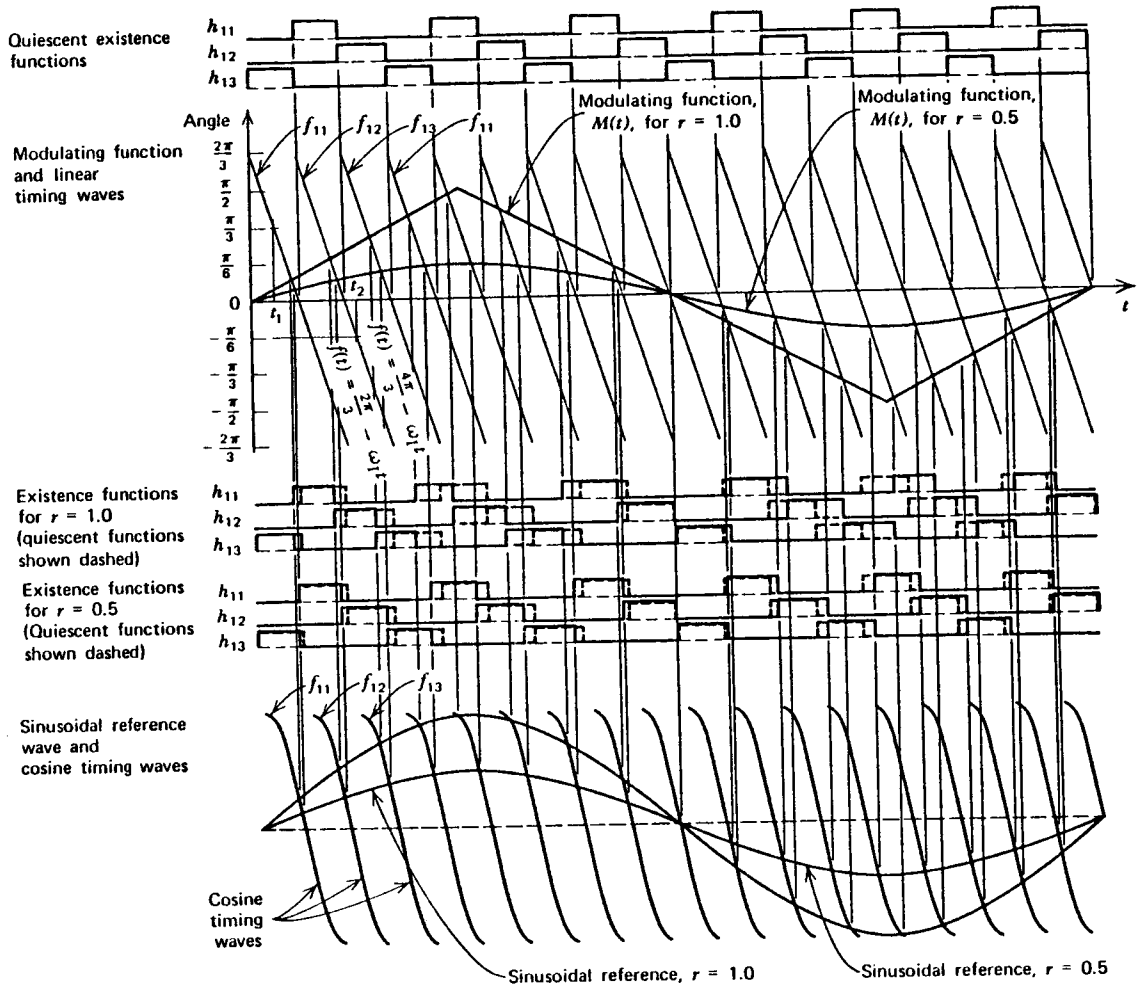
where V_o is the amplitude of a desired output component, and max V_o is the peak value of the output component.

Figure 2-7 shows that a modulating function affects the variation of two complementary output waves, by the "Cosine Wave Crossing Control" method. The relationship between the mean dc output voltage v_o and the reference voltage v_R is a linear function when comparing the cosine timing wave v_T (i.e. f_{11}, f_{12}, f_{13}) and the reference voltage v_R at the two waves interaction point. The cosine of the firing angle α is proportional to the reference voltage (i.e. $v_R/v_o = \cos\alpha = v_R/v_T$). The modulating function M(r,t) of Equation (2-39) represents the required angular deviation of the corresponding quiescent existence functions h(t) at any given time. Each zero output point is determined by the crossing (intersection) point of a correspondind timing wave v_T with the reference wave v_R. These six timing waves, consisting of three positive and negative banks, are opposite half-cycle sections of sine waves. These sine waves are synchronized to the input voltages with a phase relationship, such that at zero reference point the mean output voltages v_o and $v_{o\pi}$ is zero. The reference wave shown in Figure 2-7 is the resulting output wavform given as follows:



A. Positive-type and Negative-type Waveform Generation

Figure 2-7. Cosine wave crossing control method applied to a cyclo-converter.



B. Variation of the Sinusoidal Reference Affects the Firing Instants

Figure 2-7. (Continued)

$$v_R = v_T(r \sin \omega_o t) \tag{2-41}$$

The mathematical proof of the control ability of the sinusoidal mean output voltage with modulating function M(r,t) is given in [1] and [2]. The following equation is obtained for the positive-type output waveform,

$$\text{(a)} \quad \left[v_O(r) = \frac{3\sqrt{3}}{2\pi} V_I \left\{ r \sin \omega_O t + \sum_{k=1}^{\infty} 2A_{[3(2k-1)],0} \sin\{3(2k-1)\omega_I t\} + \sum_{k=1}^{\infty} \left(\sum_{n=1}^{2n=3(2k-1)+1} A_{[3(2k-1)],2n} \sin\{[3(2k-1)\omega_I \pm 2n\omega_O]t\} \pm \sum_{n=1}^{2n-1=6k+1} B_{6k,(2n-1)} \sin\{[6k\omega_I \pm (2n-1)\omega_O]t\} \right) \right\} \right.$$

$$\text{(b)} \quad \left[+ \frac{3\sqrt{3}}{2\pi} V_I \left\{ \sum_{k=1}^{\infty} 2A_{6k,0} \sin 6k\omega_I t + \sum_{k=1}^{\infty} \sum_{n=1}^{\infty} \left(A_{6k,2n} \sin\{[6k\omega_I \pm 2n\omega_O]t\} \pm B_{[3(2k-1)],(2n-1)} \sin\{[3(2k-1)\omega_I \pm (2n-1)\omega_O]t\} \right) \right\} \right. \tag{2-42}$$

The above equation is expressed in two parts, (a) and (b). For positive-type output voltage, it may be rewritten using the simple form

$$v_o(r) = (a) + (b) \tag{2-43}$$

The general expression for the negative-type output may be written as

$$v_{o\pi}(r) = (a) - (b) \tag{2-44}$$

where (a) and (b) are given in Equation (2-42).

The amplitude coefficients A and B are functions of the output voltage ratio r, shown in Figure 2-8, given by the expressions

$$A_{[3(2k-1)],0} = \frac{1}{2}\left(\frac{a_{[3(2k-1)+1],0}}{3(2k-1)+1} + \frac{a_{[3(2k-1)-1],0}}{3(2k-1)-1}\right) \tag{2-45}$$

$$A_{[3(2k-1)],2n} = \frac{1}{2}\left(\frac{a_{[3(2k-1)+1],2n}}{3(2k-1)+1} + \frac{a_{[3(2k-1)-1],2n}}{3(2k-1)-1}\right) \tag{2-46}$$

$$B_{6k,(2n-1)} = \frac{1}{2}\left(\frac{b_{(6k+1),(2n-1)}}{6k+1} + \frac{b_{(6k-1),(2n-1)}}{6k-1}\right) \tag{2-47}$$

$$A_{6k,0} = \frac{1}{2}\left(\frac{a_{(6k+1),0}}{6k+1} + \frac{a_{(6k-1),0}}{6k-1}\right) \tag{2-48}$$

$$A_{6k,2n} = \frac{1}{2}\left(\frac{a_{(6k+1),2n}}{6k+1} + \frac{a_{(6k-1),2n}}{6k-1}\right) \tag{2-49}$$

$$B_{[3(2k-1)],(2n-1)} = \frac{1}{2}\left(\frac{b_{[3(2k-1)+1],(2n-1)}}{3(2k-1)+1} + \frac{b_{[3(2k-1)-1],(2n-1)}}{3(2k-1)-1}\right) \tag{2-50}$$

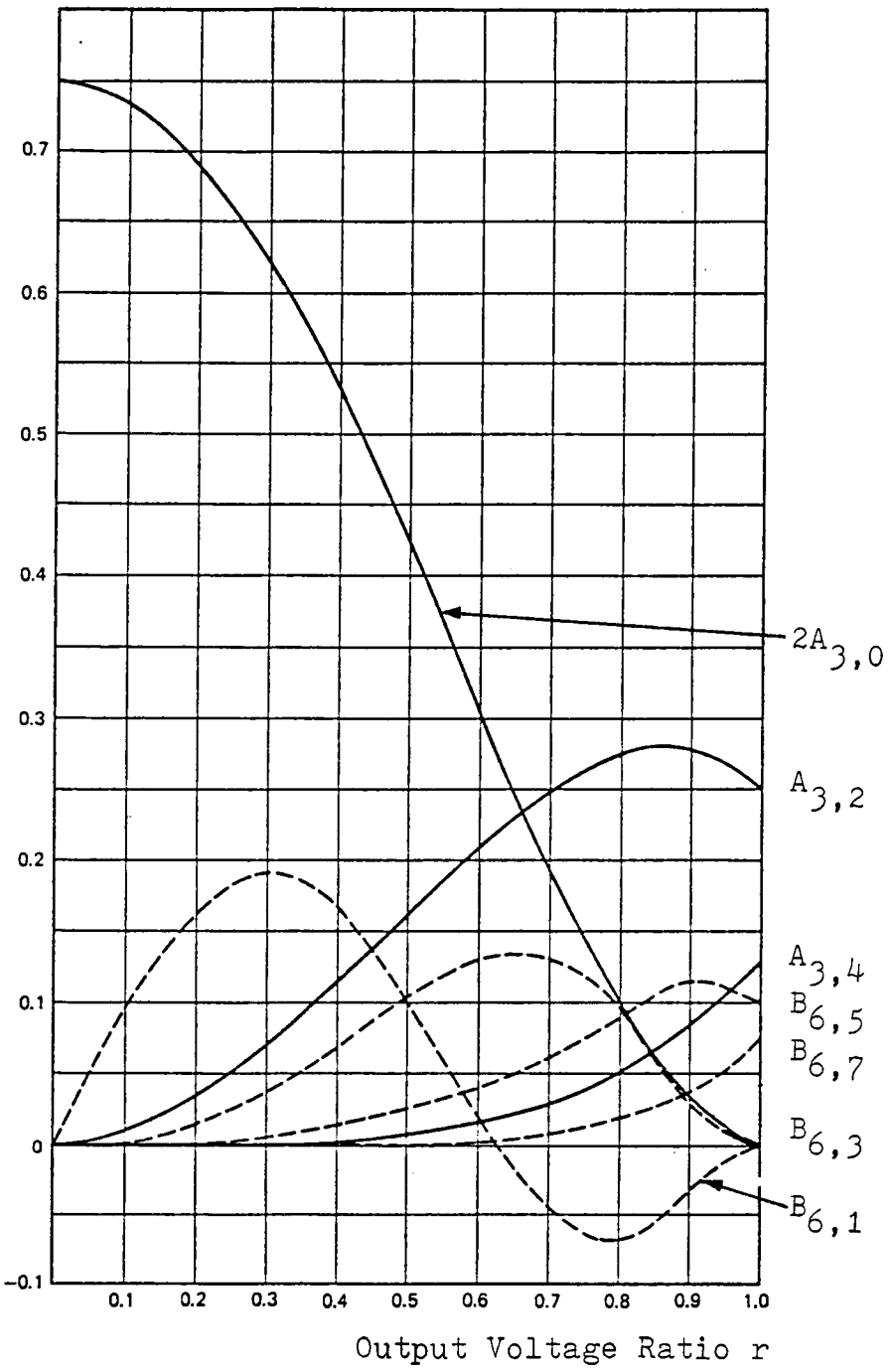


Figure 2-8. Curves showing the approximate variation of the coefficients with the output voltage ratio r.

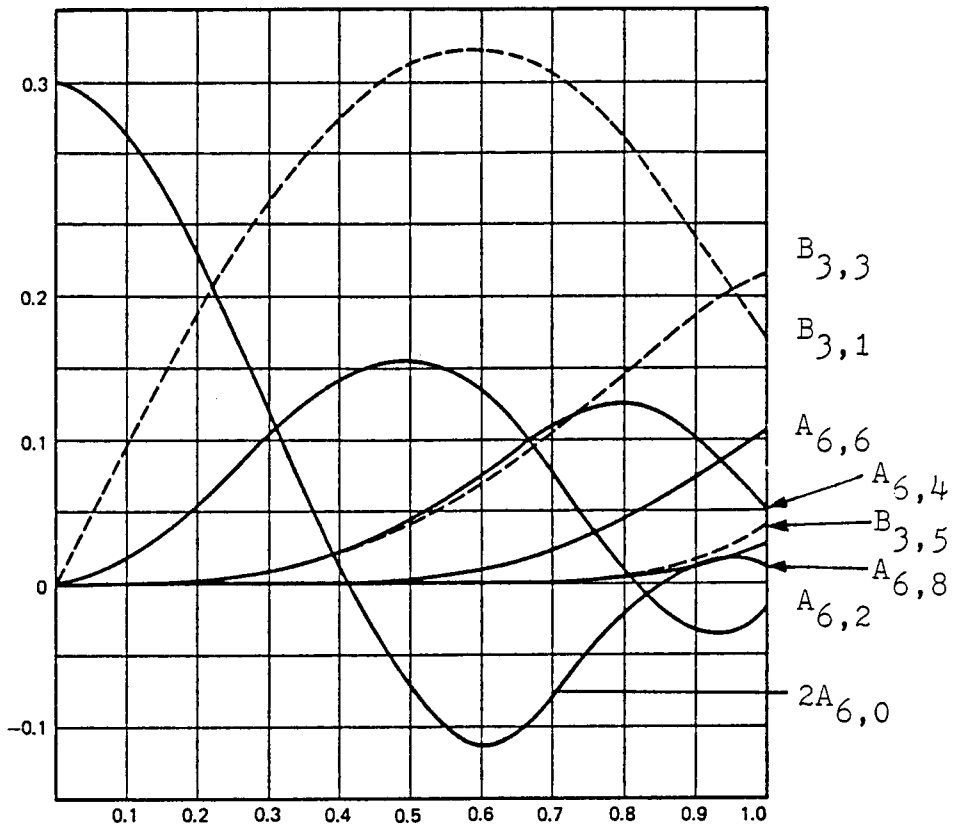


Figure 2-8. (Continued)

When r is varying, the coefficients A and B will change and will increase or decrease the output sinusoidal mean voltage. But the amplitude variation will not have a great affect upon the spectral characteristics of the output waveform. When r is approaching zero, the coefficient term $A_{3,0}$ jumps up very rapidly at that instants with frequencies of $3kf_I$, and then becomes dominate. Where r is equal to zero, the sinusoidal mean output is zero and only the components with frequencies of $3kf_I$ are present. To obtain the amplitude of each wanted or unwanted component, are added the coefficents of all terms with the same frequency. The other numerical values for a and b in the coefficient terms of the harmonic series from Equation (2-45) through (2-50) are given in Table A.3 in the Appendix.

2-2-2 Performance of Input Current Wave

To investigate the input current of the frequency changer, we assume a balanced three-phase load which output current waveforms are symmetrical. The ac input source is assumed to have zero internal impedance (neglecting the winding resistance and leakage reactance). Each current wave in a given input line is composed of segments produced by the thyristor switching function. For analytical purposes, the input current wave can be divided into two components, "Fundamental" (included real and quadrature) and "Extrabasal" component. The fundamental component of an

input current wave is defined as having an input component containing only ac input frequency f_I. The extrabasal components of an input current wave is defined as having input components in addition to a fundamental component which have frequencies that are not integrally related to the fundamental component.

Equation (2-12) may be written for an input current wave by similar description as in Equation (2-30).

$$[i_I(\rho)] = ([E(\rho)]\,[H])^T + ([E_\pi(\rho)]\,[H_\pi])^T \begin{bmatrix} i \\ o \end{bmatrix} \qquad (2\text{-}51)$$

The general expression for the three-pulse positive-type and negative-type input current waveform, related to the periodic modulating function $M(r,t) = \sin^{-1}(r \sin\omega_o t)$, is given [1] and [2], that is,

$$
\begin{aligned}
\text{(a)}\quad & \text{I}\left[i_I = \frac{\sqrt{3}}{2\pi} I_O r \cos\phi_O \sum_{p=1}^{3} \sin\{\omega_I t - (p-1)2\pi\}\right. \\
& \text{II}\left[- \frac{\sqrt{3}}{4\pi} I_O r \sum_{p=1}^{3} \sin\left((\omega_I \pm 2\omega_O)t \pm \phi_O \pm (p-1)\frac{2\pi}{3}\right)\right. \\
& \text{III}\left[+ \frac{I_O}{3} \sum_{p=1}^{3} \sin\left(\omega_O t + \phi_O - (p-1)\frac{2\pi}{3}\right)\right. \\
& \text{IV}\left[+ \frac{\sqrt{3}}{2\pi} I_O \sum_{p=1}^{3} \sum_{u=-1}^{1} \sum_{k=1}^{\infty} \left\{ \sum_{n=0}^{2n=3(2k-1)-u} \frac{a_{\{3(2k-1)-u\},2n}}{3(2k-1)-u}(\pm u)\right.\right. \right. \\
& \times \sin\left(\{[3(2k-1)-u]\omega_I \pm \omega_O\}t \pm \phi_O \mp (p-1)\frac{2\pi}{3}\right) \\
& \times \cos\left(2n\left[\omega_O t - (p-1)\frac{2\pi}{3}\right]\right) + \sum_{n=0}^{2n+1=6k-u} \frac{b_{(6k-u),(2n+1)}}{6k-u}(\pm u) \\
& \times \cos\left([(6k-u)\omega_I \pm \omega_O]t \pm \phi_O \mp (p-1)\frac{2\pi}{3}\right) \\
& \left.\left.\left. \times \sin\left((2n+1)\left[\omega_O t - (p-1)\frac{2\pi}{3}\right]\right)\right\}\right] \\
\text{(b)}\quad & \text{V}\left[+ \frac{\sqrt{3}}{2\pi} I_O \sum_{p=1}^{3} \sum_{n=0}^{\infty} a_{1,2n} \left\{ \mp \sin\left([\omega_I \pm \omega_O]t \pm \phi_O \mp (p-1)\frac{2\pi}{3}\right)\right.\right. \\
& \left.\left. \times \cos\left(2n\left[\omega_O t - (p-1)\frac{2\pi}{3}\right]\right)\right\}\right] \\
& \text{VI}\left[+ \frac{\sqrt{3}}{2\pi} I_O \sum_{p=1}^{3} \sum_{u=-1}^{1} \sum_{k=1}^{\infty} \sum_{n=0}^{\infty} \left\{ \frac{b_{[3(2k-1)-u],(2n+1)}}{3(2k-1)-u}(\pm u)\right.\right. \\
& \times \cos\left(\{[3(2k-1)-u]\omega_I \pm \omega_O\}t \pm \phi_O \mp (p-1)\frac{2\pi}{3}\right) \\
& \times \sin\left((2n+1)\left[\omega_O t - (p-1)\frac{2\pi}{3}\right]\right) + \frac{a_{(6k-u),2n}}{6k-u}(\pm u) \\
& \times \sin\left([(6k-u)\omega_I \pm \omega_O]t \pm \phi_O \mp (p-1)\frac{2\pi}{3}\right) \\
& \left.\left. \times \cos\left(2n\left[\omega_O t - (p-1)\frac{2\pi}{3}\right]\right)\right\}\right]
\end{aligned}
$$

(2-52)

and

$$i_{I\pi} = (a) - (b) \tag{2-53}$$

Part I contains the fundamental component with frequency of the input that is always in phase with the input voltage, regardless of the output phase angle. Therefore it may be said that the load consumes only real power. The amplitude of the fundamental component is not dependent on the pulse number. It will be three times larger if the three-phase load is balanced. The amplitudes of the extrabasal components are not dependent on the pulse number in part II. Because they have both frequency components of $f_I + 2f_o$ and $f_I - 2f_o$ and they will cancel each other in a balanced three-phase load. Part III has the same characteristics as part II except its components dependent on pulse number. In part IV, for single-phase output, they have nonzero amplitude and are dependent on pulse number. But they will become zero for balanced three-phase output. The amplitudes variation between zero or nonzero value are completely dependent upon the index n. For part V, they have the same characteristics as part IV except they are not dependent on pulse number. Part VI is same as part IV.

The extrabasal frequency component of a waveform, for single-phase output with other pulse number, is given

$$f_E = (Pk - 1)f_o + nf_o \qquad (2\text{-}54)$$

and

$$f_E = (Pk + 1)f_o + nf_o \qquad (2\text{-}55)$$

where P is any pulse number from one to infinity, k is any integer from one to infinity, for Pk odd n is any odd integer from one to infinity, and for Pk even n is any even integer from zero to infinity [Referred to Figure 3-5]. But for balanced three-phase output, there is three times a term (nf_o) of Equation (2-54) and (2-55).

CHAPTER 3

CONTROLLABLE DISPLACEMENT FACTOR FREQUENCY CHANGER

Consider the positive-type and negative-type complementary waveforms utilized to construct the final output waveform of the output load. The deviation of two complementary output waveforms are completely controlled by frequency changers. They can be operated and controlled to form new desired output waveforms, to satisfy given output and input performance requirements. Each frequency changer has its own operating and performance characteristics. For example, a CDFFC is one of the frequency changers that can be used in a VSCF system to control input displacement angle. It accomplishes this by shifting its final output voltage waveform from approporiately choosen alternate half-cycle sections of successive segments of the positive-type and negative-type complementary waveforms. Input displacement angle can thus be controlled regardless of the output current. Controlling the input displacement factor provides new applications such as using a frequency changer for power factor correction. A consecutive composite waveform has the unique property of providing a controlled displacement factor regardless of the load. It can be expressed as the output waveform construction of a CDFFC. Synthesize to the waveform by the modulating function has been described in the previous chapter.

The development of a consecutive composite waveform technique, corresponding to various practical modulating functions, is presented in this chapter. The important equations of output voltage and input current of a CDFFC are derived in terms of the positive-type and negative-type waves, respectively. The related performance indices are computed. They provide the solution of waveform anaysis for a CDFFC in VSCF system. Some important performance data of a CDFFC are presented in graphical and tabular form.

3-1 OUTPUT VOLTAGE CHARACTERISTICS OF A CDFFC

As has been shown, Equation (2-36) can be combined with the terms in part (a) and part (b) and rewritten in the following form:

$$v_o(\rho)=\frac{3\sqrt{3}}{2\pi}V_I\Bigg(\sin(\omega_o t+\psi)+\sum_{k=1}^{\infty}\sum_{\ell=0}^{\infty}\left(A_{[3(2k-1)],(\pm 2\ell)}(\rho)\sin\{[3(2k-1)\omega_I\pm 2\ell\omega_o]t-\psi_{[3(2k-1)],(\pm 2\ell)}(\rho)\}\right.$$
$$\left.+A_{6k,[\pm(2\ell+1)]}(\rho)\sin\{[6k\omega_I\pm(2\ell+1)\omega_o]t-\psi_{6k,[\pm(2\ell+1)]}(\rho)\}\right)\Bigg) \qquad (3-1)$$

where the normalized amplitude $A(\rho)$ and phase angle $\psi(\rho)$ are dependent upon angle ρ. The absolute values dominent components $A(\rho)$ present in Equation (3-1) are given as a function of angle ρ in Table A.4 in the Appendix. It contains the numercial values of $A(\rho)$, for $\rho = 0, \pm\pi/6, \pm\pi/3$ and $\pm\pi/2$, when L_s is varying but $k = 1$.

Using the definition given by Equation (2-9) through (2-11), the output voltage performance indices of CDFFC can be determined. The frequency ratio $\nu_{ok,L}$ of the significant unwanted component to the wanted output frequency of a CDFFC is

$$\nu_{ok,L} = \begin{cases} \left| 2L + 3(2k-1)f_I/f_o \right| \\ \left| (2L+1) + 6kf_I/f_o \right| \end{cases} \qquad (3\text{-}2)$$

The amplitude ratio $\gamma_{ok,L}(\rho)$ of the significant unwanted components to the desired output voltage of a CDFFC is

$$\gamma_{ok,L}(\rho) = \begin{cases} A_{(3(2k-1)),(\pm 2L)}(\rho) \\ A_{6k,(\pm(2L\pm 1))}(\rho) \end{cases} \qquad (3\text{-}3)$$

The total rms output voltage distortion factor μ_o of a CDFFC is

$$\mu_o = \left(\sum_{k=1}^{\infty} \sum_{L=0}^{\infty} \left(A^2_{[3(2k-1)],(\pm 2\ell)} + A^2_{6k,[\pm(2\ell+1)]} \right) \right)^{\frac{1}{2}} \simeq 0.676 \qquad (3\text{-}4)$$

The output frequency spectrum is not dependent upon of the angle ρ except at $\rho = \pm\pi/2$ [Refer to Table A.4 in the Appendix]. The difference frequency containing (2L) and (2L - 1) with the negative sign are the significant wanted frequencies in the spectrum. At discrete output to input frequency ratios it becomes zero whenever the following conditions are satisfied;

$$f_o / f_I = 3(2k - 1) / 2L \qquad (3\text{-}5)$$

and

$$f_o / f_I = 6k / (2L + 1) \qquad (3\text{-}6)$$

where k = 1,2,3,.. and L = 0,1,2,3,... Indices k and L are independent of each other and it follows that the output voltage waveform $v_o(\rho)$ appears as dc components with a relative amplitude generally present over the whole output frequency range at the above discrete output to input frequency ratios $\nu_{ok,L}$.

The amplitude of the significant unwanted components of a CDFFC is completely dependent upon of the angle ρ. For example as the angle ρ moves towards $-\pi/2$, it increases the amplitude of the components with the frequencies of the spectrum $3kf_I - (3k \pm 1)f_o$ but decreases the amplitude of the components with the frequencies of the spectrum $3kf_I + (3k \pm 1)f_o$. When the angle ρ moves towards $\pi/2$, the amplitude of the components with the frequencies of the

spectrum $3kf_I + (3k \pm 1)f_o$ is decreased. At the given angle $\rho = \pm\pi/2$, the following amplitudes with the frequencies become zero at $3(2k - 1)f_I + 2Lf_o$ for the case of $2L \neq 3(2k - 1) \pm 1$ and at $6kf_I \pm (2L + 1)f_o$ for the case of $(2L + 1 \neq 6k \pm 1)$. The output waveform contains components lower than the wanted frequency (subfrequency) whose amplitudes are varying with respect to angle ρ. The maximum output to input frequency ratio f_o/f_I limit is set for a three-pulse CDFFC. Typically it is not higher than 1/3 (e.g. 1/4 1/5 ...). The numercial value of the total rms output voltage distortion factor μ_o (dependent of ρ) of a CDFFC is only 67.6 per cent.

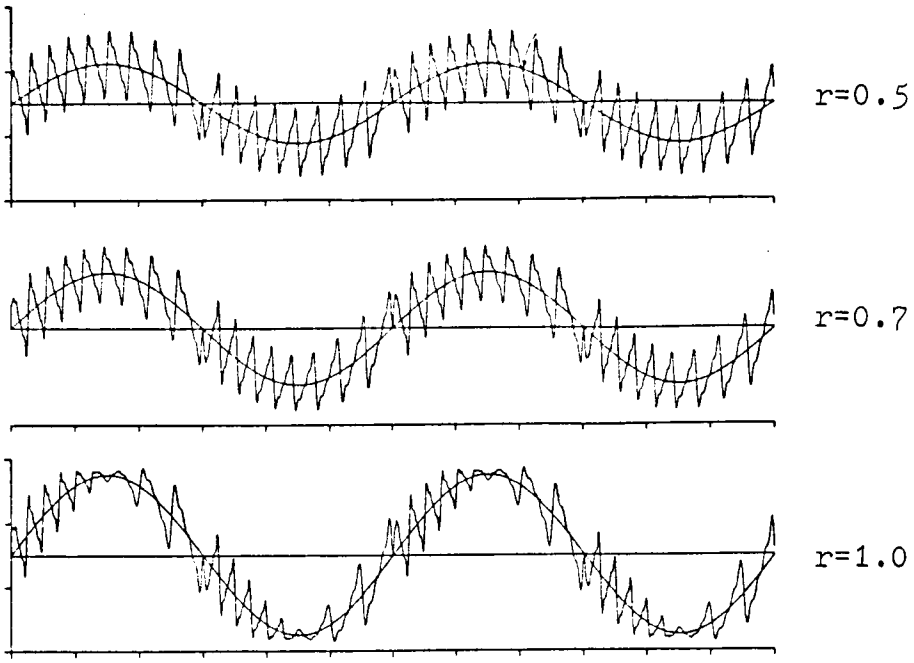
A consecutive composite output waveform $v_o(\rho)$ as an Equation (2-36) together with the output voltage ratio r (for voltage control) can be expressed as:

$$v_o(\rho,r) = a + b\left(\frac{4}{\pi}\sum_{m=1}^{\infty}\frac{1}{2m-1}\sin((2m-1)(\omega_o t + \rho))\right) \qquad (3\text{-}7)$$

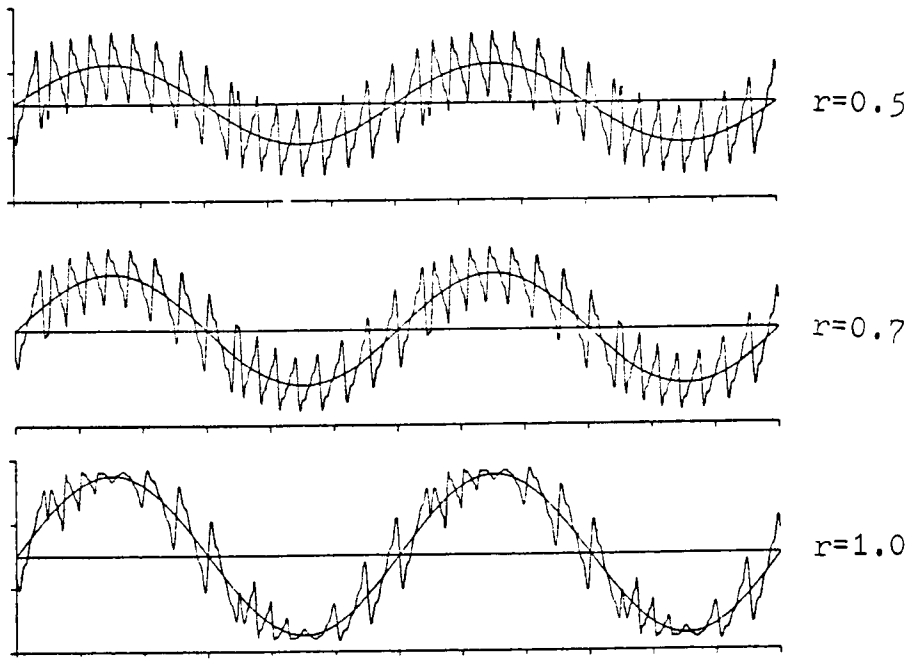
Part (a) is the dominant portion for the full voltage [Equation (2-36), r = 1] having fewer variable terms; and part (b) is the waveform structure having identical pairs of equations providing an infinite number of components of the same frequency at the time when n and m are tending to infinity. There is the final output voltage waveform of a CDFFC.

A consecutive composite output waveform of a CDFFC, with different modulating angle ρ in degrees synthesized from the terms of Equation (3-7) are shown in Figure 3-1. The CDFFC is a six-pulse converter, with different voltage ratios of r = 0.5, r = 0.7 and r = 1.0, at frequency ratio $f_o/f_I = 1/3$. The frequency spectrum of the sinusoidal mean output voltage remains independent of the output voltage ratio when it is in the range $0 \leqslant r \leqslant 1$. The amplitude of the desired output voltage does not restrict the output to input frequency ratio f_o/f_I. If the output voltage ratio is out of the normal operating range e.g. $r \geqslant 1$, the wanted component of the output waveform will be distorted. The instantaneous deriviation of the output waveform is quite small and this variation can be ignored. The numercial value of the total rms distortion factor μ_o may be assumed a constant in all cases. As the output voltage ratio approaches infinity, the output waveform becomes a square wave.

To further investigate the unwanted components in the output voltage waveform of a CDFFC, the graphical chart shown in Figure 3-2 is presented. It shows the spectrum of the first few terms of the unwanted output frequency components. The plot is the ratio of the unwanted frequency, f_U/f_I, versus the output to input frequency ratio, f_o/f_I for value of Pk up to 12 [Refer to Equation (2-35)]. In the chart the dashed line shows the wanted

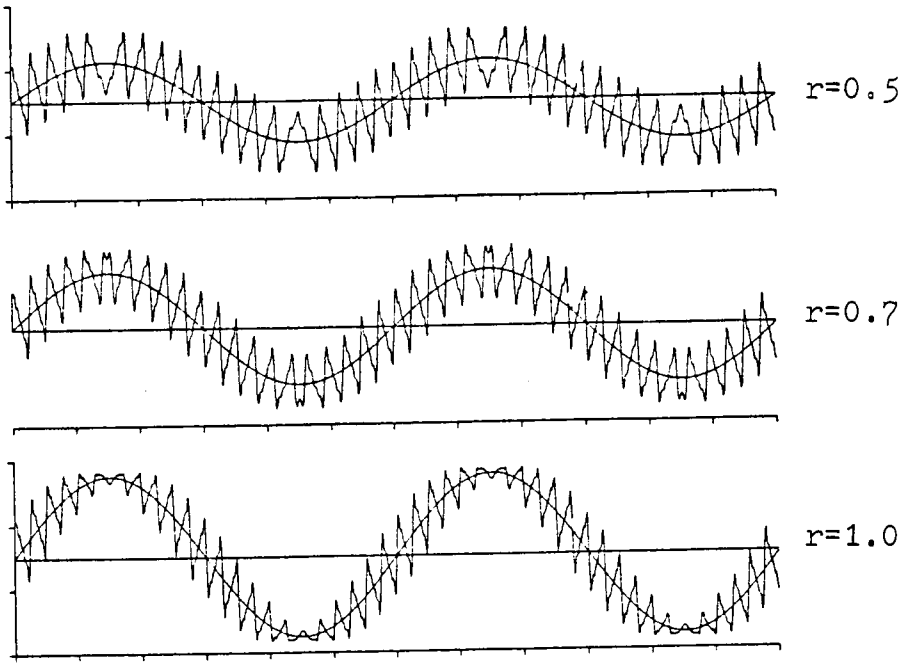


A. Output Waveforms of a Six-pulse Converter at $\rho=0^{\circ}$



B. Output Waveforms of a Six-pulse Converter at $\rho=-30^{\circ}$

Figure 3-1. Typical consecutive composite output waveforms of a CDFFC, with different modulating angle at $f_I=3f_o$.



C. Output Waveform of a Six-pulse Converter at $\rho = 90^{\circ}$

Figure 3-1. (Continued)

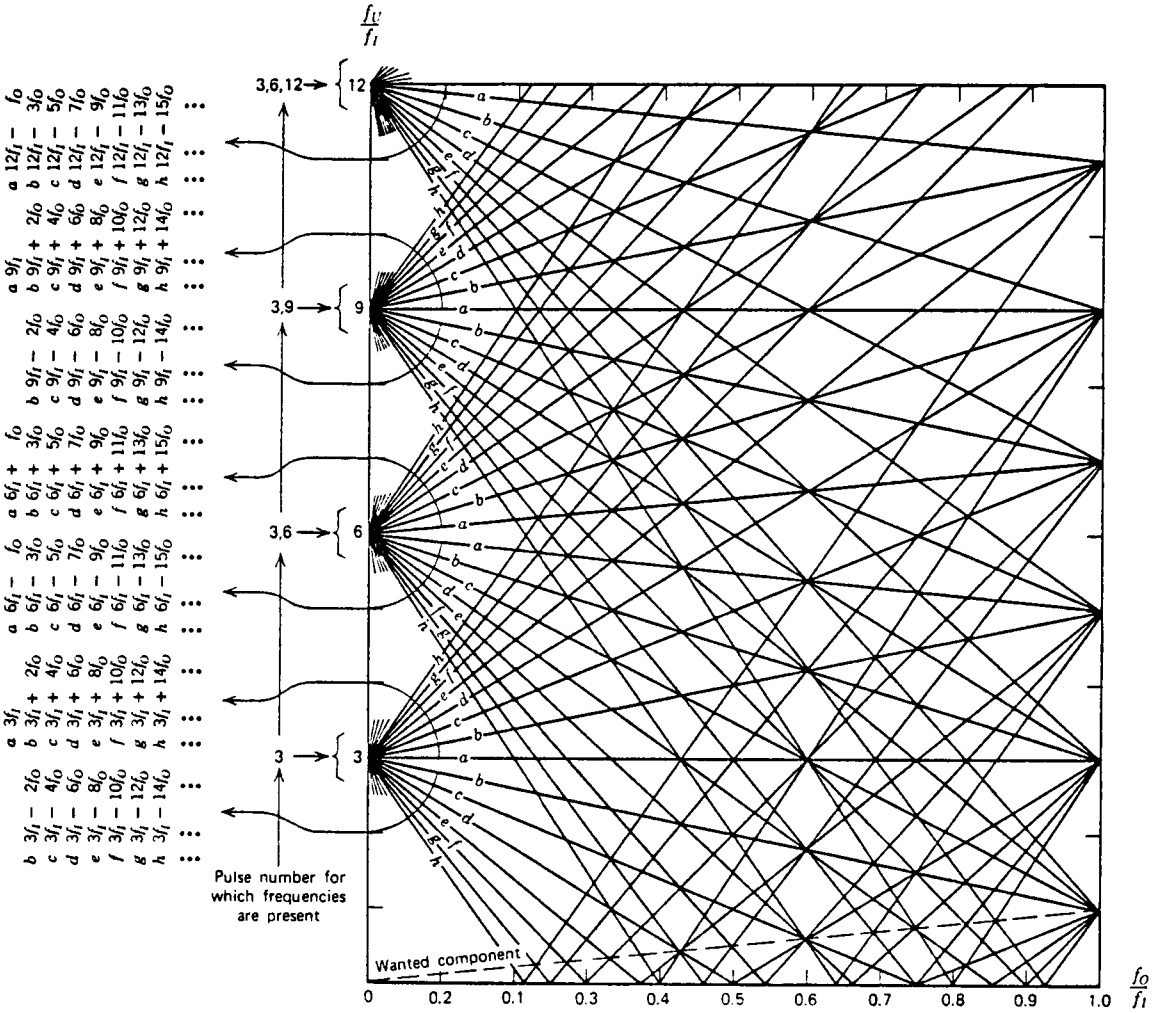
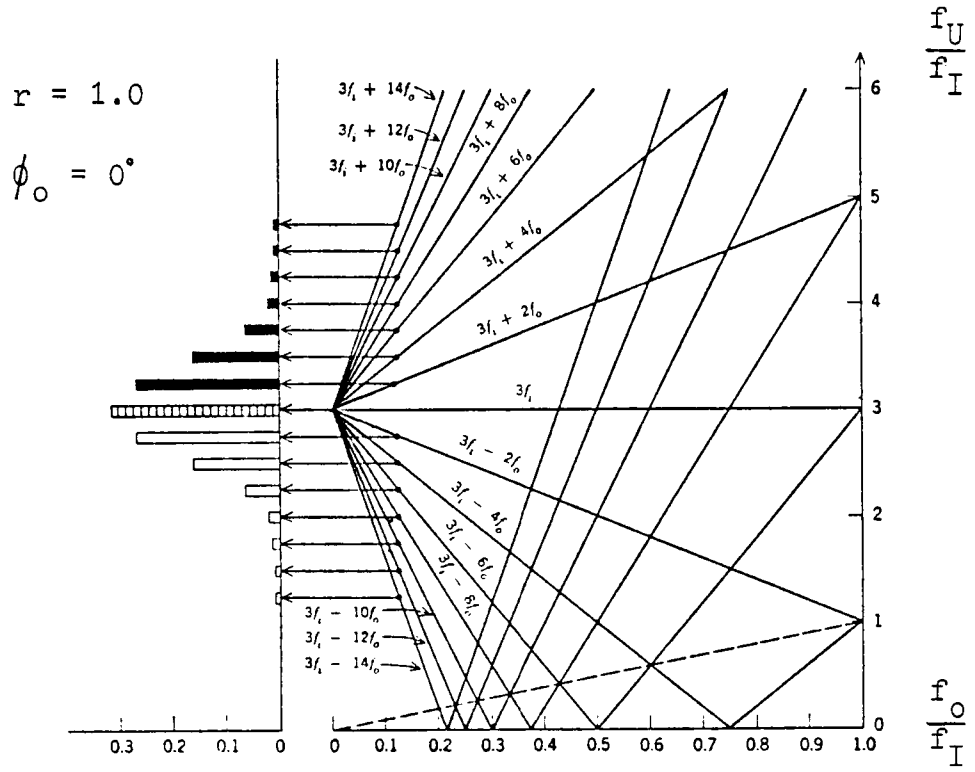


Figure 3-2. Distribution of the unwanted components in the output voltage waveform of a CDFFC.

frequency component. All unwanted frequencies below/above this line are "Subharmonic Frequencies"/"Superharmonic Frequencies". Increasing the output to input frequency ratio f_o/f_I, increases the separation between two lines of individual member of unwanted frequency. If the output to input frequency ratio f_o/f_I is too high [Referred to Figure 1-12], the output wave will deteriorate. Some unwanted frequency components (including zero frequency and some subharmonic components) close to the wanted frequency component can not be filtered out by the output filter. Thus an excessive harmonic current flows in the circuit. However using a closed loop negative feedback network, the harmonic current can be suppressed. There are several harmonic frequencies that have the same value as one another and possibly may have the same value as the wanted frequency. But the relative amplitude of those harmonic frequencies are small compared to the wanted frequency and do not affect the wanted frequency component. The output frequencies given by $f_o = 3f_I/(2n + 1)$ have only odd harmonics present at all half-cycles of the output voltage wave. But the output frequencies given by $f_o = 3f_I/2n$ have both odd and even harmonics present at all complete cycles of the output voltage wave.

Figure 3-3 shows the distribution of unwanted output frequency components for a typical three-pulse cycloconverter. It presents the amplitude of each



Per Unit Amplitude

Figure 3-3. Distribution of the predominant unwanted components in the output of the three-pulse CDFFC with amplitudes at maximum output voltage and unity load displacement factor.

predominant unwanted components in output as a function of the output voltage ratio r and output displacement angle ϕ_o regardless the frequency ratio f_o/f_I. For this particular case the output voltage r is set at maximum (r = 1) and the waveform switching angle ρ is set equal to the output displacement angle ϕ_o (i.e. $\rho = \phi_o$).

The output voltage wave is for a three-, six- and twelve-pulse cycloconverter shown in Figure 3-4 for switching angle ρ from 0 to 360 degrees. Increasing the pulse number of a cycloconverter reduces the amplitude of the unwanted components. The numerical values of the amplitude of the unwanted components shown in Figure 3-4 are in Table A.5 in the Appendix.

3-2 INPUT CURRENT CHARACTERISTICS OF A CDFFC

Equation (2-52) is the basic analytic expression of positive-type and negative-type input current waveform. Using a simple symbols, Equation (2-52) can be written in the following general form:

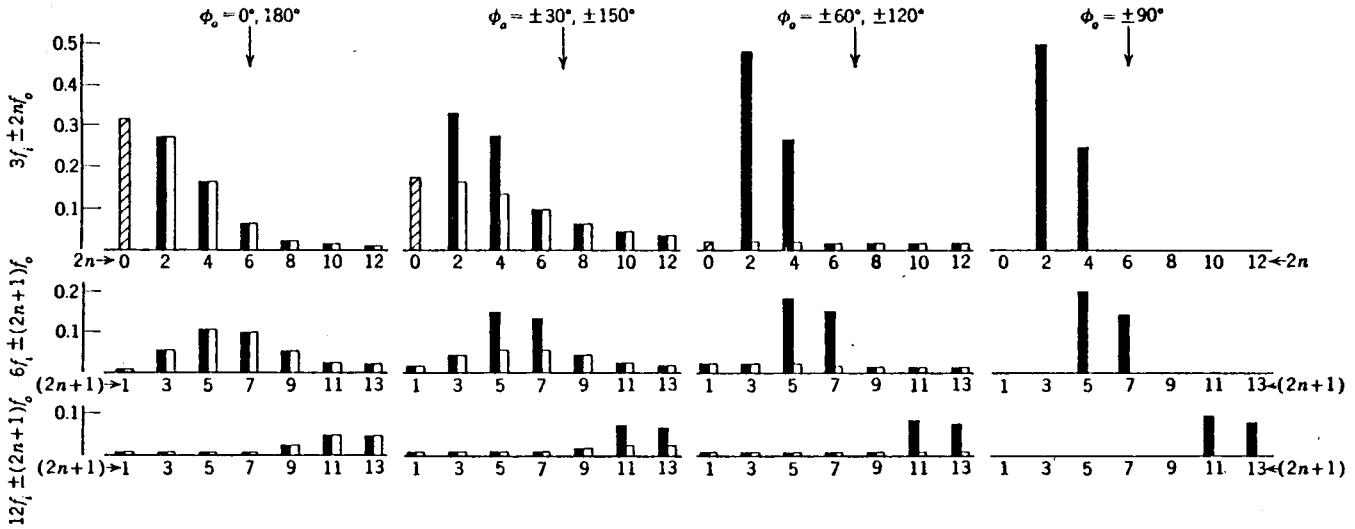


Figure 3-4. Amplitude of the unwanted component in the output voltage of the three-, six-, and twelve-pulse cycloconverter, with maximum output voltage ratio r = 1.

■ Amplitude of the "sum frequency" unwanted component for positive ϕ_o, and Amplitude of the "difference frequency" unwanted component for negative ϕ_o.

□ Amplitude of the "sum frequency" unwanted component for negative ϕ_o, and Amplitude of the "difference frequency" unwanted component for positive ϕ_o.

$$
\begin{aligned}
(a)\quad & i_I = \frac{3\sqrt{3}}{2\pi} I_O \Bigg\{ r\cos\phi_O \sin\omega_I t \\
& + \frac{1}{2}\sum_{u=-1}^{1}\sum_{k=1}^{\infty}\Bigg(\sum_{n=1}^{6n-4=3(2k-1)-u} \frac{a_{[3(2k-1)-u],(6n-4)}}{3(2k-1)-u}(\pm u) \\
& \times \sin\{([3(2k-1)-u]\omega_I \pm 3(2n-1)\omega_O)t \pm \phi_O\} \\
& \qquad + \sum_{n=1}^{6n-2=3(2k-1)-u} \frac{a_{[3(2k-1)-u],(6n-2)}}{3(2k-1)-u}(\mp u) \\
& \times \sin\{([3(2k-1)-u]\omega_I \pm 3(2n-1)\omega_O)t \mp \phi_O\} \\
& + \sum_{n=1}^{6n-1=6k-u} \frac{b_{(6k-u),(6n-1)}}{6k-u}(\pm u)\sin\{[(6k-u)\omega_I \pm 6n\omega_O]t \pm \phi_O\} \\
& + \sum_{n=0}^{6n+1=6k-u} \frac{b_{(6k-u),(6n+1)}}{6k-u}(\mp u)\sin\{[(6k-u)\omega_I \pm 6n\omega_O]t \mp \phi_O\}\Bigg)\Bigg\}
\end{aligned}
$$

$$
\begin{aligned}
(b)\quad & + \frac{3\sqrt{3}}{4\pi} I_O \Bigg\{ \mp a_{1,(6n-4)}\sin\{[\omega_I \pm 3(2n-1)\omega_O]t \pm \phi_O\} \\
& \qquad \pm a_{1,(6n-2)}\sin\{[\omega_I \pm 3(2n-1)\omega_O]t \mp \phi_O\} \\
& + \sum_{u=-1}^{1}\sum_{k=1}^{\infty}\Bigg(\sum_{n=1}^{\infty} \frac{b_{[3(2k-1)-u],(6n-1)}}{3(2k-1)-u}(\pm u) \\
& \qquad \times \sin\{([3(2k-1)-u]\omega_I \pm 6n\omega_O)t \pm \phi_O\} \\
& + \sum_{n=0}^{\infty} \frac{b_{[3(2k-1)-u],(6n+1)}}{3(2k-1)-u}(\mp u)\sin\{([3(2k-1)-u]\omega_I \pm 6n\omega_O)t \mp \phi_O\} \\
& + \sum_{n=1}^{\infty} \frac{a_{(6k-u),(6n-4)}}{6k-u}(\pm u)\sin\{[(6k-u)\omega_I \pm 3(2n-1)\omega_O]t \pm \phi_O\} \\
& + \sum_{n=1}^{\infty} \frac{a_{(6k-u),(6n-2)}}{6k-u}(\mp u)\sin\{[(6k-u)\omega_I \pm 3(2n-1)\omega_O]t \mp \phi_O\}\Bigg)\Bigg\}
\end{aligned}
$$

(3-8)

and

$$i_{I\pi} = (a) - (b) \tag{3-9}$$

Using the general definition given by Equation (2-51) input current i_I modulated by M(r,t) but dependent of angle ρ can be written in the following form

$$i_I(\rho) = a + b\left(\frac{4}{\pi}\sum_{m=0}^{\infty}\frac{1}{2m+1}\sin\left((2m+1)\left\{\omega_o t + \rho - (p-1)2\pi/3\right\}\right)\right) \tag{3-10}$$

where part (a) is represented the fundamental (wanted) component that is in phase with the input voltage wave and supplies real power to the load. Part (b) represents the extrabasal (unwanted) components that have multiples of output frequency of different families and supplies reactance power to the load. Evidently part (a) is not affected by variable switching angle ρ and only part (b) of Equation (3-10) need be considered. The new expression can be written in the following form after substituting part (b) of Equation (3-10) to Equation (2-52).

$$
\mathrm{V}\left[\begin{array}{l}
i_{Ib}(\rho) \\
= \dfrac{\sqrt{3}}{2\pi^2} I_O \sum\limits_{p=1}^{3} \left\{ \sum\limits_{n=0}^{\infty} \sum\limits_{m=0}^{\infty} \dfrac{a_{1.2n}}{2m+1} \right. \\
\quad \times \left[-\cos\left([\omega_I \pm 2(n-m)\omega_O]t \pm \phi_O \mp (2m+1)\rho \mp 2(n-m)(p-1)\dfrac{2\pi}{3} \right) \right. \\
\quad + \cos\left([\omega_I \pm 2(n-m-1)\omega_O]t \mp \phi_O \mp (2m+1)\rho \mp 2(n-m-1)(p-1)\dfrac{2\pi}{3} \right) \\
\quad - \cos\left([\omega_I \pm 2(n+m)\omega_O]t \mp \phi_O \pm (2m+1)\rho \mp 2(n+m)(p-1)\dfrac{2\pi}{3} \right) \\
\quad \left. \left. + \cos\left([\omega_I \pm 2(n+m+1)\omega_O]t \pm \phi_O \pm (2m+1)\rho \mp 2(n+m+1)(p-1)\dfrac{2\pi}{3} \right) \right]
\end{array}\right.
$$

$$
\begin{aligned}
\mathrm{VI} \quad & + \sum_{u=-1}^{1} \sum_{k=1}^{\infty} \sum_{n=0}^{\infty} \sum_{m=0}^{\infty} \frac{1}{2m+1} \left[\frac{b_{[3(2k-1)-u],(2n+1)}}{3(2k-1)-u} u \right. \\
& \times \left\{ \begin{matrix} + \\ \mp \end{matrix} \cos \left(\{ [3(2k-1)-u]\omega_I \pm [2(n-m)+1]\omega_O \} t \right. \right. \\
& \qquad \left. \pm \phi_O \mp (2m+1)\rho \mp [2(n-m)+1](p-1)\frac{2\pi}{3} \right) \\
& \quad \mp \cos \left(\{ [3(2k-1)-u]\omega_I \pm [2(n+m+1)+1]\omega_O \} t \right. \\
& \qquad \left. \pm \phi_O \pm (2m+1)\rho \mp [2(n+m+1)-1](p-1)\frac{2\pi}{3} \right) \\
& \quad \begin{matrix} + \\ \mp \end{matrix} \cos \left(\{ [3(2k-1)-u]\omega_I \pm [2(n+m+1)-1]\omega_O \} t \right. \\
& \qquad \left. \mp \phi_O \pm (2m+1)\rho \mp [2(n+m+1)+1](p-1)\frac{2\pi}{3} \right) \\
& \quad \mp \cos \left(\{ [3(2k-1)-u]\omega_I \pm [2(n-m)-1]\omega_O \} t \right. \\
& \qquad \left. \left. \mp \phi_O \mp (2m+1)\rho \mp [2(n-m)-1](p-1)\frac{2\pi}{3} \right) \right\} \\
& \qquad + \frac{a_{(6k-u),2n}}{6k-u} u \\
& \times \left\{ \begin{matrix} + \\ \mp \end{matrix} \cos \left([(6k-u)\omega_I \pm 2(n-m)\omega_O] t \right. \right. \\
& \qquad \left. \pm \phi_O \mp (2m+1)\rho \mp 2(n-m)(p-1)\frac{2\pi}{3} \right) \\
& \quad \mp \cos \left([(6k-u)\omega_I \pm 2(n+m+1)\omega_O] t \right. \\
& \qquad \left. \pm \phi_O \pm (2m+1)\rho \mp 2(n+m+1)(p-1)\frac{2\pi}{3} \right) \\
& \quad \mp \cos \left([(6k-u)\omega_I \pm 2(n+m)\omega_O] t \right. \\
& \qquad \left. \mp \phi_O \pm (2m+1)\rho \mp 2(n+m)(p-1)\frac{2\pi}{3} \right) \\
& \quad \begin{matrix} + \\ \mp \end{matrix} \cos \left([(6k-u)\omega_I \pm 2(n-m-1)\omega_O] t \right. \\
& \qquad \left. \left. \left. \mp \phi_O \mp (2m+1)\rho \mp 2(n-m-1)(p-1)\frac{2\pi}{3} \right) \right\} \right] \Bigg\}
\end{aligned}
$$

(3-11)

Part V in the above equation has components with frequencies that are sums and differences of input frequency and odd multiples of the output frequency. But part VI has components with frequencies that are sums and differences between multiples of the input frequency and multiples of the output frequencies. After carrying out the multiplication in the equations, some additional fundamental components from part V of Equation (2-52) are formed whenever indices m and n satisfy the following condition

$$m = n \tag{3-12}$$

and

$$m = n - 1 \tag{3-13}$$

The multipliers of frequency ω_o becomes zero for the appropriate terms of the series. These new fundamental components are called "Quadrature Components" because they have a phase shift from the corresponding input voltage of $\pi/2$. It is a reactive component containing the fundamental frequency of the ac source. By appropriate substitution of the above conditions,

$$i_{IQ}(\rho) = \frac{\sqrt{3}}{\pi^2} I_O \sum_{p=1}^{3} \sum_{n=0}^{\infty} a_{1,2n} \left(\frac{\cos\{\phi_O + (2n-1)\rho\}}{2n-1} - \frac{\cos\{\phi_O - (2n+1)\rho\}}{2n+1} \right)$$

$$\times \cos\{\omega_I t - (p-1)2\pi\} \qquad (3\text{-}14)$$

The total fundamental input current $i_{IF}(\rho)$, can be obtained by summing the two fundamental components. One of each component given by part (a) of Equation (3-8) is the "Real Component" $i_{IR}(\rho)$ which contains the fundamental frequency of the ac source. For single-phase output, the total fundamental input current $i_{IF}(\rho)$ is given here,

$$i_{IF}(\rho) = i_{IR}(\rho) + i_{IQ}(\rho)$$

$$= \frac{\sqrt{3}}{2\pi} I_O \left\{ r \cos\phi_O \sin\omega_I t + \frac{2}{\pi} \sum_{n=0}^{\infty} a_{1,2n} \left(\frac{\cos\{\phi_O + (2n-1)\rho\}}{2n-1} - \frac{\cos\{\phi_O - (2n+1)\rho\}}{2n+1} \right) \cos\omega_I t \right\}$$

(3-15)

The total rms values of the input current waveform I_{rms} is given by the following expression.

$$I_{rms} = \left(I_{IR}^2 + I_{IQ}^2 + \sum_{L=1}^{\infty} I_{EL}^2 \right)^{\frac{1}{2}} \qquad (3\text{-}16)$$

where I_{EL} is the extrabasal component of an input current wave. The total real component I_{IR} of an input current is

$$I_{IR} = P\ S\ (\sqrt{3} I_o / 2\pi)\ (r \cos\phi_o) \qquad (3\text{-}17)$$

or

$$I_{IR} = P\ S\ (\sqrt{3} I_o / 2\pi)\ I_{IR,PU} \qquad (3\text{-}18)$$

where P is the number of output phase, S is the number of pulse group in series or cascade connection in each output phase and $I_{IR,PU}$ is a per-unit real component of input current. The total quadrature current I_{IQ} of input current is

$$I_{IQ} = P\ S\ (\sqrt{3} I_o / 2\pi)\ I_{IQ,PU} \qquad (3\text{-}19)$$

To further investigate the extrabasal components in the input current waveform of a CDFFC, a graphical chart is presented in Figure 3-5. The numerical values of the amplitudes of the extrabasal components in the input current wave of a CDFFC with sinusoidal mean output voltage (single- and balanced three-phase output) is shown in Table A.6 in the Appendix. These numerical values are the function of the output voltage ratio r, the output displacement angle

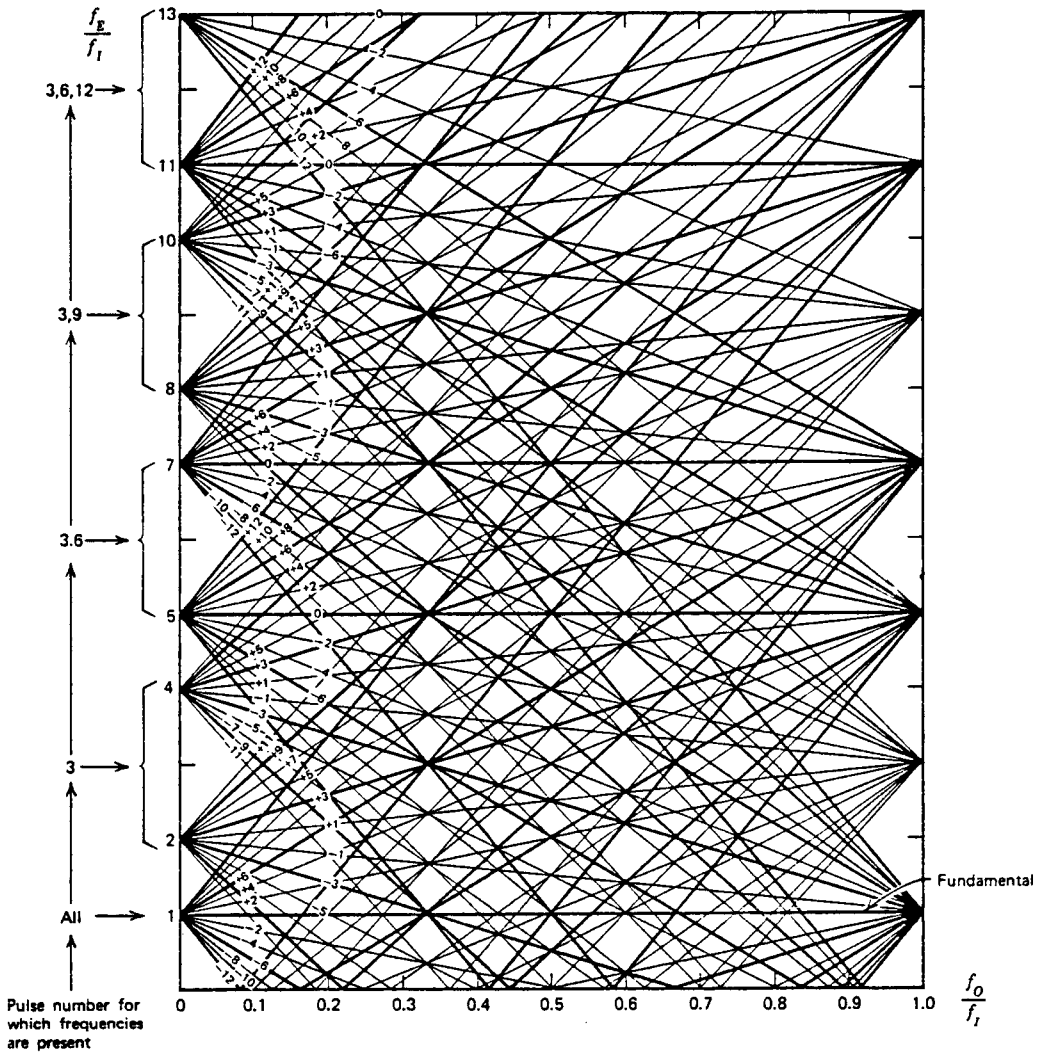


Figure 3-5. Distribution of the extrabasal components in the input current waveform of a CDFFC. For single-phase output, all frequencies shown are present. For balanced three-phase output, only frequencies shown by heavy lines are present.

ϕ_o, and also the control angle σ. Table A.6 is a special case for setting the control angle σ at 180° (i.e. $\rho = \phi_o$), with different output displacement angle ϕ_o. For other settings of control angle, the numerical values of the amplitudes of the extrabasal components can be computed by using Equation (3-11).

The relationship between the per-unit quadrature component of the input current $I_{IQ.PU}$, the output load displacement factor ϕ_o, and the output voltage ratio r, of a CDFFC is shown in Figure 3-6.

The half-period section of the final output current waveform of a CDFFC can be defined for a given input displacement angle by the control angle σ, measured at $\omega_o = 2\pi f_o$, specifying the point of changover between v_o and $v_{o\pi}$ with respect to the zero crossing point of the output current wave, rather than respect to the output voltage wave. The control angle σ is defined by

$$\sigma = \phi_o - \rho - \pi \qquad (3\text{-}20)$$

The relationship between pre-unit quadrature component of input current $I_{IQ,PU}$, output displacement angle ϕ_o, and output voltage ratio r, for CDFFC with $\sigma = \phi_o$ and $\sigma = \pi + \phi_o$ are shown in Figure 3-7.

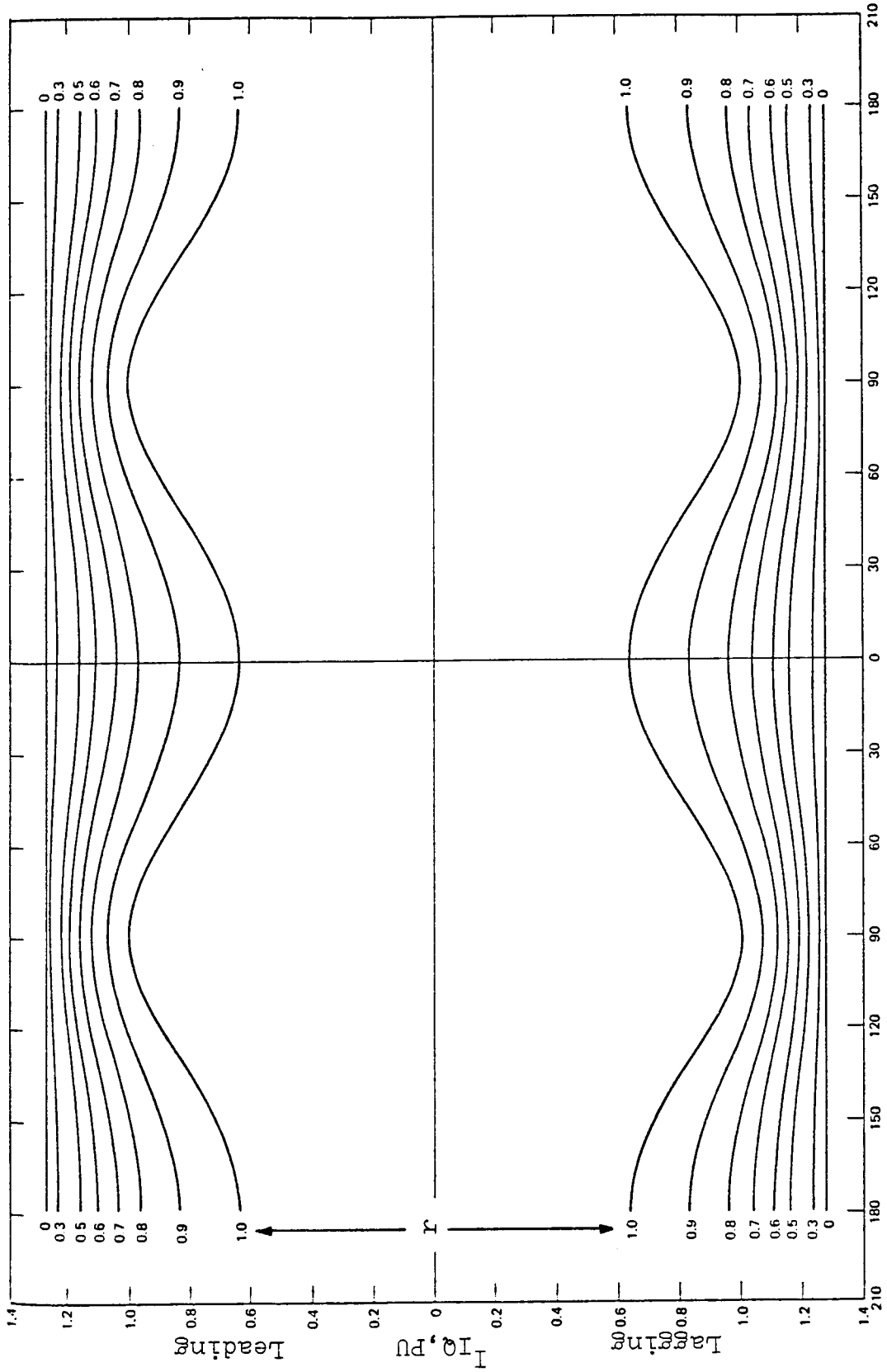


Figure 3-6. Per unit quadrature component of input current of the CDFFC as a function of the output displacement angle ϕ_o and output voltage ratio r.

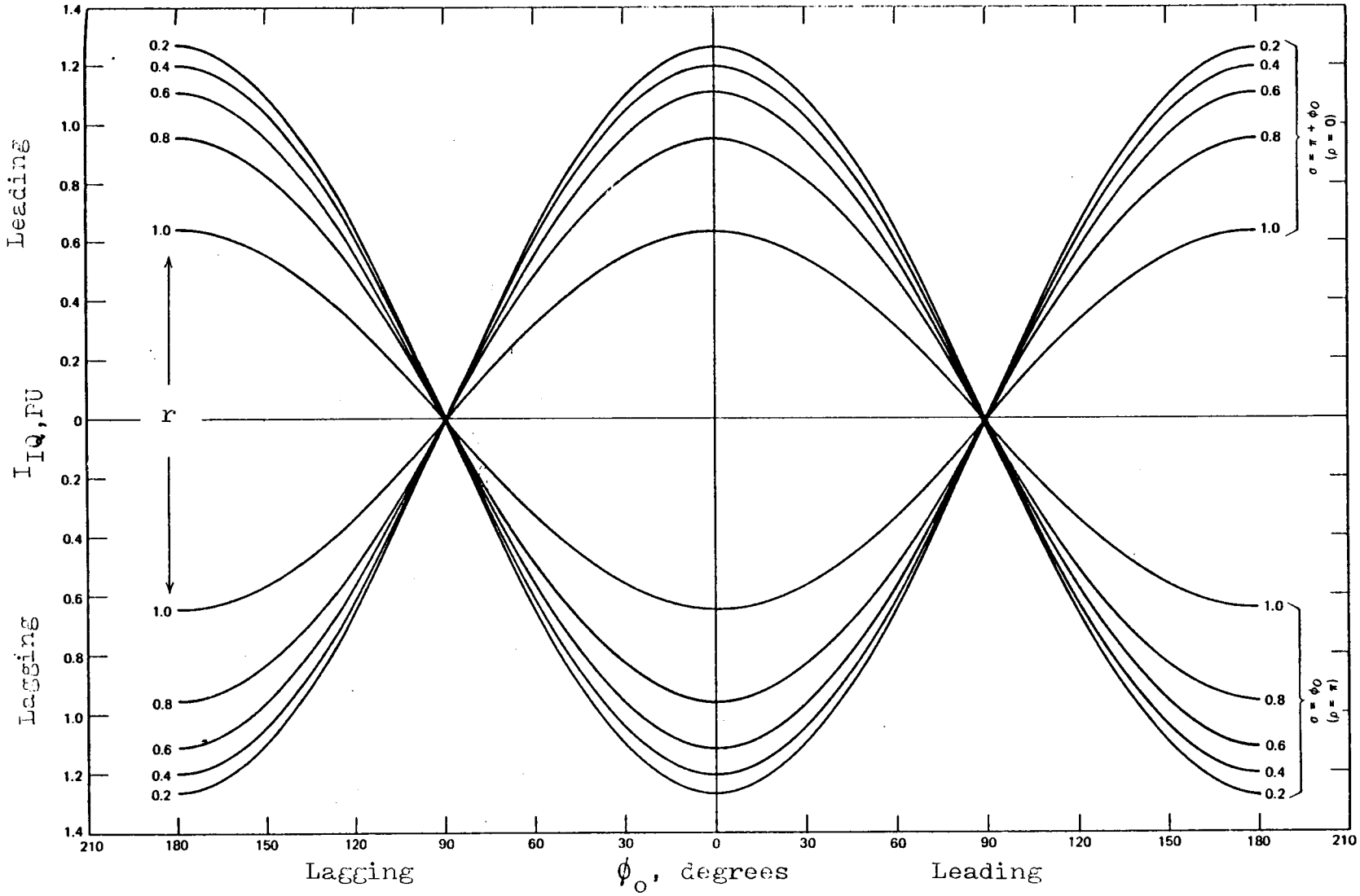


Figure 3-7. Relationship between per unit quadrature component of input current, output displacement angle and output voltage ratio, for CDFFC with $\sigma = \phi_o$ and $\sigma = \pi + \phi_o$.

The input displacement angle $\phi_I(\rho)$ may be measured lagging, leading, or unity regardless of the phase angle of the output load which is given

$$\phi_I(\rho) = \tan^{-1}\left\{\frac{\frac{2}{\pi}\sum_{n=0}^{\infty} a_{1,2n}\left(\frac{\cos\{\phi_o + (2n-1)\rho\}}{2n-1} - \frac{\cos\{\phi_o - (2n+1)\rho\}}{2n+1}\right)}{r\cos\phi_o}\right\} \tag{3-21}$$

where an angle is measured between input current (fundamental component) and the line-to-neutral input voltage. The relationship between the load phase angle ϕ_o, control angle σ and input phase angle ϕ_I is shown in Figure 3-8.

The interactions between the input displacement angle ϕ_I, the control angle σ, and the output voltage ratio r for a CDFFC are shown in Figure 3-9.

The operating range of a CDFFC with variations in the input phase angle under any given load condition is shown in Figure 3-10. The plot of the input phase angle against the load phase angle consists of two curves, one has lagging angle characteristic and other has an angle with the same amplitude but opposite polarity.

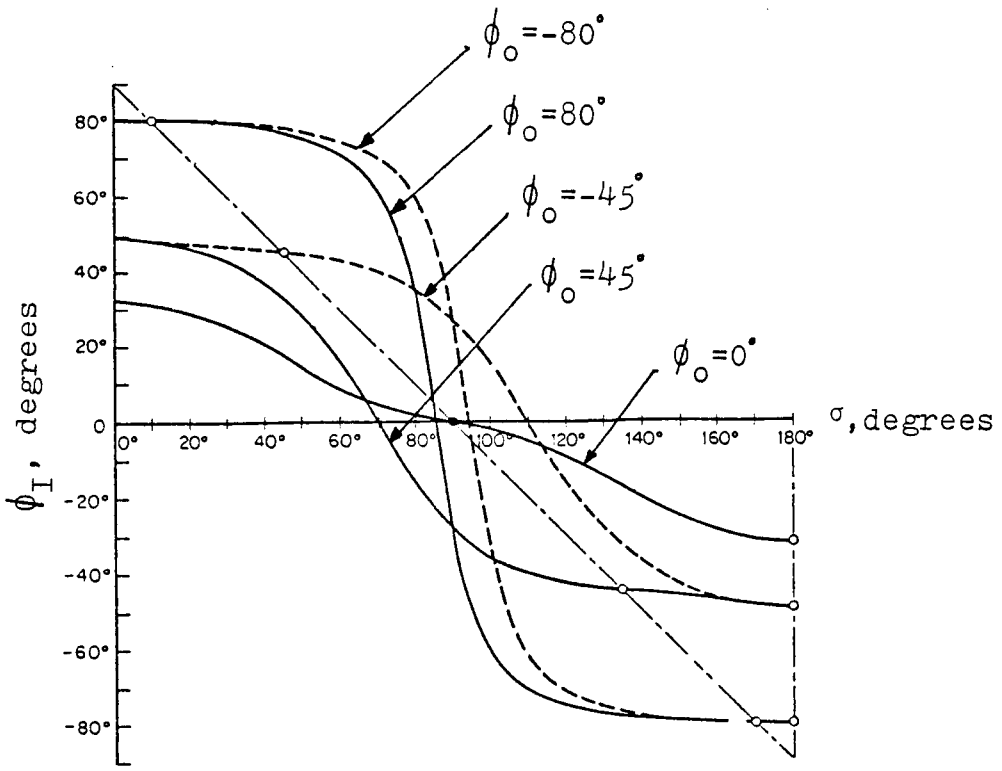


Figure 3-8. Relationship between the load phase angle, control angle and input phase angle, with maximum output voltage ratio.

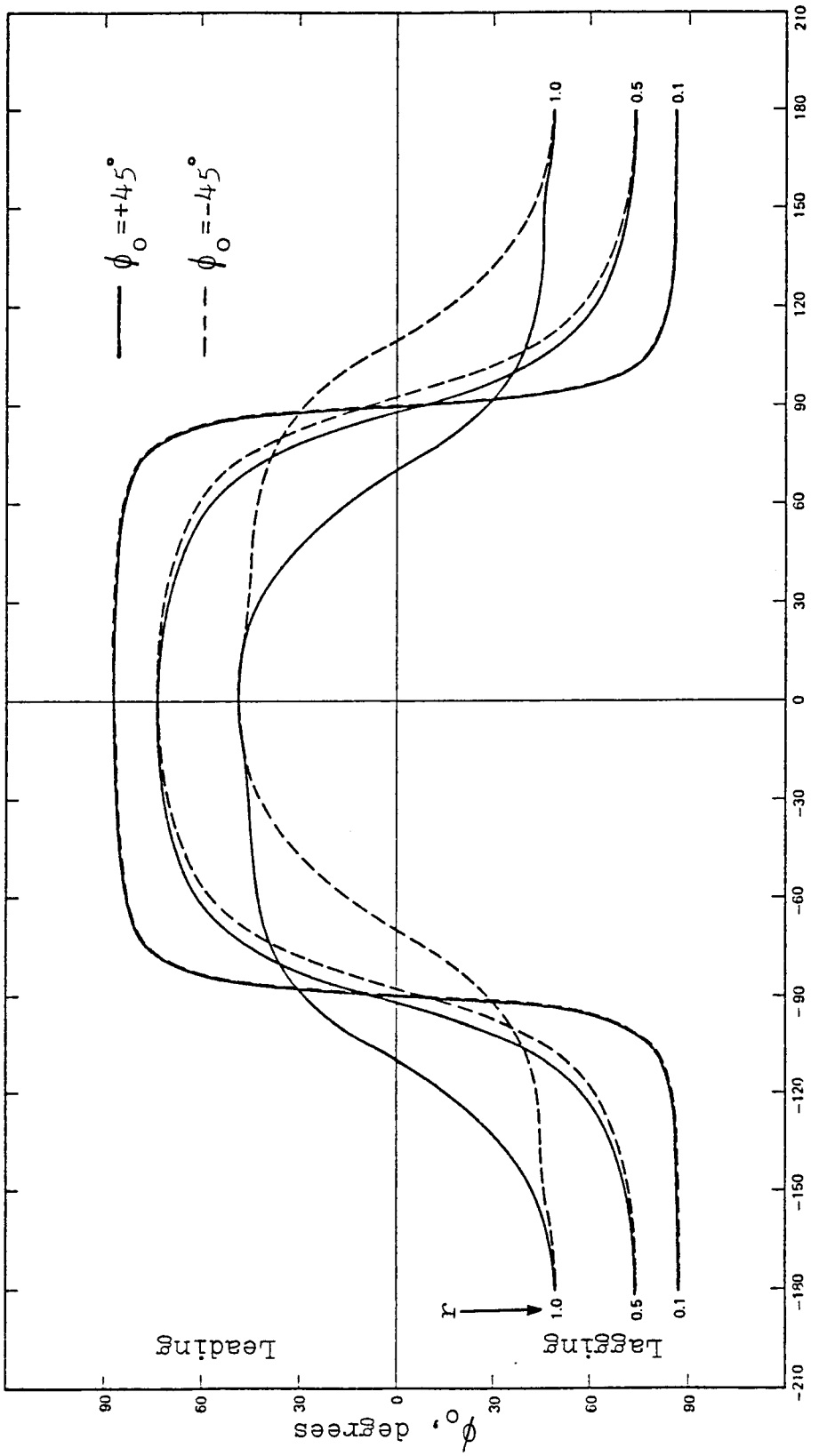


Figure 3-9. Relationship between the control angle for different output voltage ratios and two load phase angles.

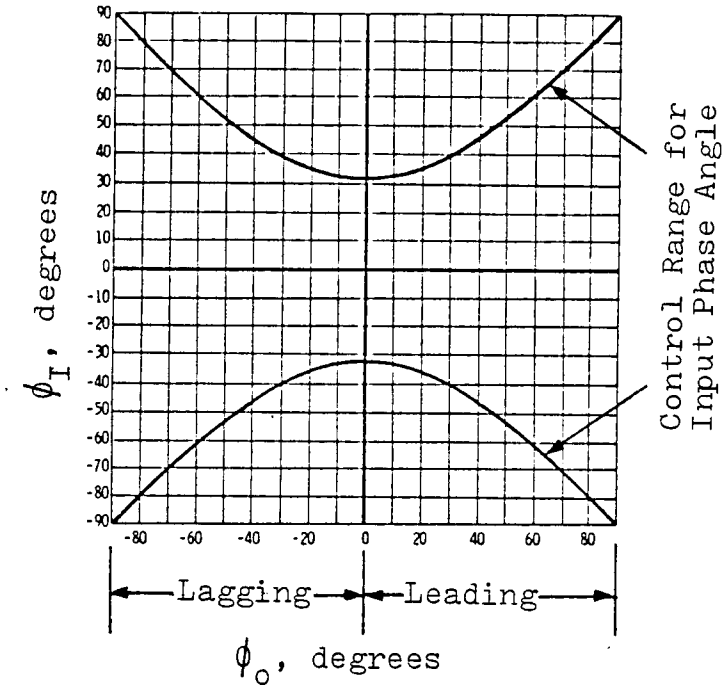


Figure 3-10. Relationship between load phase angle and control range of input phase angle for CDFFC.

Some other important input parameters are determined for the case of switching angle $\rho = 0$, $\phi_o = 0$ (unity power factor) and r = 1 (full output voltage). The frequency ratio $\nu_{Ik,L}$ of the extrabasal components to the input fundamental component of a CDFFC is given

$$\nu_{Ik,L} = \begin{cases} 1 \pm 6(L+1)(f_o / f_I) \\ [3(2k-1) \pm 1] + 3(2L+1)(f_o / f_I) \\ [3(2k-1) \pm 1] - 3(2L+1)(f_o / f_I) \\ (6k \pm 1) + 6L(f_o / f_I) \\ (6k \pm 1) - 6L(f_o / f_I) \end{cases}$$

$$k = 1,2,.. \qquad L = 0,1,2,.. \qquad (3\text{-}22)$$

The input displacement factor δ_I of a CDFFC is given

$$\delta_I = \cos \phi_I = I_{IR} / (I_{IR}^2 + I_{IQ}^2)^{\frac{1}{2}} = 0.842 \qquad (3\text{-}23)$$

This factor is important in determining the size and weight of the generator because it has the same direct relationship to the demagnetizing effect of armature reaction as does the power factor of a generator. When the leading load or lagging load delivers reactive power to the frequency changer, the output phase delay will increase and the displacement factor will reduce. The current overlap between phases, depend on the generator leakage reactance, will also reduce the displacement factor. Therefore, the

generator leakage reactance must be minimized for high frequency generation. The input distortion factor μ_I of a CDFFC is given

$$\mu_I = I_{IR,rms} / I_{I,rms} = 0.9 \qquad (3\text{-}24)$$

This distortion factor may be improved by decreasing the copper losses in the armature and damper winding, due to the harmonic current flowing in the generator. The input power factor λ_I of a CDFFC is given

$$\lambda_I = V_{I,rms} I_{IF,rms} \cos \phi_I / V_{I,rms} I_{I,rms} \cos \phi_I \qquad (3\text{-}25)$$
$$= \cos \phi_I = 0.759$$

It should be noted that the total current $i_I(\rho)$ [Referred to Equation (3-10)] of a frequency changer, generally nonsinusoidal, is constituted from three components [Equation (3-15) and (3-16)]. These are the fundamental real component $i_{IR}(\rho)$, fundamental quadrature components $i_{IQ}(\rho)$, and extrabasal components $i_{EL}(\rho)$.

The fundamental real component of the input current is always in phase with the corresponding supply voltage, regardless of the load angle ϕ_o. In other words, the input displacement factor ϕ_I of the system does not vary with load. Since the frequency changer was specified to be lossless, the real input and output power must be equal. It

follows that the real component of the input current is proportional to the product of the real component of the output current and the output voltage ratio r, but is independent of the output voltage waveform construction. Consequently, purely inductive or capacitive loads result in a zero fundamental input current component.

The fundamental quadrature components have a phase shift from the corresponding input voltage of $\pi/2$. They are dependent on the output voltage waveform construction and load phase angle ϕ_o . When a quadrature current component appears at the output, there will no other quadrature current component at the input, and the converse is also true.

The extrabasal current components related to the output waveform construction, is appearred in addition to the fundamental current component dependently of the output displacement angle ϕ_o, the pulse number, and the number of output phase. From an inspection of the general expression for input current, it is possible to classify the spectrum of extrabasal frequencies into two groups, "Pulse Number Dependent" and "Pulse Number Independent."

The Pulse Number Dependent extrabasal component may be removed by increasing the output phases number of the frequency changer. For example, if components having frequencies of $(6 \pm 1)f_I \pm Pnf_o$ are present. The frequency

changer is a six-pulse changer with ia p-phase balanced output, and n is an integer number which is dependent upon the method of output voltage waveform construction. As the number of output phases approaches infinity, the pulse number dependent term $(6 \pm 1)f_I$ of the extrabasal component will become predominent. Conversely, when the pulse number of a frequency change is increased, there will no pulse number dependent extrabasal component in the input current wave, regardless of the number of output phases.

The pulse number independent extrabasal components are determined only by the number of balanced output phases. There are two types of components having the frequencies $(f_I \pm 2f_o)$ and $(f_I \pm Pnf_o)$, in this group. With a single-phase or unbalance output, the first harmonic current components having frequencies of $(f_I \pm 2f_o)$ are present only in the input current, regardless of the circuit phase number. But for a balanced three-phase output, the pulse number independent extrabasal components are absent, and the distortion of the input current wave is generally reduced. The second components having frequencies of $(f_I \pm Pnf_o)$ will contain no pulse number dependent extrabasal components, regardless of the circuit pulse number when the number of output phases approaches infinity.

3-3 INPUT AND OUTPUT POWER CHARACTERISITICS OF CDFFC

The ideal frequency changer is theoretically lossless, therefore the real power suplied by the generator must be equal to the real power consumed at the output (i.e. $P_I = P_o$). Consider now a frequency changer with an infinite pulse number producing a single-phase output from a three-phase input. The frequency changer has a infinite pulse number, therefore its output wave will not contain any pulse number dependent extrabasal component. Thus output voltage v_o and output current i_o can be assumed sinusoidal. The instantaneous power output, with a "Resistive" load, is given by

$$P_o = V_o \sin \omega_o t \; I_o \sin(\omega_o t + \phi_o) \tag{3-26a}$$

$$= \underbrace{\frac{V_o I_o}{2} \cos \phi_o}_{\text{Steady component}} - \underbrace{\frac{V_o I_o}{2} \cos(2\omega_o t + \phi_o)}_{\text{Oscillatory component}} \tag{3-26b}$$

Thus the output power consists of two components; a "Steady Component" and an "Oscillatory Component". The amplitude of steady component of power is dependent on the output displacement angle ϕ_o. But the amplitude of the oscillatory component of power, having twice the output frequency is not dependent on the output displacement angle. The reactive component of current at the output terminal or the extrabasal component of current at the input terminal

appears in the term of the oscillatory component in Equation (3-26b), regardless the load. Thus reactive power can be delivered by the frequency changer.

In the ideal converter, the steady power component must be to equal the products of the fundamental real input current component I_{IR} and input voltage V_I. Another fundamental quadrature component of input current, dependent on the output voltage construction and load phase angle, will be disscussed. The steady component of power, with three input terminals, is given by

$$\begin{aligned}\text{Steady component of input power} &= V_I \sin \omega_I t \, I_{IR} \sin \omega_I t \\ &\quad + V_I \sin\left(\omega_I t - \frac{2\pi}{3}\right) I_{IR} \sin\left(\omega_I t - \frac{2\pi}{3}\right) \\ &\quad + V_I \sin\left(\omega_I t - \frac{4\pi}{3}\right) I_{IR} \sin\left(\omega_I t - \frac{4\pi}{3}\right) \\ &= \frac{3V_I I_{IR}}{2} = \frac{V_O I_O}{2} \cos \phi_O\end{aligned} \tag{3-27}$$

For three-phase balanced output, the extrabasal components of input current will cancel. Therefore the input current wave is essentially sinusoidal. The steady component of three-phase output power is three times bigger than the steady component of single-phase output power. But all the oscillatory components of the output power are absent in this three-phase balanced system and the total

instantaneous ouput power is given by

$$\begin{aligned} P_o &= V_o \sin \omega_o t \, I_o \sin(\omega_o t + \phi_o) \\ &\quad + V_o \sin\left(\omega_o t - \frac{2\pi}{3}\right) I_o \sin\left(\omega_o t + \phi_o - \frac{2\pi}{3}\right) \\ &\quad + V_o \sin\left(\omega_o t - \frac{4\pi}{3}\right) I_o \sin\left(\omega_o t + \phi_o - \frac{4\pi}{3}\right) \\ &= \frac{3V_o I_o}{2} \cos \phi_o \end{aligned} \tag{3-28}$$

Now consider a frequency changer that has an infinite pulse number and is connected to a single-phase "Reactive" load. Of course, in this case it is not possible to have output current containing a real power or input current containing reactive power. Since reactive power is not necessarily conserved in this system, the current drawn from the input source is zero because no fundamental and extrabasal components flow through the frequency changer. The frequency changer can have self-sufficient to supply a reactive power exchange between the load phases. Generally, the frequency changer has the ability to supply a reactive current at the output/input with no input/output reactive current supplied, depending upon the diffenent types of output waveforms. Therefore the load may either absorb or deliver reactive power.

The only component of the input current of the frequency changer capable of supplying a mean component of power at the output, is the fundamental real component of

input current. This is true since the mean power due to the fundamental quadrature component of input current is necessarily zero. The net instantaneous power at the three-phase input due to the quadrature components of input current is zero:

$$\begin{aligned} P_Q &= V_I \sin \omega_I t \, I_{IQ} \cos \omega_I t \\ &\quad + V_I \sin\left(\omega_I t - \frac{2\pi}{3}\right) I_{IQ} \cos\left(\omega_I t - \frac{2\pi}{3}\right) \\ &\quad + V_I \sin\left(\omega_I t - \frac{4\pi}{3}\right) I_{IQ} \cos\left(\omega_I t - \frac{4\pi}{3}\right) \\ &= 0 \end{aligned} \tag{3-29}$$

The presence of the lagging/leading quadrature component of input current, which is inherent in the basic control mechanism of the cycloconverter, represents that a reactive power exchange establishes between the phases of the input/output through the frequency changer.

3-4 SUMMARY

At this point it would appear to be advantageous to summarize the relative functions of the frequency changer. The relationship between the input and/or output voltage and current waveforms of a CDFFC are illustrating in Figure 3-11. It is obvious to express the phase relationship of output load displacement angle ϕ_O, control angle σ and the input displacement angle ϕ_I in the input current wave and output voltage wave of a three-pulse frequency circuit, with

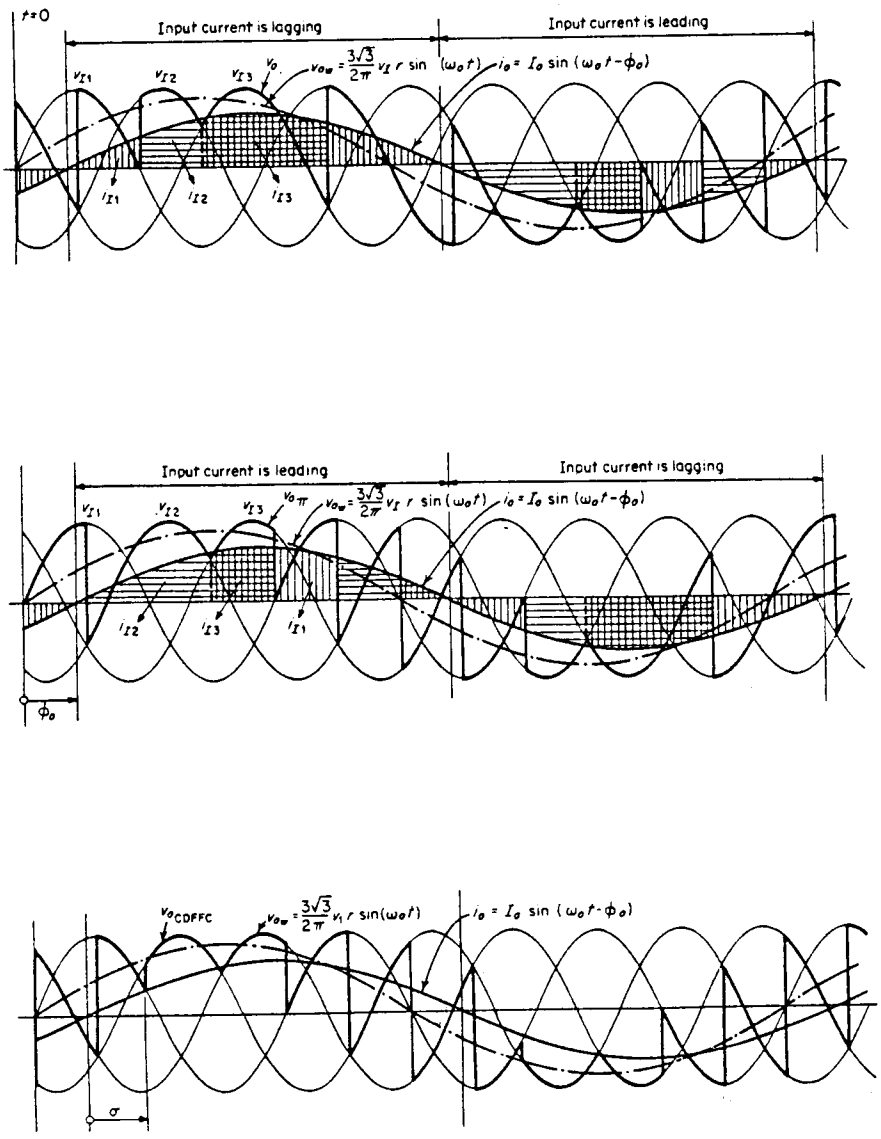


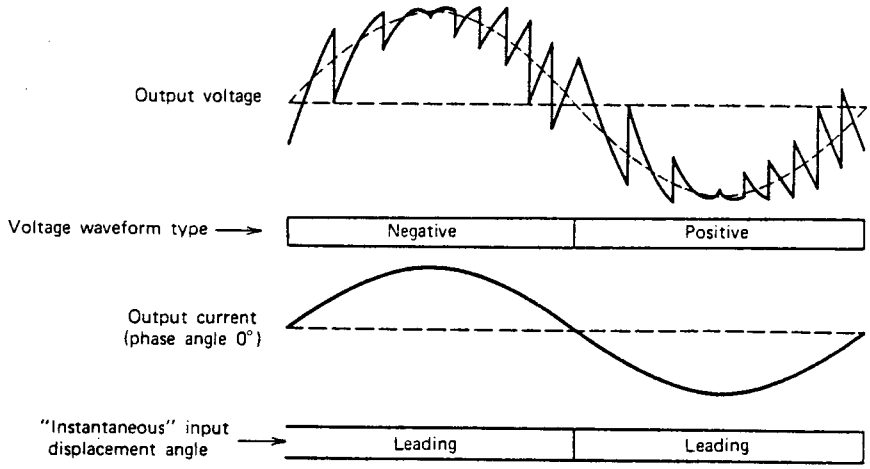
Figure 3-11. Phase relationship between the output or input voltage and current of the CDFFC.

single-phase output [Refer to Figure 2-2(A)]. The phase position (leading, lagging or unity) of the input current is dependent upon the construction method of the output voltage waveform. Different combinations of the voltage waveform type and output current polarity determine the input phase position shown in Table 3.1. Figure 3-12 shows different phase shift of the positive-type and negative-type waveform at the output affecting the input displacement angle of a CDFFC. The characteristics of a six-pulse (P = 6) CDFFC are summarized in the Table 3.2.

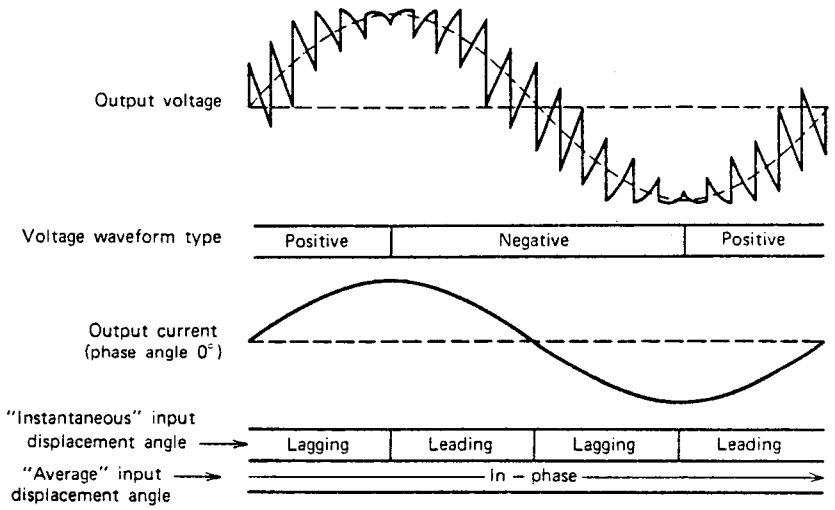
In order to reduce the harmonic content of the output wave, the firing signals to the frequency changer must operate in such a way that the output voltage contains a large wanted component and a small unwanted components and the input current contains a large fundamental component and a small extrabasal components.

Table 3.1. Conditions determine input displacement angle : Leading or Lagging.

Voltage Waveform	Polarity of the Output Current	Input Displacement Angle
Positive-type	Positive	Lagging
	Negative	Leading
Negative-type	Positive	Leading
	Negative	Lagging

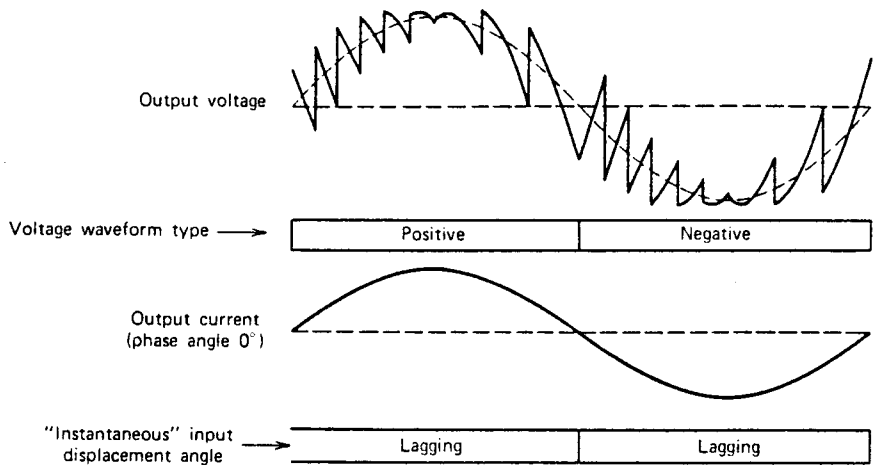


A. Input Current is Leading



B. Input Current is In-phase

Figure 3-12. Construction method of the output voltage waveform affects the input displacement angle.



C. Input Current is Lagging

Figure 3-12. (Continued)

Table 3.2. Summary of the characteristics of a six-pulse CDFFC.

Commutation	Forced
Input Displacement Angle	$\cos \phi_I = F(\sigma, \cos \phi_o)$ Controllable; $\sigma = \phi_o - \rho - \pi$
Maximum Output/Input Frequency Ratio	$(f_o / f_I)_{max} = (P - 2) / P$
Desired Output Frequency Spectrum of the Unwanted Voltage Components	$f_{od1} = \lvert P(2k - 1)f_I \pm (2L)f_o \rvert$ $f_{od2} = \lvert P(2K)f_I \pm (2L + 1)f_o \rvert$
Desired Input Frequency Spectrum of the Extra-basal Current Components	$f_{Id1} = \lvert [P(2k - 1) \pm 1]f_I \pm 3(2L + 1)f_o \rvert$ $f_{Id2} = \lvert [P(2k) \pm 1]f_I \pm (6L)f_o \rvert$ where k = 1,2,3,.. L = 0,1,2,..

CHAPTER 4

PRINCIPLE OF CAPACITOR-EXCITED INDUCTION GENERATOR

If an induction machine is driven at speeds slightly above synchronism, the stator current reverses, and supplies power back into the line. The performance characteristics of the induction generator depend upon the prime mover, and upon the circuit to which the machine is connected. The induction generator requires a source of leading current for excitation. If a lagging reactive power input is equated with a leading reactive power output, then the generator can be described as operating with a leading power factor [Refer to Table B.1 in Appendix]. A self-excited capacitance which normally carries leading current may be used to excite the machine to build-up voltage. The induction generator receives its excitation from the external capacitance, and generated voltages at different frequencies at the output are largely dependent upon the size of the capacitance.

In order to study the influence of terminal capacitors on steady-state behaviour of an induction machine, a magnetization curve is developed in which the nonlinear effect of magnetic saturation is taken into account for investigation in any "Build-up" voltage analysis of the problem. The technique is utilizing for improve the saturation curve with external reactors is developed. Some

equations related to slip and voltage regulation are derived. Further improvements of the output voltage regulation, such as using series capacitor and saturable reactors, are introducted. The experimental results of an external performance of machine, included with shunt load and compound load connection, are measured and plotted.

4-1 PERFORMANCE FROM MAGNETIZATION CURVE

To determine its voltage and frequency, and to supply its lagging reactive magnetizating power, an induction generator is connected to an energized power network with capacitors. Provided that the rotor has an adequate remanent field, the machine will self-excite. The voltage at which the machine will operate is dependent upon its no-load excitation characteristics at that frequency, the criterion to be satisfied being that the lagging volt-amperes of excitation is equal to the leading volt-amperes of the capacitor. The self-excited induction machine is governed by the saturation of the main flux paths. The internal characteristic of an induction generator is known as its magnetization curve, or the saturation curve. It is the no-load output phase voltage V_1 plotted against the excitation current I_E (phase current) with the generator operated at rated speed.

A test machine used for the experiment is a 1/2-HP, 206-230/460 V, 4-pole, three-phase squirrel-cage induction machine that is driven at a constant speed of 1800 rpm. The machine has the impedence parameters referred to a stator phase at normal operating temperature shown in Table 4.1.

The output voltage V_1 will be related to the excitation current I_E as shown in Figure 4-1. The no-load magnetizing curve OS is shown to vary with frequency and exciting current. At no load, $I_E = V_1 \omega_c = V_1/X_c$ must be equal magnetizating current $I_m = V_1/X_m$. But V_1 is a function of I_m so that stable operation requires the line $I_m X_c$ to cut the voltage/excitation characteristics.

At rated speed the generated output voltage $V_1 = K\Phi N_1$ is directly related to flux Φ, since the rotating speed N_1 is held constant (neglect the slip) and K is the machine constant of proportionality. The excitation current I_E must increase from zero to a maximum voltage (saturation) value to maintain stable operation. At such a high degree of saturation, many forms of losses become significant, and these produce space harmonics of air-gap flux that may affect the regulation of the output voltage.

As the excitation current is increased, the curve coincides with the straight-line portion (linear region) of the magnetization characteristics and under these conditions the circuit will be in different equilibrium since the

Table 4.1. Test parameters of the induction machine.

Stator Resistance per phase	R_1 = 5.6 ohms
Referred Rotor Resistance per phase	R_2 = 1.38 ohms
Stator & Rotor Leakage Reactance ($X_1 + X_2$) per phase referred to Stator	X_T = 8.2 ohms
Unsaturated Magnetizing Reactance per phase	X_m = 92.0 ohms
Magnetizing Branch Resistance per phase	R_m = 308.0 ohms

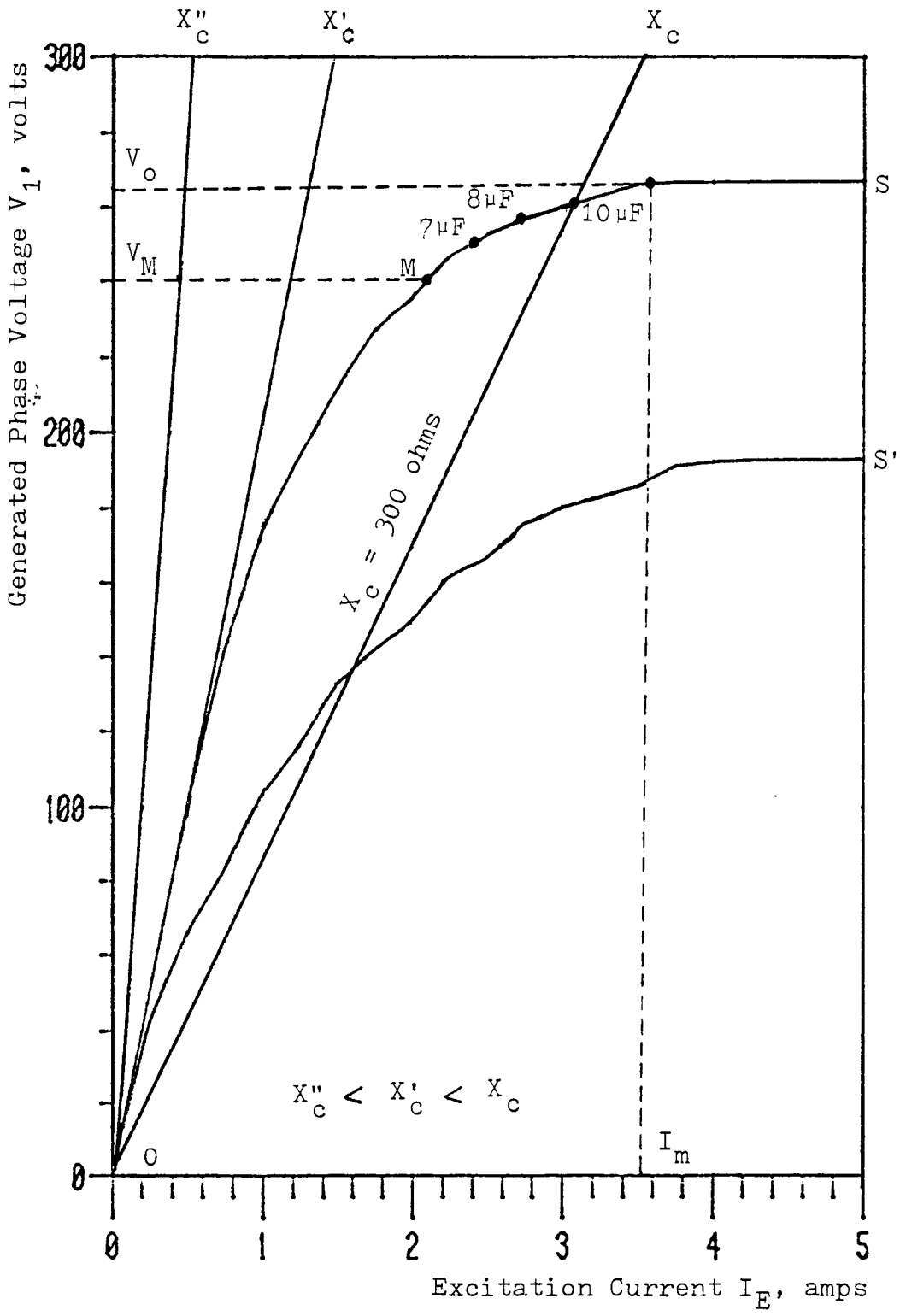


Figure 4-1. Build-up Characteristics of the Capacitor-excited Induction Generator.

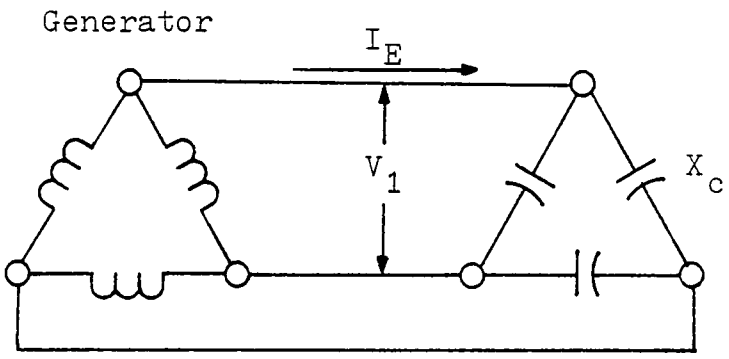
OS = No-load Saturation Curve, at Rated Speed.

OS' = No-load Saturation Curve, slightly under Rated Speed.

OX_c = Excitation Line.

OX'_c = Air-gap Line (Critical Excitation Line).

A. No-load Saturation Curve



B. Test Circuit

Figure 4-1. (Continued)

equation $V_1 = I_E X_c$ is satisfied at all voltages along the region of coincidence. The end of the straight-line portion is M and at this point the iron starts to saturate slowly, at first, but increases as I_c increased. This process is continuous and finally an equilibrium is reaches at point S when the magnetic circuit is saturated. Here the process stops. The intersection point of the magnetizing curve OS and the excitation line OX_c determines the no-load voltage of a generator ($I_E = I_m$ at no-load condition). The slope of the line OX_c equals the value of terminal excitation reactance X_c at the generated frequency. As the excitation reactance increases from line OX_c to OX'_c, the no-load voltage gradually decreases and the machine will not build-up an appreciable voltage if the excitation reactance X_c is greater than the critical value (line OX'_c), which is the slope of the line just tangent to the no-load saturation curve. This line is often called the air-gap line which gives a critical value for the excitation reactance X_c. Line OX''_c in Figure 4-1 represents a value of reactance that is too large for machine operation. The dotted magnetization curve OS' represents a machine operating slightly under rated speed. For voltage to build-up in an induction generator, the following factors are necessary:

(1) There must be a residual magnetism in a rotor circuit before starting.

(2) The value of an excitation reactance X_c must

be equal to or less than the critical value, determined by the slope of the excitation line OX'_c.

(3) The speed of the prime mover may be high enough to obtain the desired output frequency f_o as it is proportional to the actual speed of the rotor N_2 minus the slip speed S i.e. $f_o \propto (N_2 - S)$.

(4) The terminal capacitive reactance X_c must be equal to or less than the magnetizing reactance X_m of the machine i.e. $X_c \leq X_m$ [Refer to Figure 1-15].

The output voltage of an induction machine operating as an generator, will be substantially higher than the normal rated voltage V_M of a motor. This is caused by the saturation of leakage flux paths, for this reason the core losses will be greater than that at normal operation. As the result an induction generator has rather poor voltage regulation characteristics. In order to improve the voltage regulation of the machine, it may be necessary to change the machine constants or connect a non-linear saturable reactor X_R externally with the generator unit. If the rating of the parallel reactor X_R is equal to a generator magnetizing reactance X_m, a new saturation curve with a very low loss characteristics results. Figure 4-2 shows an improved saturation curve ON that is a combination of two curves OS (no-load saturation curve) and OR (reactor characteristic

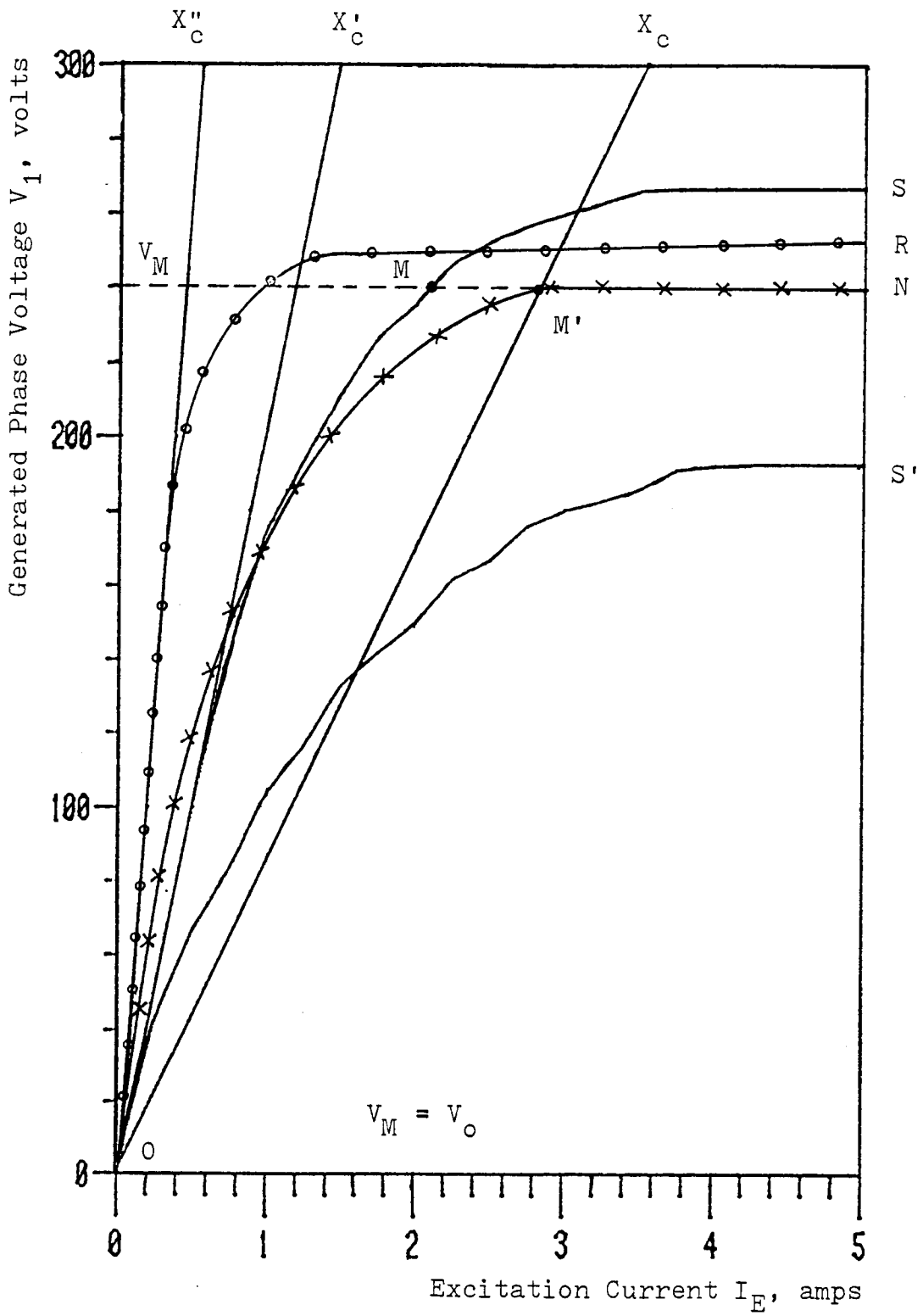
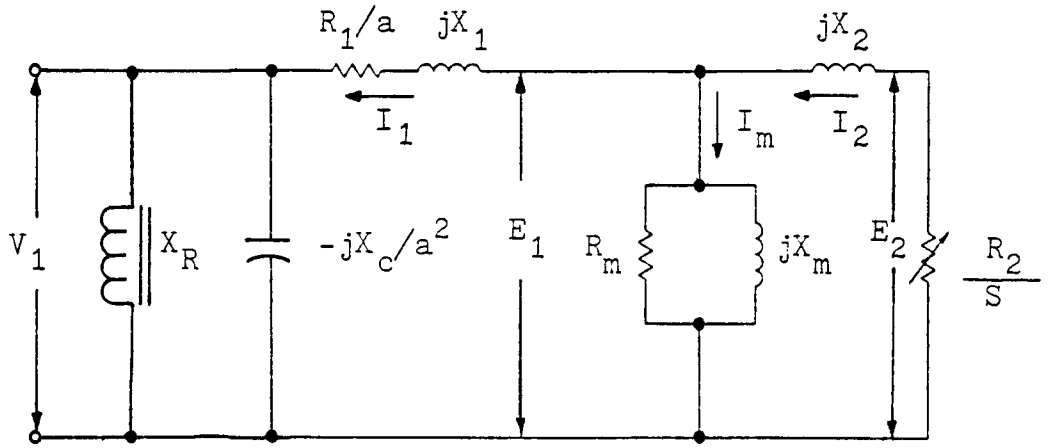


Figure 4-2. Improved the build-up characteristic of the capacitor-excited induction generator with external reactor.

OS = No-load Saturation Curve.
OR = Reactor Characteristic Curve.
ON = New No-load Saturation Curve.

A. No-load Saturation Curve



$a = \omega_e / \omega_1$

ω_e : self-excited frequency
ω_1 : normal angular frequency

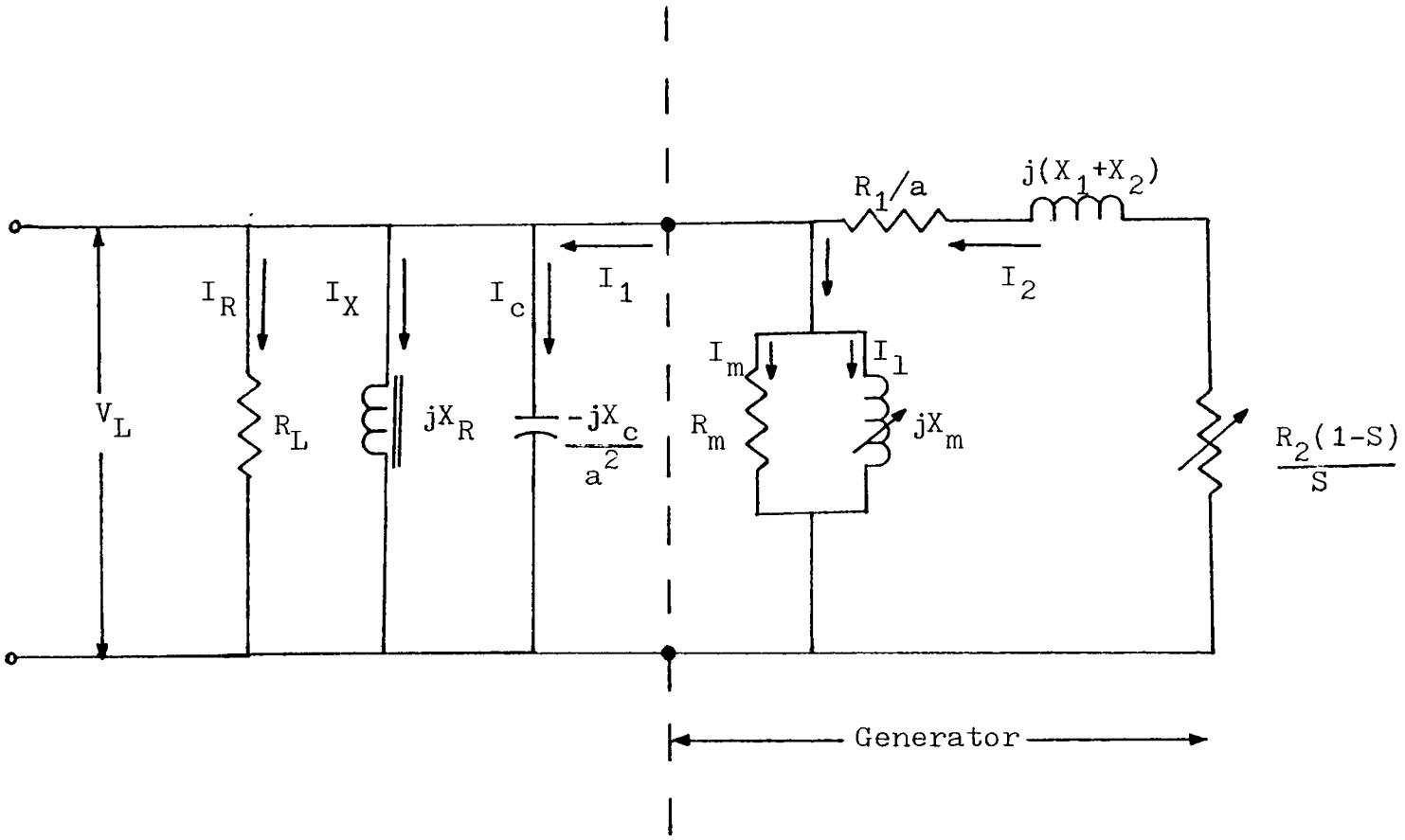
B. Per-phase Equivalent Circuit

Figure 4-2. (Continued)

curve). Under this condition, the generated no-load voltage V_o is much reduced (close to or equal to V_M). A per phase equivalent circuit of a machine connected with a capacitive reactance X_c and a saturable reactor X_R, is shown in part (B) of Figure 4-2. The equivalent circuit for any given self-excited frequency ω_e can be expressed in terms of the parameters R_1, R_2, X_1, X_2, R_m, X_m and X_c all referred to the normal angular frequency ω_1 by using a factor $a = \omega_e / \omega_1$. When $a = 1$, it means the frequency of excitation is very close to the synchronous frequency corresponding to the speed of rotor.

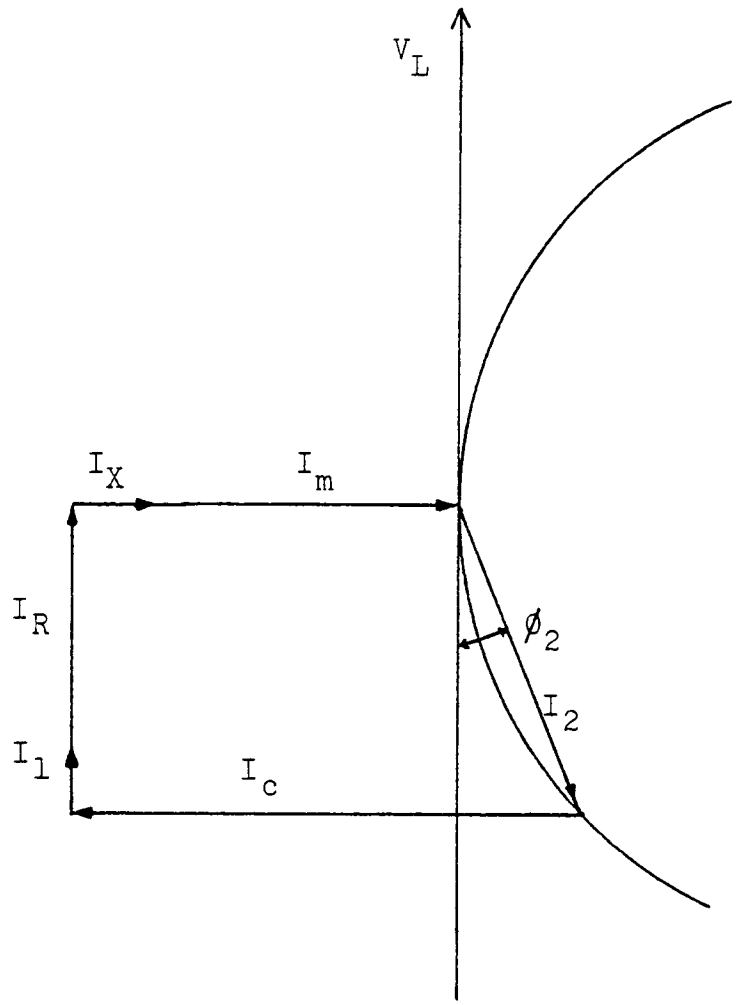
4-2 SLIP AND LOAD RELATIONSHIP

In the proceeding section the theory was developed for no-load performance. In this section a pure "Resistive" load is applied to the terminal of the induction generator and its external load-voltage characteristics will be discussed. Figure 4-3 illustrates an approximate per phase equivalent circuit of an induction machine with a resistive load R_L in parallel with the reactor X_R and excitation reactance X_c at the output terminal. Since the induction generator operates with a very small (2 to 5 %) slip, the slip-dependent resistance R_2/S in the equivalent rotor circuit shown in Figure 4-2(B) may be replaced in the approximate rotor equivalent circuit by $R_2(1-S)/S$. The slip S of the rotor can be defined as



A. Per-phase Equivalent Circuit

Figure 4-3. Capacitor-excited induction generator with external reactor and resistive load.



B. Current Phase Diagram

Figure 4-3. (continued)

$$S = \frac{\text{Rotor Copper Loss}}{\text{Power Transferred Across Air-Gap}} \qquad (4\text{-}1)$$

But under load condition, the generated power $V_L I_2 \cos \phi_2$ [Refer to Figure 4-3(B)] provides for the load power in R_L and the loss in R_m. The reactive currents must sum to zero,

$$\frac{V_L}{X_R} + \frac{V_L}{X_m} + I_2 \sin \phi_2 = \frac{V_L}{X_c} \qquad (4\text{-}2)$$

which determines the capacitive reactance X_c for a given load and voltage. The formula for the slip of an induction generator which related to the value of load resistance R_L, is given in [11], that is

$$\left[R_1 + \frac{R_L}{S}\right]^2 + \left[R_1 + \frac{R_2}{S}\right]\left[\frac{R_L R_m}{R_L + R_m}\right] + X_T^2 = 0 \qquad (4\text{-}4)$$

where $X_T = X_1 + X_2$. Because of the slip is independent of voltage and current, therefore the output (stator) frequency f_1 of an machine may not reliable when load is changing. In order to maintain a constant output frequency, the speed of the prime mover must rise with increase of load, to counteract the effect of the slip.

4-3 VOLTAGE REGULATION

Changes in load current can cause appreciable terminal voltage drop, but this drop can be avoided by installing a series capacitor between the output terminals and the load. Connecting a parallel reactor at the load decreases the effects of machine losses and terminal voltage waveform distortion.

In order to calculate the value of the reactor X_R, the equivalent circuit shown in Figure 4-3 must first be modified and replaced by the parallel connection shown in Figure 4-4. The value of the equivalent machine resistance R_P and equivalent machine reactance X_P are given in [11] and are

$$R_P = S[(R_1 + R_2/S)^2 + X_T^2] \; / \; (SR_1 + R_2) \qquad (4\text{-}4)$$

$$X_P = [(R_1 + R_2/S)^2 + X_T^2] \; / \; X_T \qquad (4\text{-}5)$$

The reactor X_R is used to minimize output voltage waveform distortion and to improve voltage regulation, therefore all the reactive currents in the circuit are set to zero [Referred to Equation 4-2 and Figure 4-3(A)]. The mathematical expression of a non-linear saturable reactor X_R is given by [11] that is in terms of the variable load resistance R_L as follows:

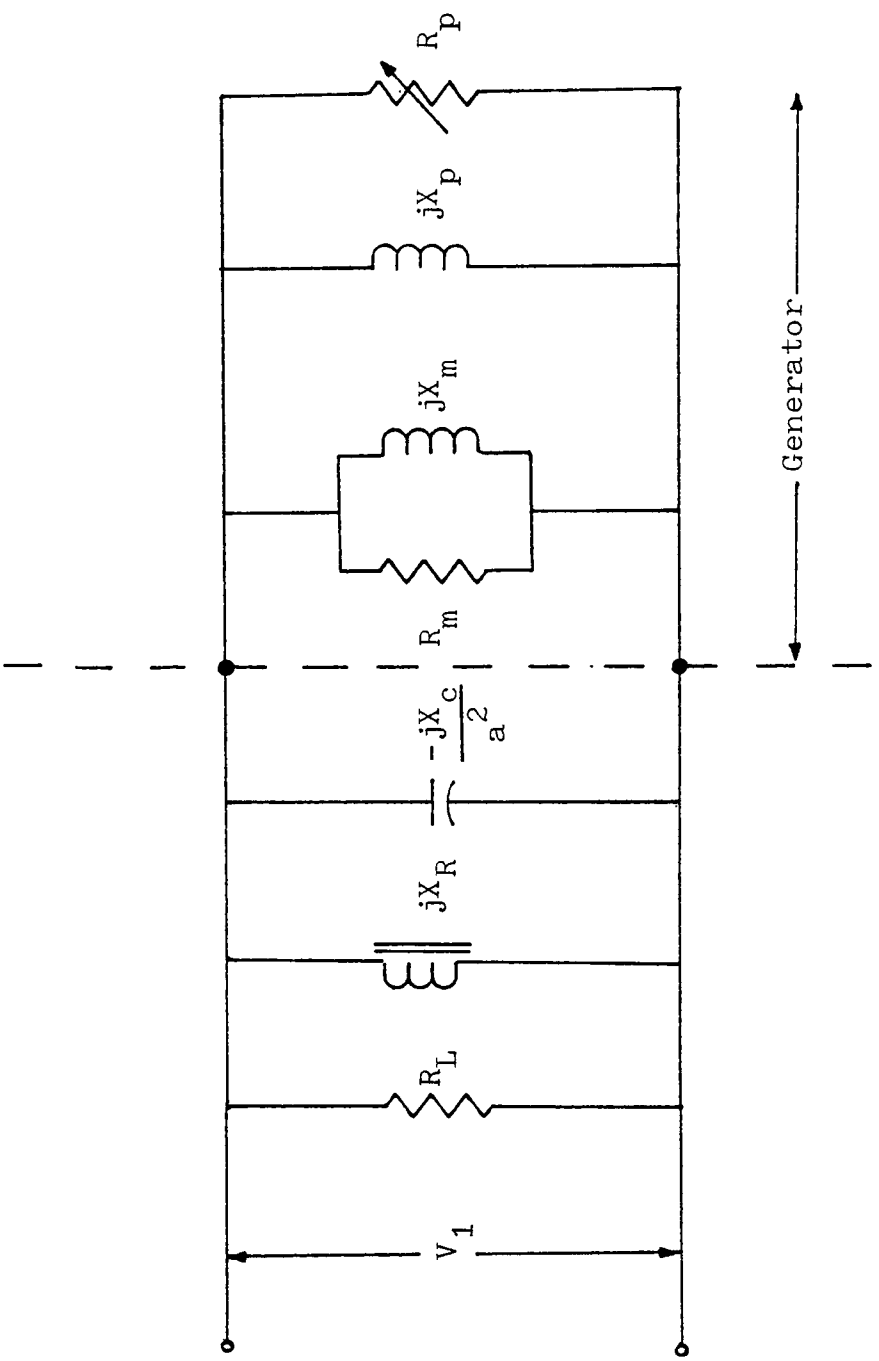


Figure 4-4. Per phase equivalent circuit of the capacitor-excited induction generator with modified internal machine parameters.

$$\frac{1}{X_R} = \frac{1}{X_c} - \frac{1}{X_m} - \frac{1}{2X_T} + \sqrt{\frac{1}{4X_T^2} - \left(\frac{1}{R_L} + \frac{1}{R_m}\right)^2} \qquad (4\text{-}6)$$

According to the above expressions, the amount of change in voltage or speed resulting from a load change is related to a particular value of $1/X_R$ which can be predicted by using the circle diagram. Although the external saturable reactor can be improved the output voltage regulation, it has some disadvantages. Due to the nature of the core material in the reactor, voltage waveform distortion appears as fifth and seventh harmonics. To improve the distorted output harmonic components in three-system, the reactor circuit can be re-connected, with a star to delta configuration, shown in Figure 4-5.

4-4 EXTERNAL LOAD CHARACTERISTICS

The induction generator, for any load, must operate at a definite power factor, regardless of the character of the external load. The current must lead the terminal voltage by an angle determined by the voltage and load on the machine. The performance of an induction generator can be limited by "Overloading" and "Sustained Short Circuits" occurring at the output. Due to these abnormal condition, an induction generator can collapse its terminal voltage and at the same time to collapse its excitation. To restore the residual magnetism in the machine, several methods may be used as follows:

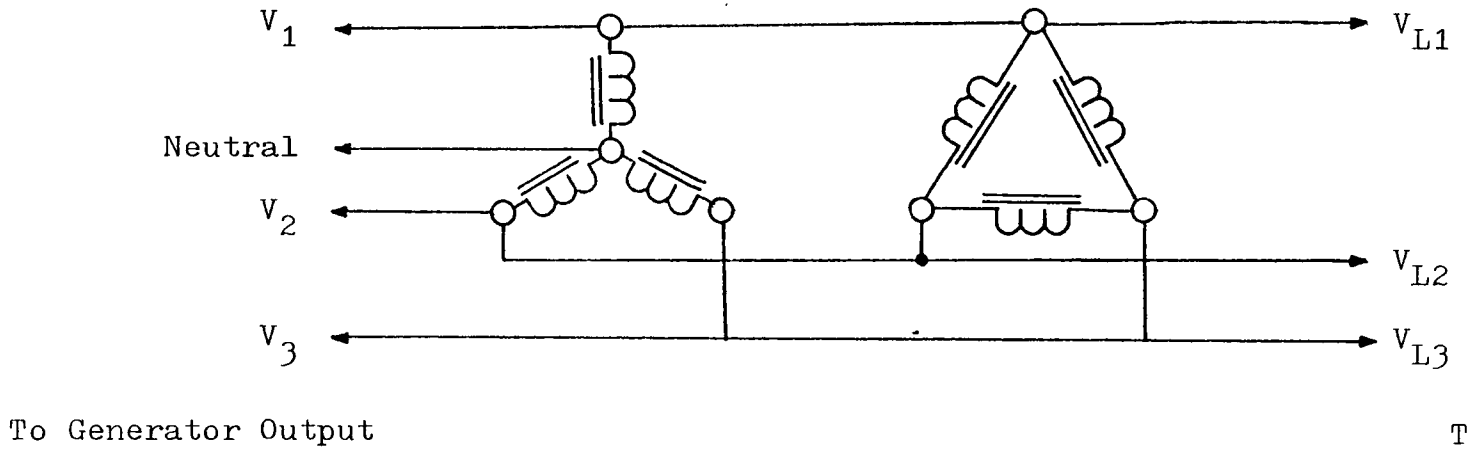


Figure 4-5. Reactor operating in parallel with wye and delta in three-phase system.

(1) Connect an external storage battery across the terminal.

(2) Run the machine as a motor.

(3) Discharge a condenser through the stator windings.

The power factor of an induction generator must at all loads be equal or bigger than the power factor of the whole system. In some cases the power factor of an external load is higher than that of the generator, therefore the induction generator will not build-up. After the power factor is corrected, the latter excites and its terminal voltage rises until saturation of the magnetic circuit is achieved.

4-4-1 With Shunt Load Connection

The generated voltage relationship shown in Figure 4-1 is corrected for no-load conditions only. When an external load is applied to the generator terminal, of course, the generated voltage characteristics are modified. Since the speed of the prime mover is decreasing with load, the reduction of a line frequency and speed occurs therefore the speed of the prime mover must be higher than that of the normal speed of the generator, to counteract the amount of slip. The speed of an induction generator increases to

increase the power output. The change of frequency with load will be much the same as the drop in the rotor speed with load in an induction motor.

Now consider an unity power factor load connected to the terminal of an induction generator. The load-voltage characteristics are shown in Figure 4-6. The curve falls off is rapidly with the load is increasing. To reduce the rate of voltage drop and maintain an machine with a high degree of saturation, the terminal voltage must be held up. By inserting a series capacitor [Refer to Figure 4-7(B)], the output voltage curve approaches zero voltage regulation. Leading loads can maintain the terminal voltage, but lagging loads decrease the terminal voltage rapidly.

A short circuit of an induction generator would not cause a serious rise in current, such as occurs in synchronous generators, because the series initial rush of current is limited by the leakage reactance of the machine. The short-circuit current is equal to the terminal voltage divided by its leakage reactance. The sustained short-circuit current is zero since the excitation to the machine would go to zero automatically.

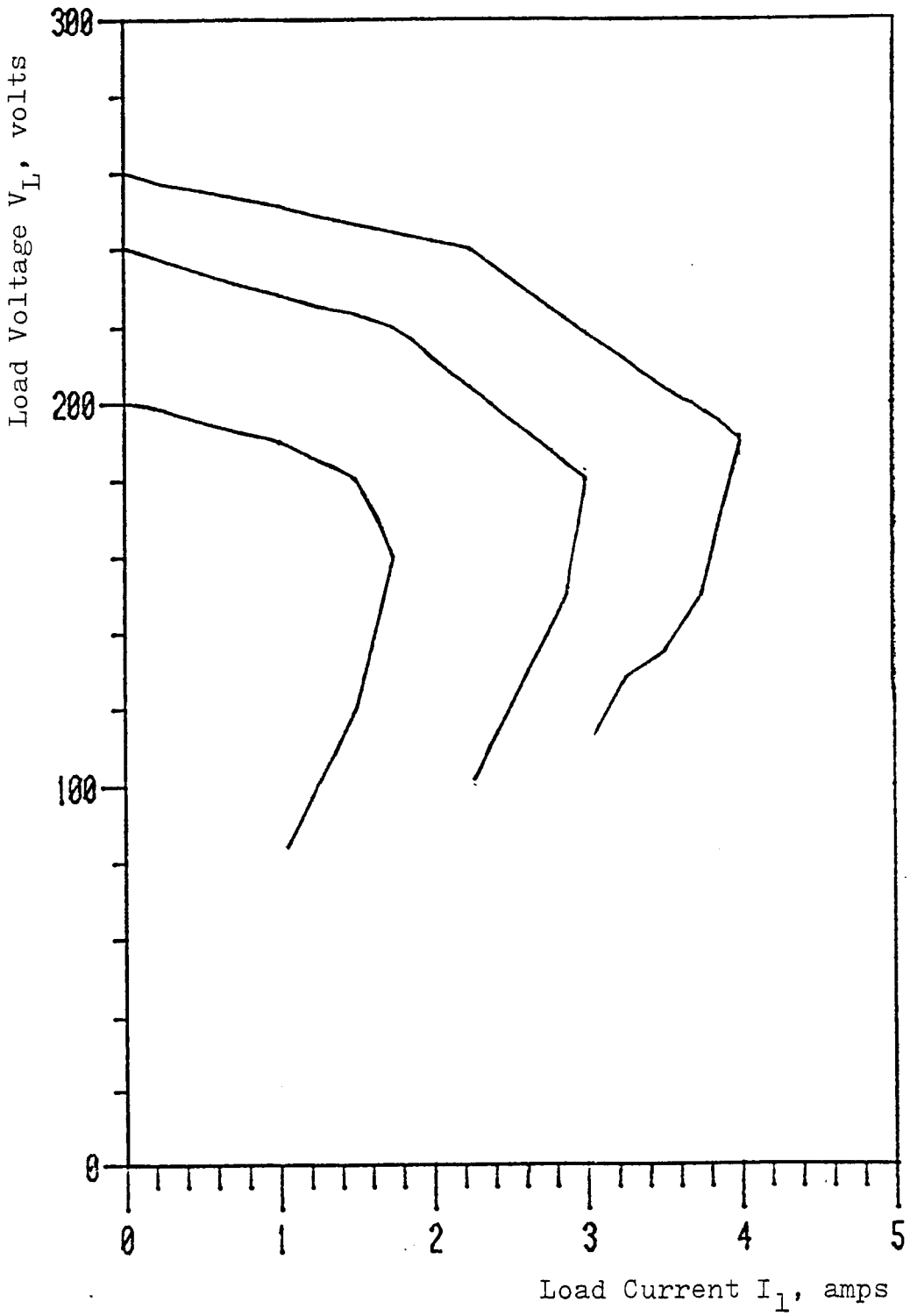
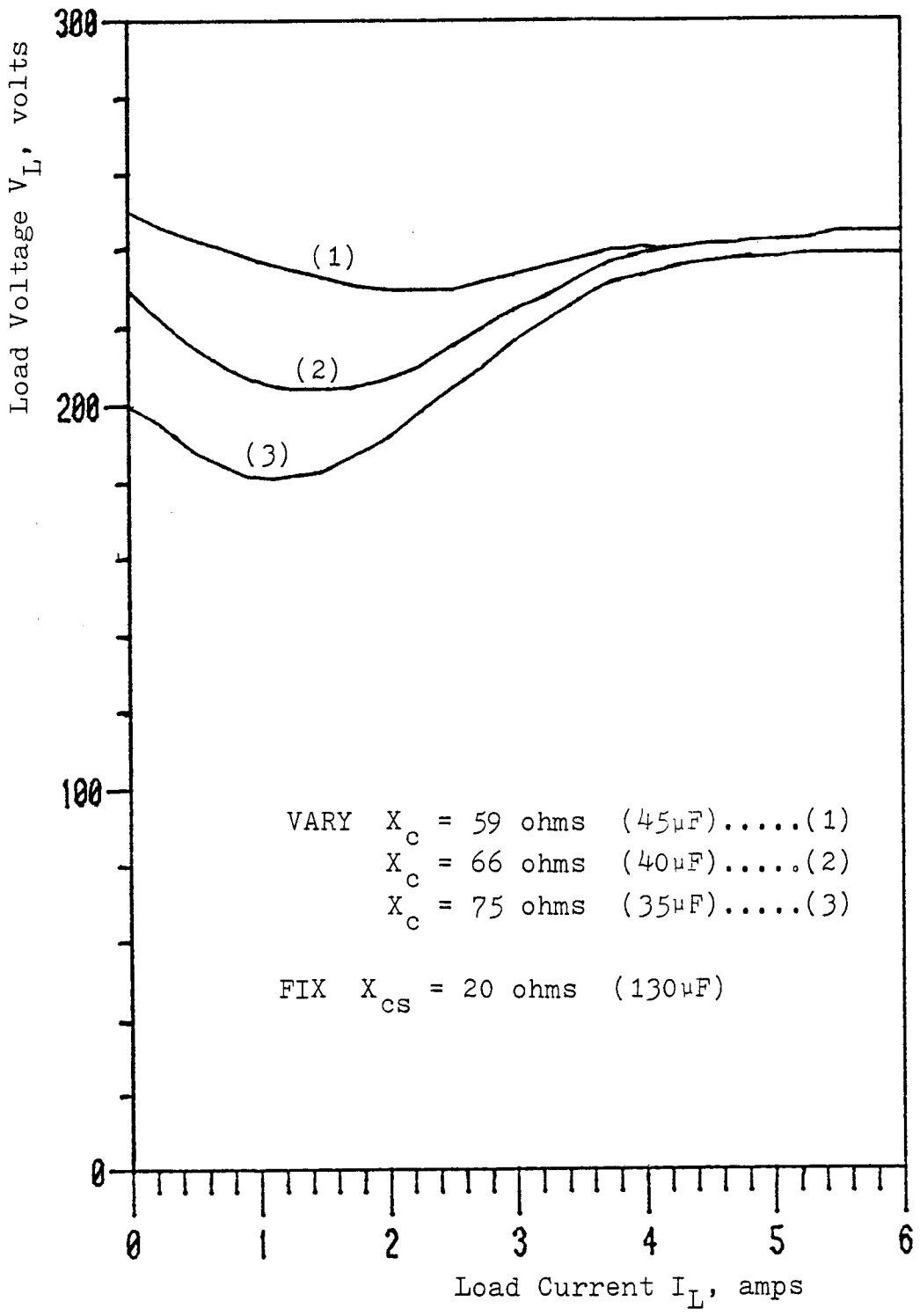


Figure 4-6. External performance of the induction generator with a unity power factor load.

4-4-2 Compound Load Connections

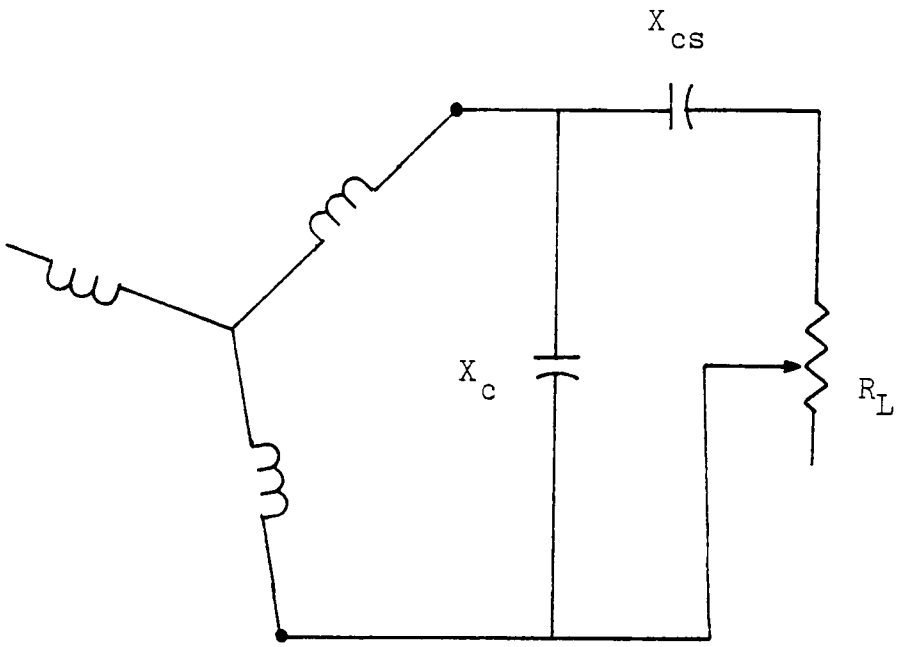
In order to maintain terminal voltage, series capacitors may be placed between the excitation capacitance and the output load. The capacitor provides power factor improvement and maintains a leading current to the load causing the terminal voltage to hold up longer. Figure 4-7 shown the test results of the machine by inserting series capacitor with load. The optimum value of a series capacitive reactance X_{cs} is approximate equal to the effective induction reactance X_m of the machine winding, to get the best hold up voltage characteristics. The series capacitor can be thought of as a negative reactance that neutralizes the machine inductive reactance, leaving only the resistance component. In this case, fluctuating loads will have a little effect on voltage drop.

Some typical load characteristics of the machine, are plotted (1) with the machine terminal voltage V_1 and load voltage V_L in Figure 4-8, (2) with the slip S in Figure 4-9, and (3) with the power factor p.f. in Figure 4-10, and (4) with efficiency η in Figure 4-11 against the real power output. In the Appendix B.2.2, it given the expressions for those powers and the methods of calculation.



A. Characteristic Curve

Figure 4-7. External performance of the induction generator by inserting series capacitor with load.



B. Test Circuit

Figure 4-7. (Continued)

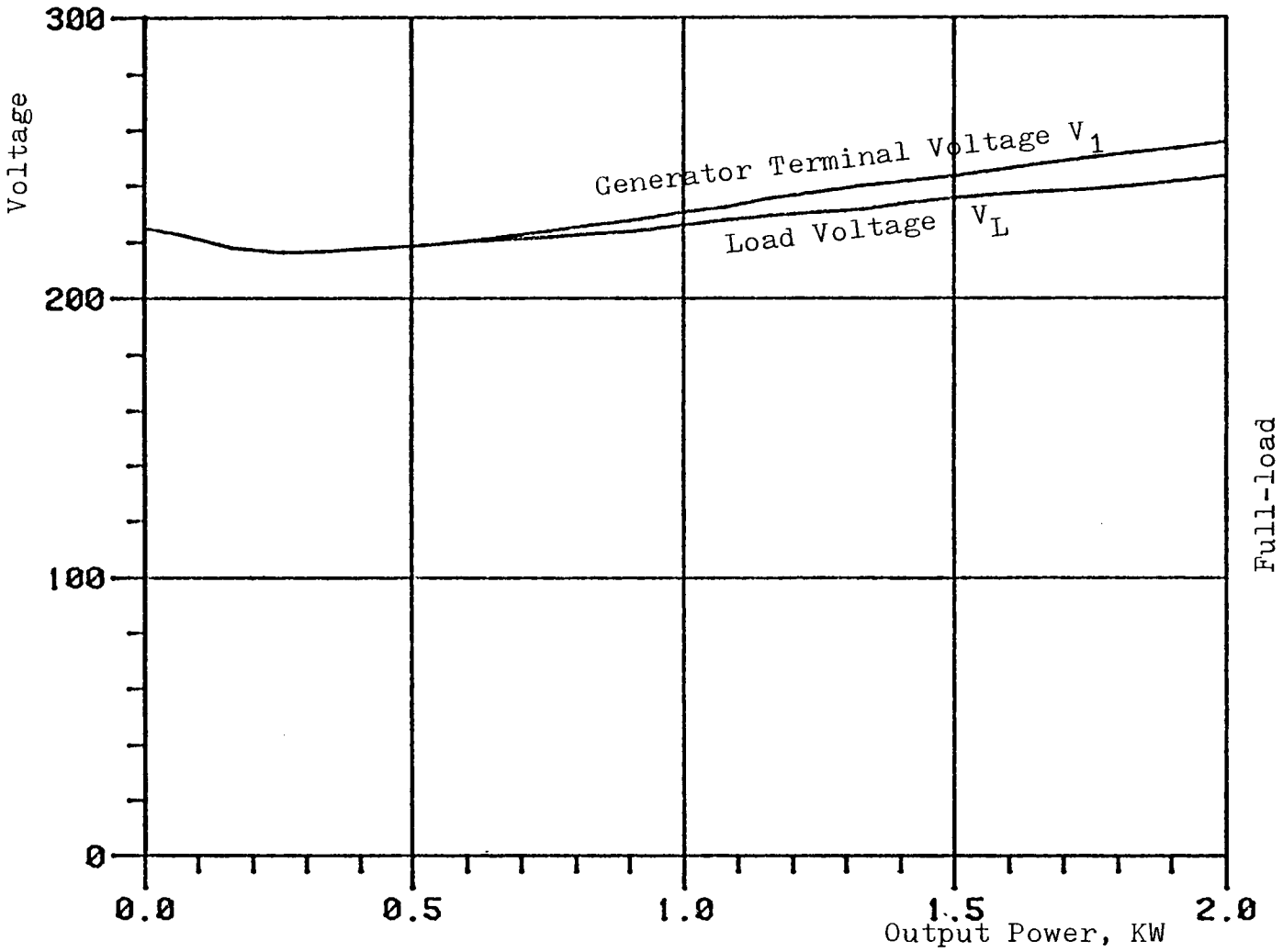


Figure 4-8. Terminal voltage and load voltage versus output power of the induction generator.

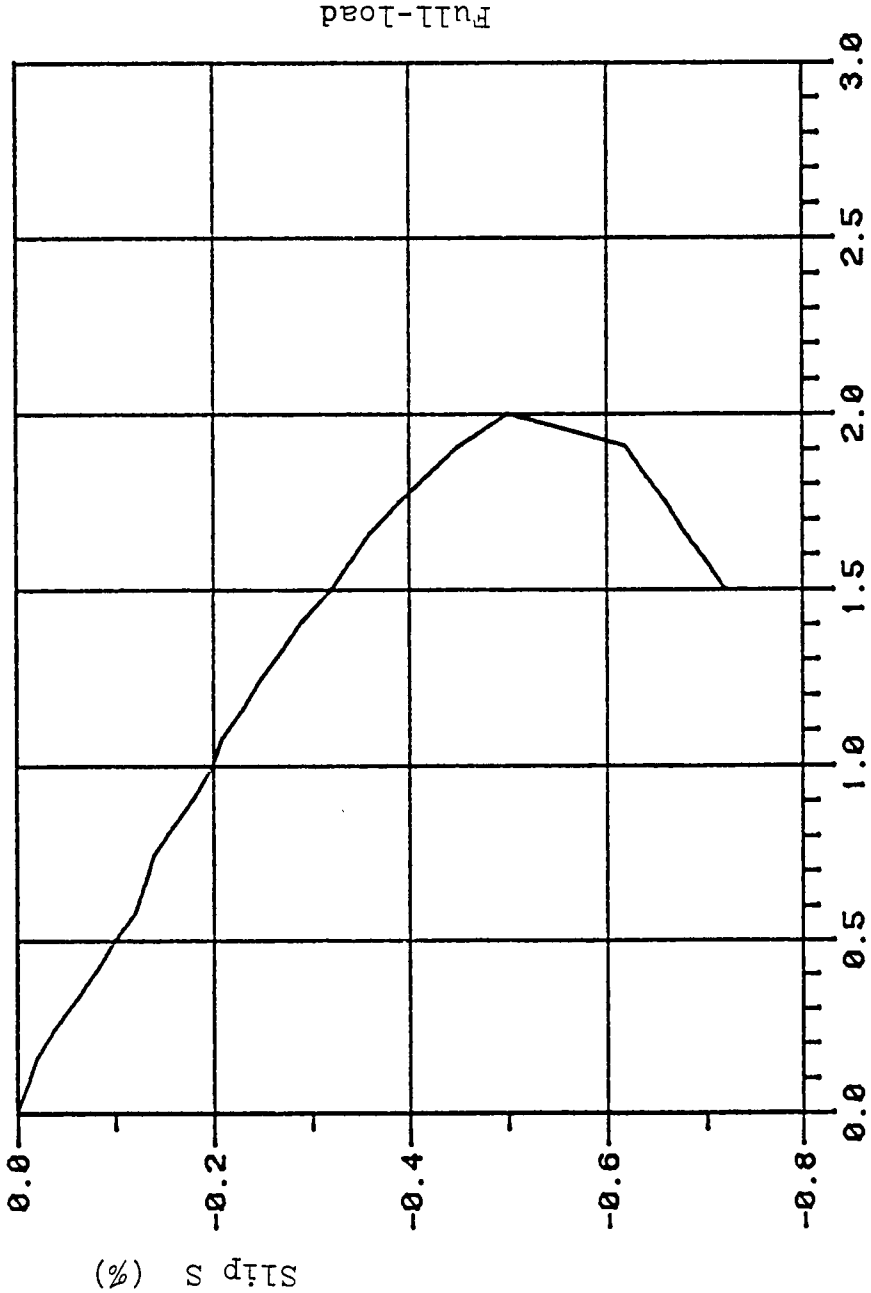


Figure 4-9. Slip versus output power of the induction generator.

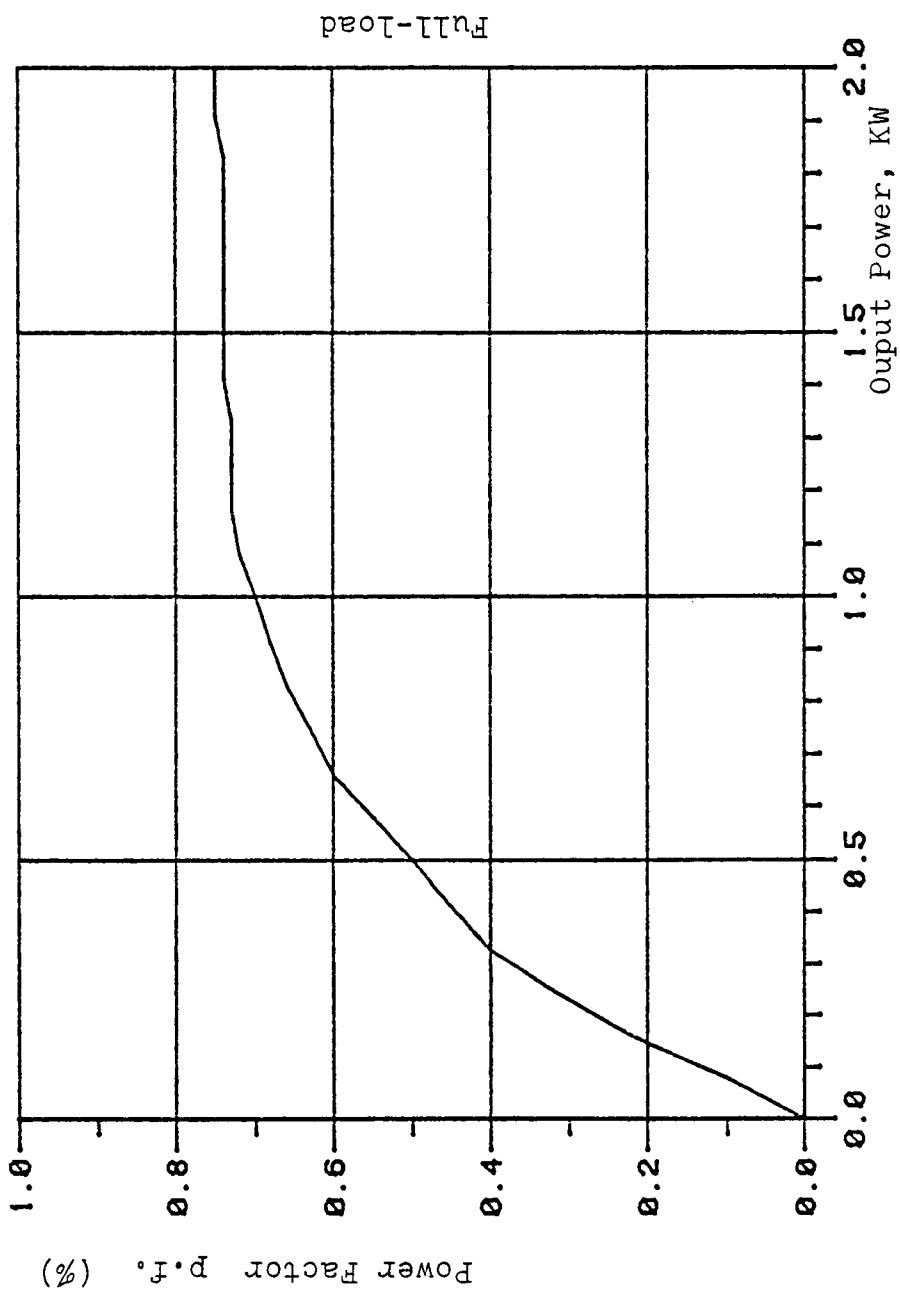


Figure 4-10. Power factor versus output power of the induction generator.

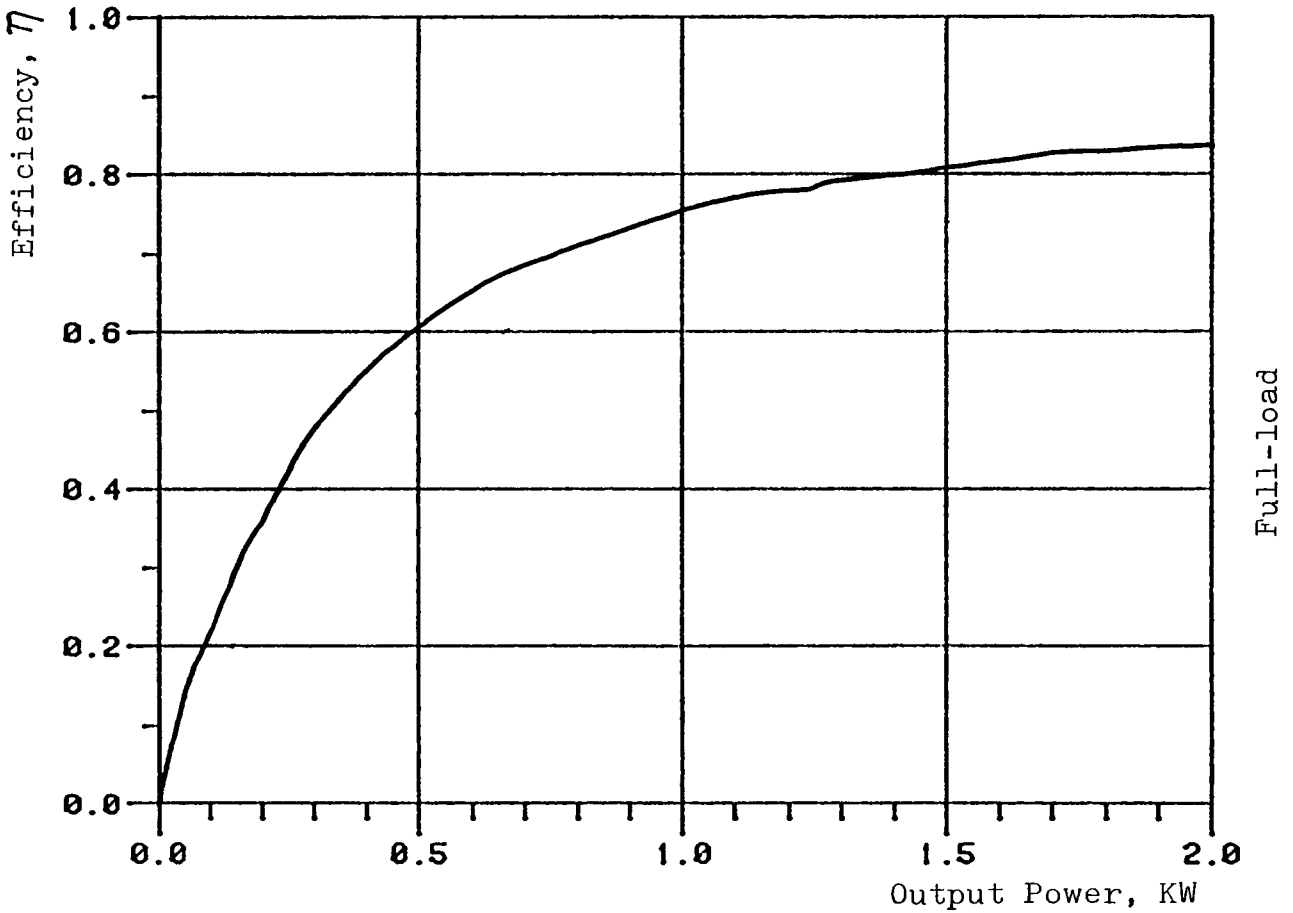


Figure 4-11. Efficiency versus output power of the induction generator.

4-5 CONCLUSION

With the magnetizating reactive power provide by an exciting capacitance bank, an external ac supply is not needed; but the operating frequency and the generated voltage are affected by the speed, load and capacitor rating. The exciting capacitor must also supply any lagging reactive power demand which means that the machine operates at a leading power factor at its output.

The capacitive-excited induction generator has rather poor regulation characteristics, which can be improved inserting parallel saturable reactors with a rating equal to the generator magnetizing reactance. The VSCF power generating system did not use saturable reactors therefore there was a tendency for the machine to overheat during operation. The main advantages of using an induction generator may be summarized as follows:

(1) Self-excited type of installation may make a profitable an independent source of sine wave power.

(2) Construction and operation are simpler than that of an equivalent synchronous machine.

(3) Overspeeding causes no over-voltage but increase in frequency, both of which are dependent upon the capacitor rating.

(4) A line fault causes no serious rise in current

because it is limited by the leakage reactance of the machine.

(5) The machine can be handle all types of load if the power factor of the external circuit is equal to or lower than the power factor of the induction generator. If not we can insert a series capacitor and the load power factor would be improved.

(6) A squirrel-cage induction machine is so common and much easier to offer. This type of machine can have capable to performing both duties (motoring and generating mode) with high efficiency.

The main disadvantages of using an induction generator may be summarized as follows:

(1) The weight of the bulk of capacitors necessary for excitation are heavier than a synchronous generator and exciter.

(2) The voltage regulation is poor if a saturable reactor and a series capacitor are not available.

(3) The output frequency and voltage are restricted by the speed, load and capacitor rating.

(4) Restoration of the rotor magnetism is necessary when (i) a line fault causes loss of the terminal voltage since loss of voltage means loss of excitation, and (ii) overloading causes loss

of terminal voltage because it is impossible to have an infinite energy output since the excitation is fixed by the design requirement.

CHAPTER 5

APPLICATION IN A VSCF SYSTEM

This chapter describes the theory necessary for designing the controller of a frequency changer. Proper controlling of the CDFFC in a VSCF system will provide a lagging power for machine excitation obviating the necessity of external static capacitors.

A new firing control technique called "Integral Control" is introduced which employs closed-loop feedback to control the thyristor firing instants. Compared to the well-known cosine wave crossing method [Refer to Figure 2-7], the present control method is complicated and more reliable in a variable-speed system. The experimental waveforms of a six-pulse frequency changer, evaluated in the laboratory, compared well with the theortically waveforms of a six-pulse frequency changer.

5-1 CONTRUCTION OF A VSCF SYSTEM

A block diagram of the VSCF system is shown in Figure 5-1. The system consists of an induction generator driven by an unregulated prime mover, which supplies variable generator frequency ac power to a CDFFC. The CDFFC uses TRIACs as a cycloconverter converting the variable input frequency power to one which is at a precisely controlled lower output frequency.

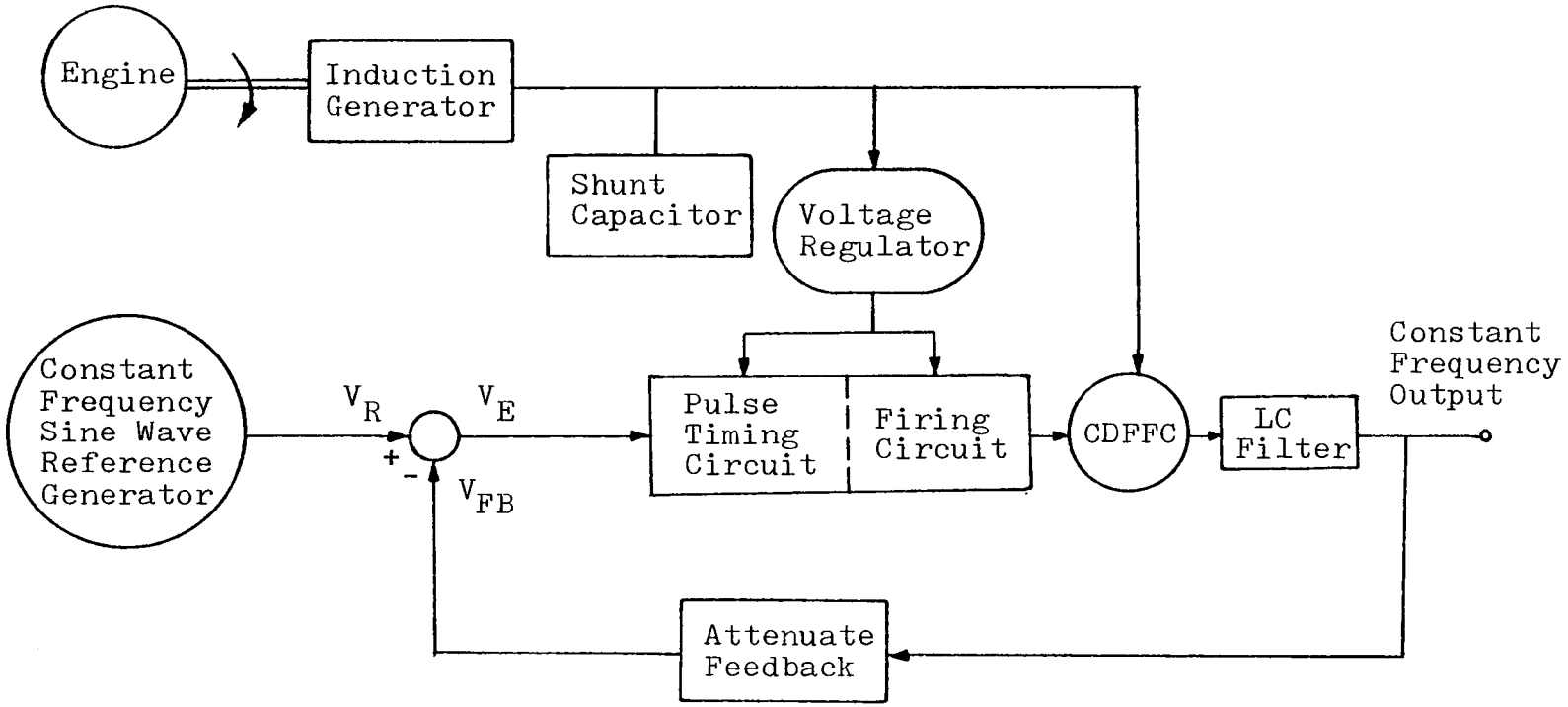


Figure 5-1. Block diagram of the VSCF power-generating system.

The capacitor-excited induction generator operates over a speed range of 1500 to 2100 rpm and delivers power at 45 to 80 Hz. The system output is rated 240 volts, single-phase and 20Hz. The CDFFC programmed with a 20Hz sinusoidal reference wave and regulated voltage waves derived from the generator, is given an output that is essentially 20Hz plus some high ripple frequencies. The output waveform of the frequency changer is then filtered by a small LC filter. The size and weight of this type of filter can be reduced by increasing the frequency or decreasing the amplitude of the ripple to meet specifications on waveshape.

The timing signals of the corresponding control block output, determined by the analogue error signal V_E which is derived by comparing a reference input signal V_R against a negative feedback signal V_{FB}, vary the phase position of the pulse trains at different instants of time. These timing pulses go through a firing circuit triggering the switches of a frequency changer and controlling the desired output frequency f_o, output voltage V_o, and input displacement angle ϕ_I. After the correction is made, the feedback signal V_{FB} causes the reduction of an error signal and maintains stability of the system within desired limits.

Proper control of the leading or lagging input current by the CDFFC allows any desired input displacement factor to be obtained independently. Since the output LC filter is always capacitive, the CDFFC has the ability to supply/draw the leading/lagging reactive current to/from the generator for machine excitation. In order to avoid generator failure due to an abnormal condition, a stand-by system is required consisting of shunt capacitors placed between the output lines to supply lagging reactive power. This method is universally applied on power system to suply the KVAR necessary for a desired power factor improvement. In some static system, the input shunt capacitor is common used as a turn-off device (thyristor commutation) and/or input filter. But in this VSCF system, it becomes an excitation device and input filter. It provides a low impedence path to suppress switching transients, filter the extrabasal component, and cancel the quadrature component of the input current.

The generator voltage regulator produces an error signal to the CDFFC, to adjust the leading/lagging input displacement angle ϕ_I by sensing the input reactive current. For optimum control, the input displacement factor of the frequency changer should be set as leading as possible (more capacitive) for the initial build-up voltage of the generator.

5-2 CONTROL SYSTEM OF A CDFFC

In order to generate positive-type waveforms or negative-type waveforms for half the total operating period at the output, it is necessary to have two separate timing control channels. These channels require some control mechanism for switching from one waveform type to the other. Each timing channel in continuous operation provides a continuously running wave either positive-type or negative-type. Figure 5-2 is the basic control system of CDFFC which consists of two timing control channels. In correspondence with the output switching signal $E(\rho)$ and $E_{\pi}(\rho)$ on these channels, output frequency and input phase angle are independently controlled that is the unique operating characteristics of a CDFFC.

The phase position ϕ_o of the positive-type segments and the negative-type segments at the output voltage waveform controls the input displacement factor ϕ_I of a frequency changer. Generally the CDFFC allows a circulating current to flow in the load during any conducting period of time. Therefore bidirectional switches (i.e. TRIAC) are required. The firing pulses to a single array of bidirectional switches of a CDFFC are generated by a single set of firing circuits. These pulses are transmitted through the timing channels to control the switching mechanism from one waveform type to other.

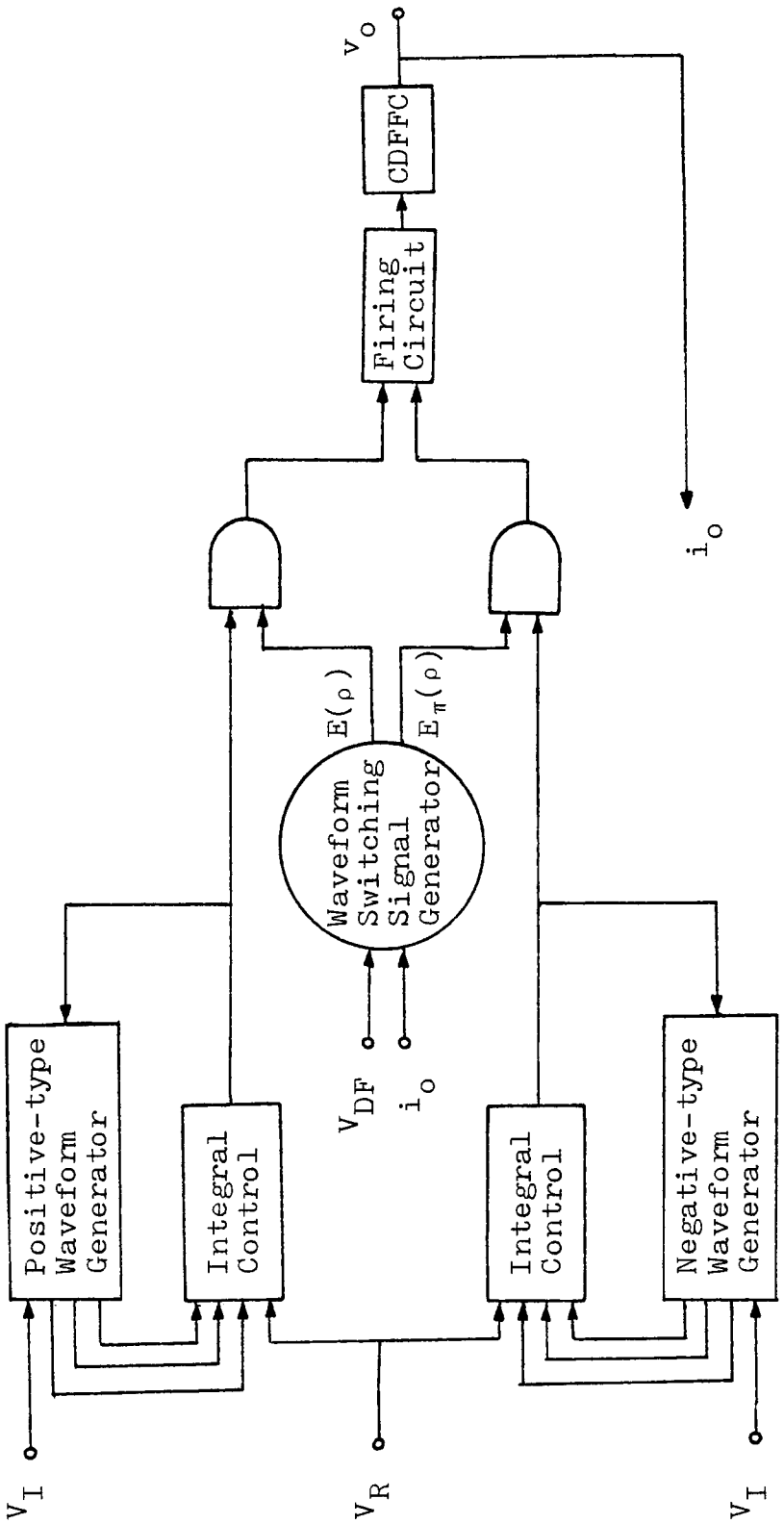


Figure 5-2. Control system of a CDFFC.

The output voltage waveform of a CDFFC is dependent on two variables, switching angle ρ and output voltage ratio r [Refer to Equation (3-7)]. The phase shift of the output voltage is adjusted by the periodic switching functions $E(\rho)$ and $E_{\pi}(\rho)$ [Refer to Equation (2-26) and (2-27)]. If the amplitude of the periodic switching signal $E(\rho)$ or $E_{\pi}(\rho)$ is unity ("On" state), the output would become positive-type or negative-type waveform, respectively. By shifting the positive-type segments and the negative-type segments waveform at the output with respect to the output current wave, the output phase angle of a frequency changer will be varied. The intervals during which the converter switches are operated at high and low rates $(f_I + f_o)$ and $(f_I - f_o)$ depend upon the control angle σ.

The block diagram of the adjustable phase control circuit is shown in Figure 5-3. It provides the waveform switching signals $E(\rho)$ and $E_{\pi}(\rho)$ synchronized to the output current of a frequency changer. The amplitude of the displacement factor reference V_{DF} (external supply) controls the output phase delay of the switching signals $E(\rho)$ and $E_{\pi}(\rho)$, with respect to the input current wave i_o. In the case of an increase/decrease of V_{DF}, the frequency of the voltage controlled oscillator (VCO) output will be increased/decreased, and the output phase delay switching signals $E(\rho)$ and $E_{\pi}(\rho)$ will be advanced/retarded. In order to maintain a stable system, V_{DF} must be set within the

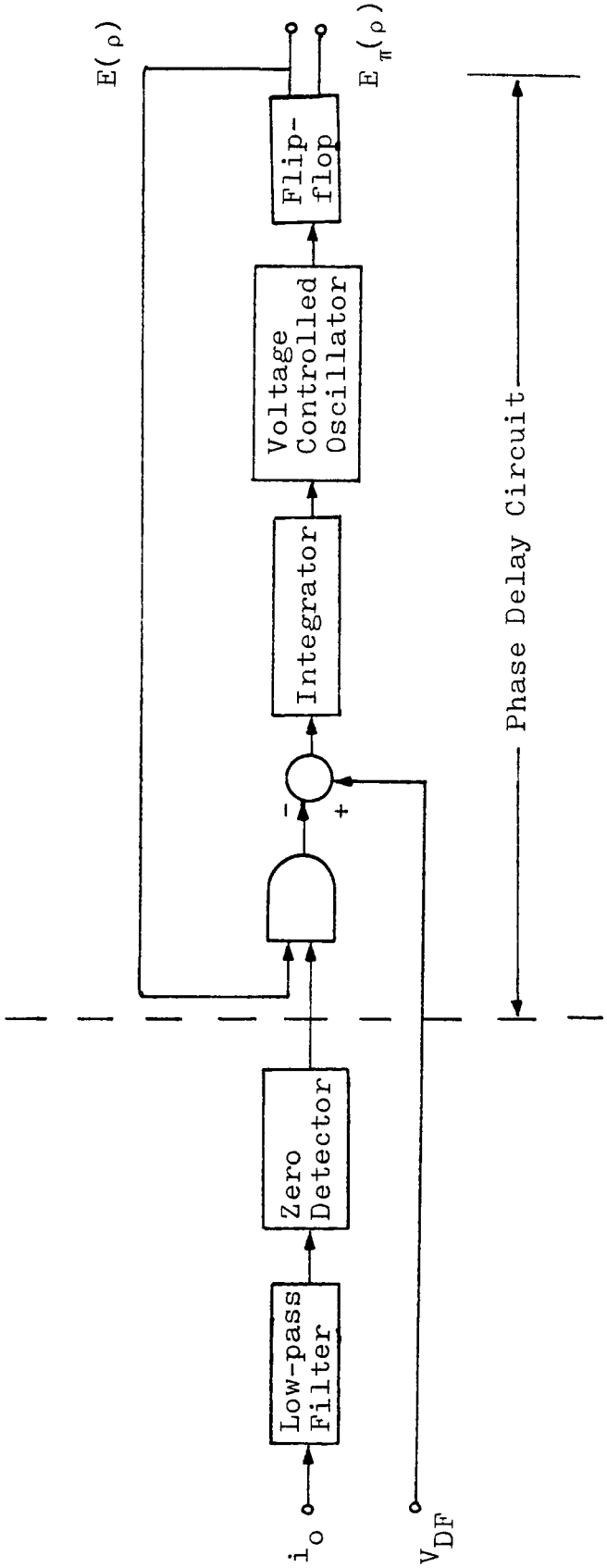


Figure 5-3. Phase control circuit of a CDFFC.

required maximum and minimum limits. Failure to maintian V_{DF} within these strict limits will cause the input displacement factor of a frequency change not to be controlled. The "End-Stop Control" method shown in Figure 5-5 is one practical technique for ensuring that V_{DF} stays within the limits.

Due to the difficulty of using the cosine wave crossing control method [Refer to Figure 2-7] in a variable-speed system, another timing control technique "Integral Control" method is utilized as shown in Figure 5-4. It provides a self-contained corrective feedback to control the firing delay. The difference voltage between the reference voltage V_R and the feedback voltage V_{FB} from the output is applied to the integrator. Since the gain of integrator is inversely proportional to the frequency of the input, it is similar as a low-pass filter (i.e. Gain = $1/j\omega RC$). After integration, it may have some ripple voltage amplified and appeared at the output of integrator. This integral of ripple voltage is a correction signal which determined the switching instants of the timing signals and is applied at the input of the zero detector. When the zero detector detects the zero crossing points of the integral of the riple voltage, a train of pulses are produced and act as the triggering input to the clock pulse generator.

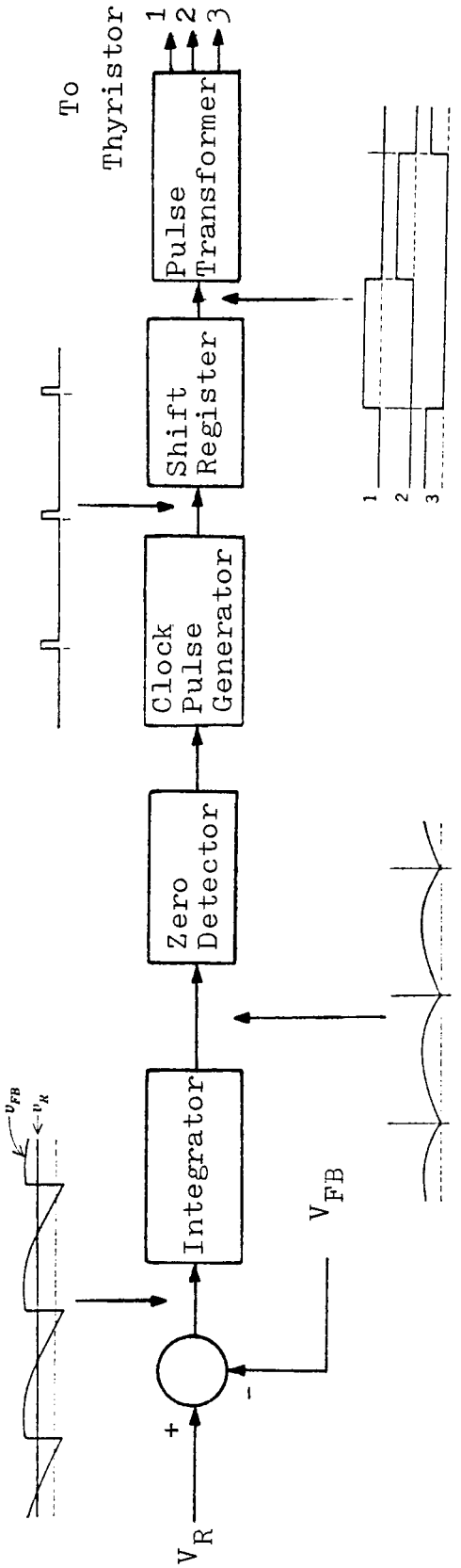


Figure 5-4. Firing pulse generator using integral control principle.

This firing control scheme is a close-loop feedback that automatically changes the firing instant in order to improve the output performance. When the output voltage of the frequency changer is increased/decreased, the feedback voltage magnitude will increase/decrease and then the integral of ripple voltage will increse/decrease at the output of integrator. Therefore the zero crossing points of the ripple voltage will be retarded/advanced, and the output voltage of the frequency changer will automatic decrease/increase.

The practical firing control scheme for a six-pulse CDFFC is shown in Figure 5-5 utilizing the integral control method. To provide a separate continuously running positive-type and negative-type waveform, two generators are required which are "Positive-type Waveform Generator" and "Negative-type Waveform Generator" [Refer to Figure 5-2]. Each generator consists of a group of low power circuits with three outputs [Refer to Figure 5-8], a six-pulse frequency changer which is the same as the power circuit of the CDFFC.

The typical waveforms from a six-pulse frequency changer in the positive timing channel, with zero reference voltage, are illustrated in Figure 5-6. The input waveforms of the half-wave integrators and main integrator are fed by the positive-type waves which are generated from the

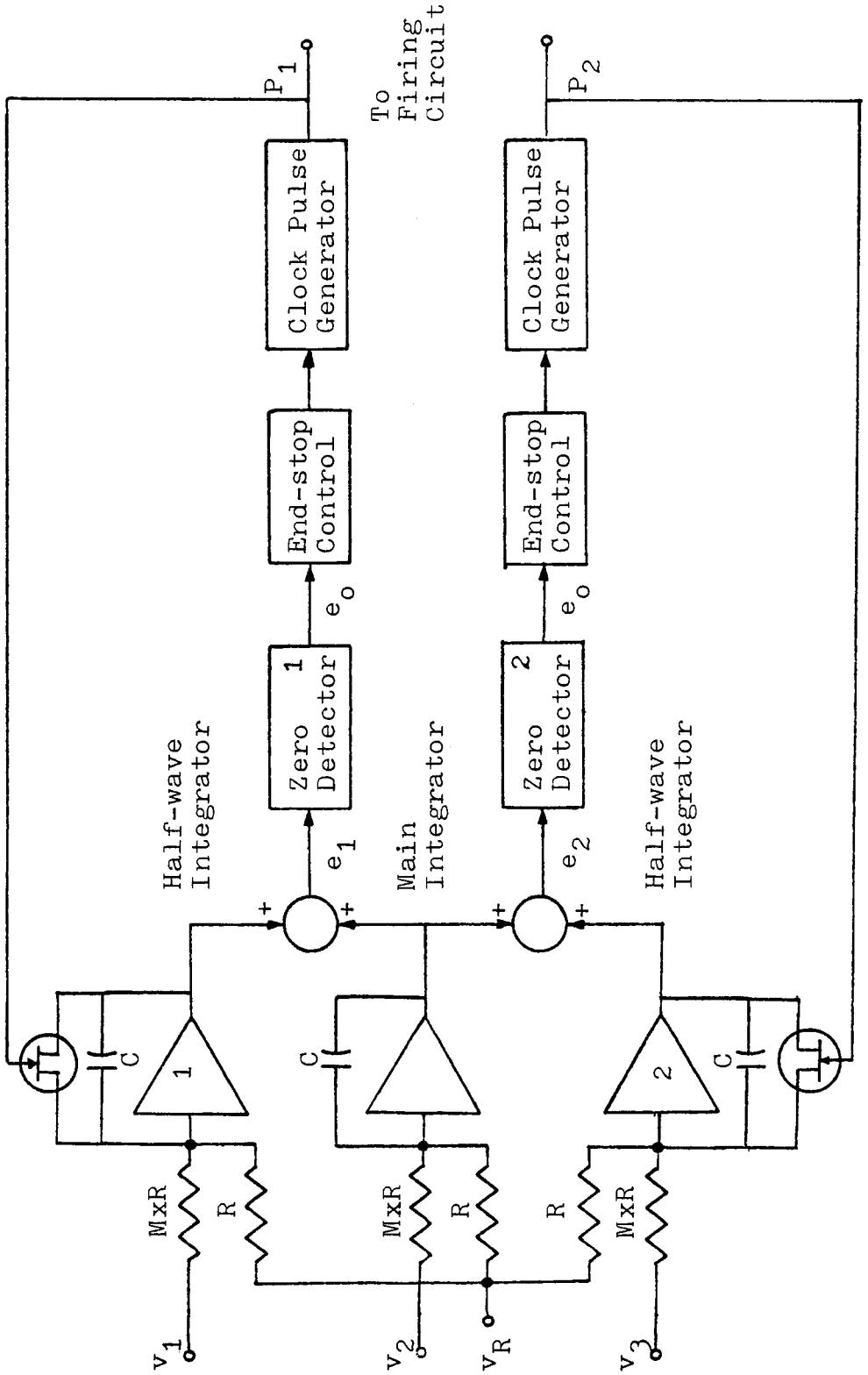
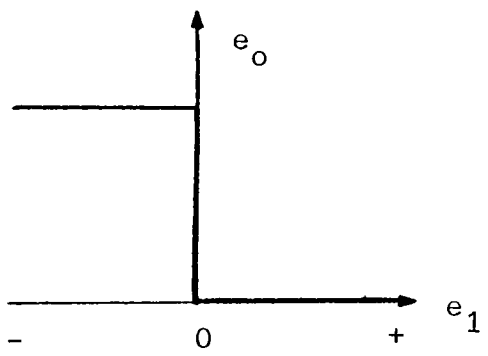
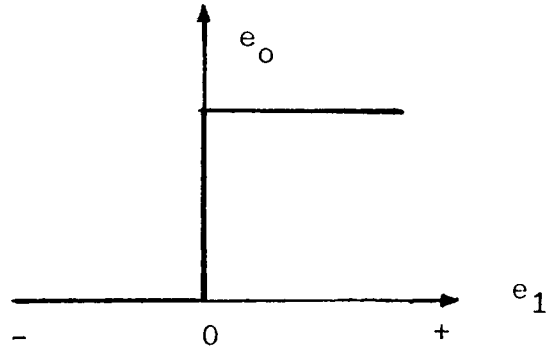


Figure 5-5. An integral control for a CDFFC.

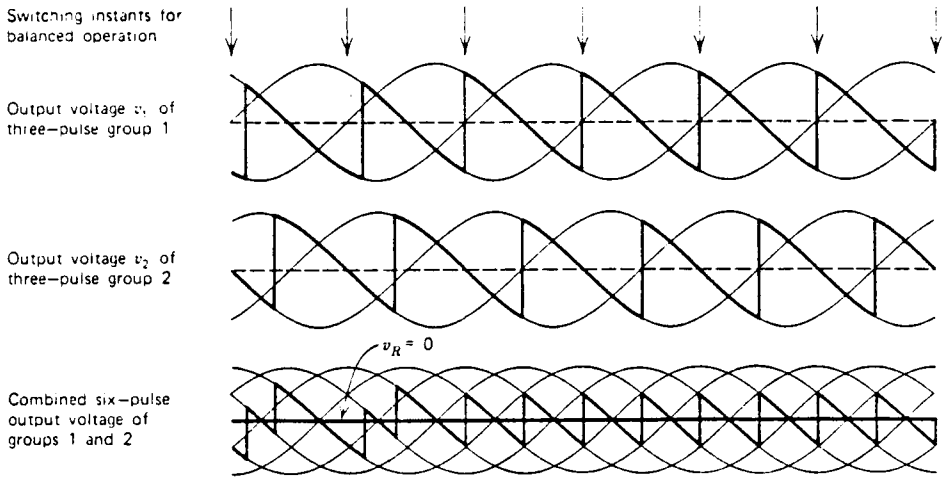


Transfer Characteristics of Zero Detector 1 and 2, for Positive-type Output Voltage v_o

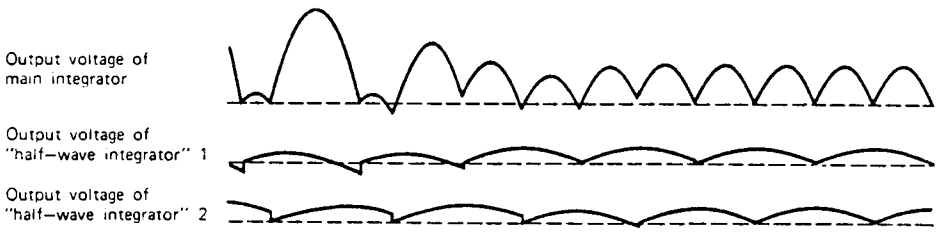


Transfer Characteristics of Zero Detector 1 and 2, for Negative-type Output Voltage $v_{o\pi}$

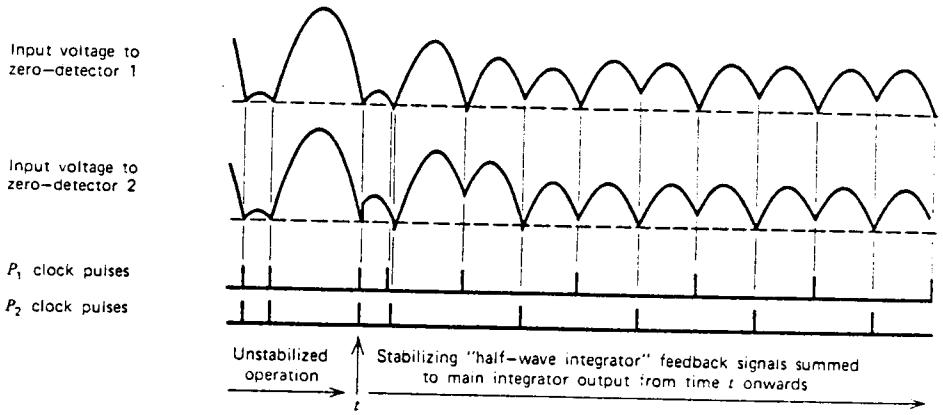
Figure 5-5. (Continued)



A. Input Waveforms of Integrators



B. Output Waveforms of Integrators



C. Zero Crossing Ripple Voltages and the clock pulses

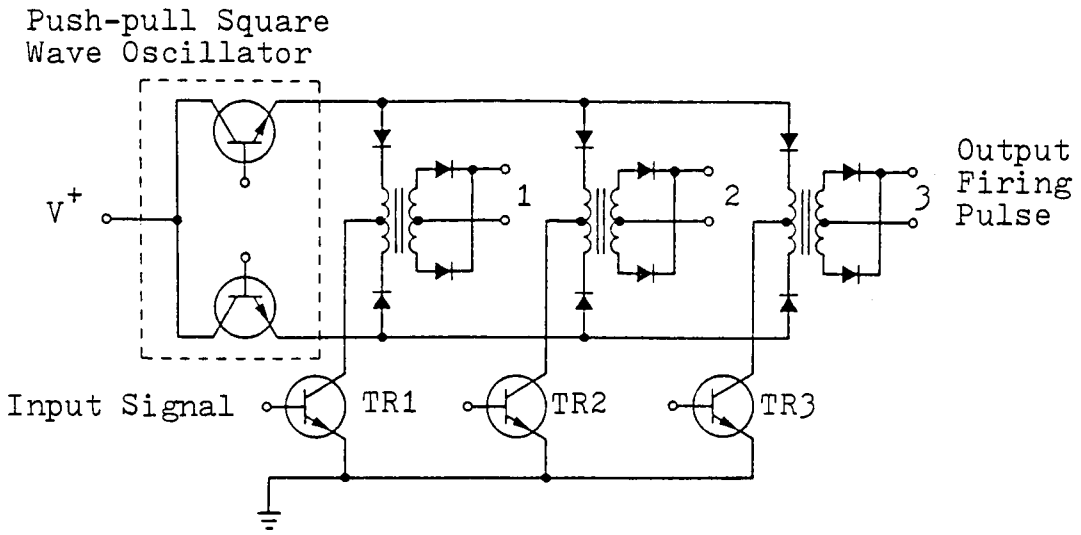
Figure 5-6. The associated waveforms of a six-pulse CDFFC, with integral control method.

positive-type waveform generator. The gain of the half-wave integrator is relatively small compared to the gain of the main integrator. M is an attenuate factor of output voltage V_o and feedback voltage V_{FB} (i.e. $M = V_o/V_{FB}$). The gain ratio of these two type of integrators is about 5 to 20. The difference between the reference voltage V_R and the output voltage of each individual groups of v_o, v_1 and v_2 are integrated by the integrators. The output of main integrator will sum with the output of half-wave integrators "1" and "2" and will transfer to zero detectors "1" and "2", respectively. The transfer characteristics of each zero detector in this control scheme is just for construct the positive-type waveform only. The zero detector detects the zero crossing points of the integral of the ripple voltage and then feeds to the input of each clock pulse generator. The successive clock pulses P_1 and P_2 change the three conduction states of each shift register and delivers a total of six separate timing signals in regular sequence at the output. These firing instants of the switches correct and improve the output waveform fabrication. The pulses P_1 and P_2 are also fed back to reset the half-wave integrators. The desired firing instants of the thyristors form the positive-type waveform at the output of the frequency changer and are produced by means of a train of clock pulses.

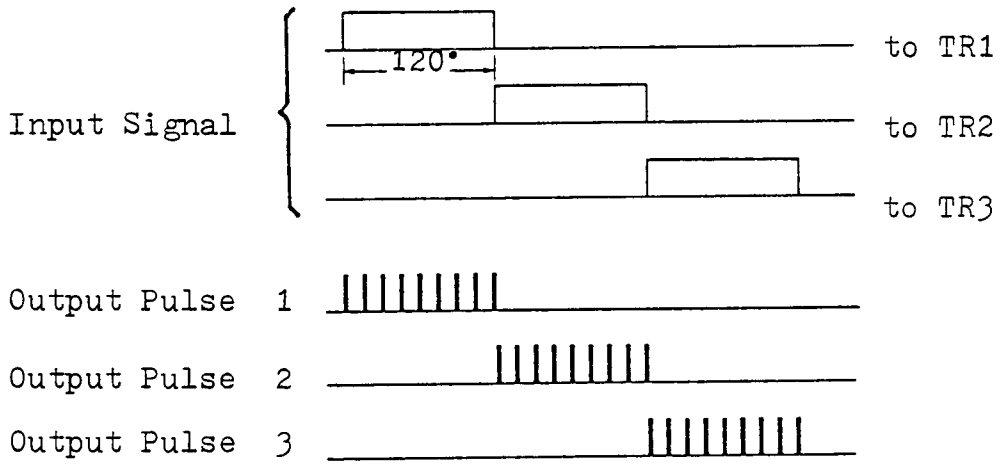
For constructing the negative-type waveform at the output of the frequency changer, a "Negative-type Waveform Generator" is required. The output waveforms of the negative-type waveform generator are fed back to another integral control scheme which is similar as the positive-type output control has been previously discussed. But ensure change the transfer characteristics of each zero detectors "1" and "2" in the control block [Refer to Figure 5-5] that is presented for construct the negative-type waveform only.

In order to obtain the high (di / dt) required to fire the thyristor more than once at any point within the period of the firing pulse, the scheme illustrated in Figure 5-7 is utilized. It uses a high frequency continuously running oscillator to produce pulse trains for a three-pulse converter group. The center-tapped pulse transformers connected in parallel with a high frequency oscillator, deliver the train of pulses to each individual thyristor at different conduction periods.

The power circuit of the CDFFC is shown in Figure 5-8 which utilizes six-pulse dual midpoint converters with an interphase transformer, to form a single-phase output. The output ripple current must be returned to the input of the waveform switching signal generator before passing through the low-pass LC filter to load. This feedback operation



A. Schemetic Diagram



B. Input Triggering Signal and Output Firing Pulses

Figure 5-7. Extended output firing pulses for a three-pulse circuit.

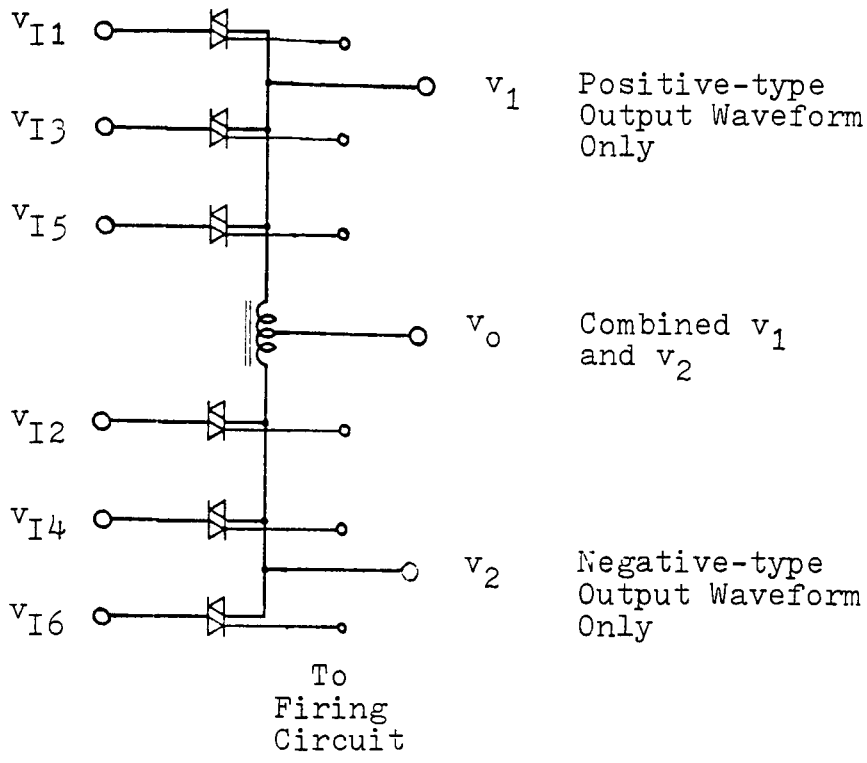


Figure 5-8. Six-pulse Frequency Changer Circuit.

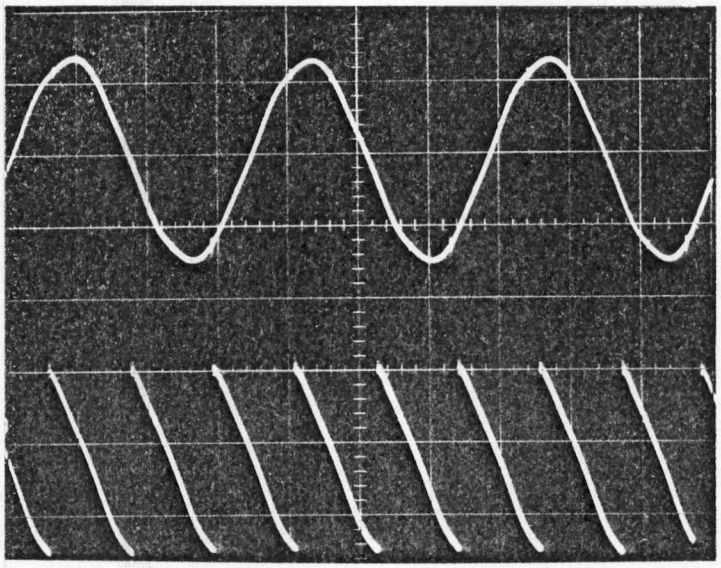
which adjusts the phase position of the switching signal is a function of angle ρ.

5-3 CONCLUSION

A complete model of the VSCF control unit utilizing a circulating type six-pulse cycloconverter has been developed and tested in the laboratory [Refer to Figure 5-10]. The experimental results were found to agree well with the theory. Figure 5-9 shows typical waveforms of the characteristics of the CDFFC [Refer to Figure 3-12]. These oscillograms are the unfiltered output voltage waveforms under unity power factor load condition. The operating frequency ranges of the input of CDFFC are in 45 to 80 Hz, and the output of CDFFC is in 20 Hz. Any input displacement angle can be controlled regardless of the output current.

This system appear to have application in modern wind power-generating system. The control scheme in this thesis can be easily extended to higer power ranges and wider controlled frequency ranges (Triacs are rated as high as 4000 V and 500 A).

With the employment of a Triac under ideal forced commutation conditions, the performance would compare favorably with conventional systems utilizing anti-parallel SCRs that is simpler, cheaper, and providing precise frequency control.

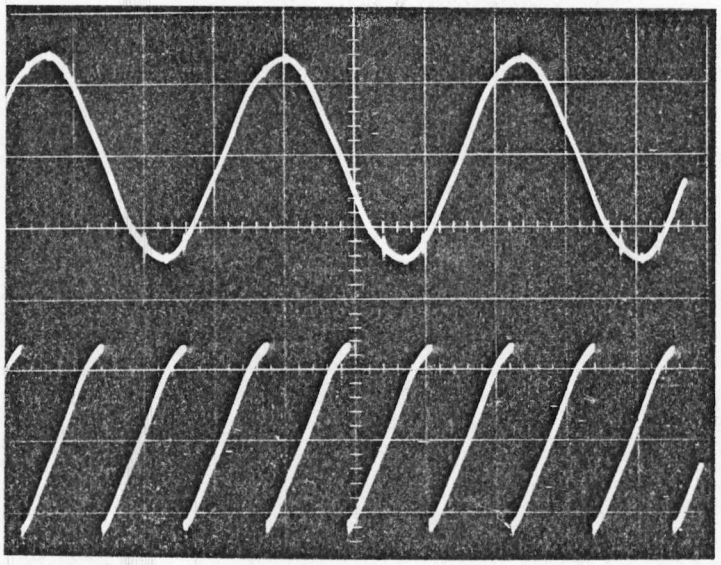


Input Voltage
20 V/ div.

60 Hz

Output Voltage
20 V/ div.

A. Three-pulse Positive-type Waveform for Zero Mean Output Voltage (see Figure 1-8)



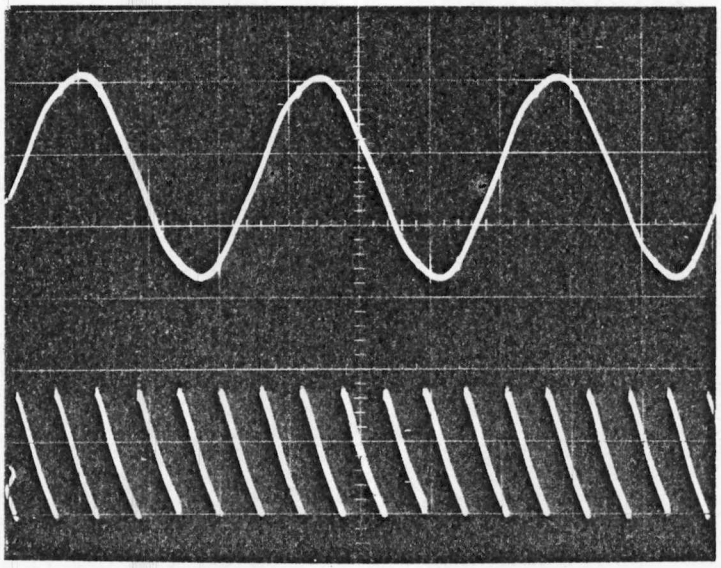
Input Voltage
20 V/ div.

60 Hz

Output Voltage
20 V/ div.

B. Three-pulse Negative-type Waveform for Zero Mean Output Voltage (see Figure 1-8)

Figure 5-9. Associated output waveforms of a six-pulse CDFFC in the VSCF power-generating system.

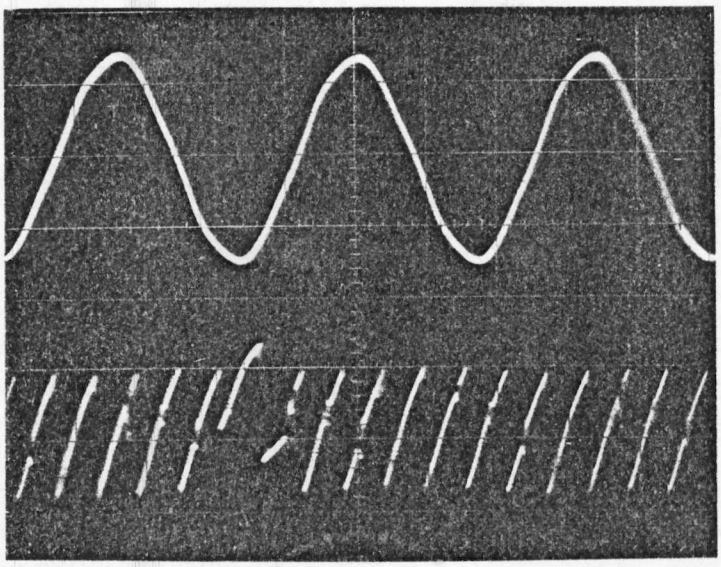


Input Voltage
20 V/ div.

60 Hz

Output Voltage
20 V/ div.

C. Six-pulse Positive-type Waveform for Zero Mean Output Voltage



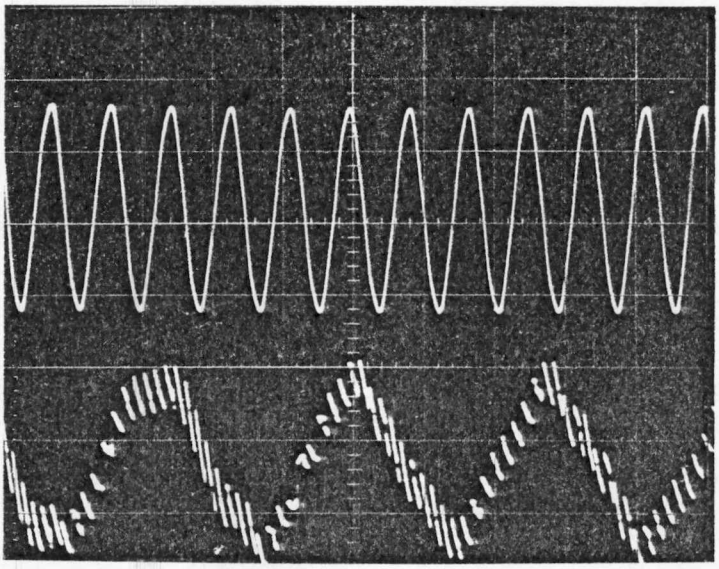
Input Voltage
20 V/ div.

60 Hz

Output Voltage
20 V/ div.

D. Six-pulse Negative-type Waveform for Zero Mean Output Voltage

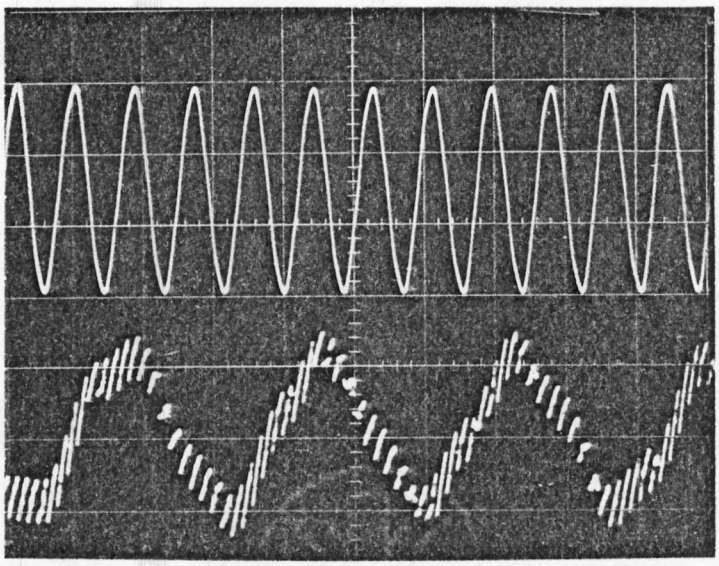
Figure 5-9. (Continued)



Input Voltage
20 V/ div.
60 Hz

Output Voltage
10 V/ div.
20 Hz

E. Positive-type Output Waveform of a Six-pulse CDFFC

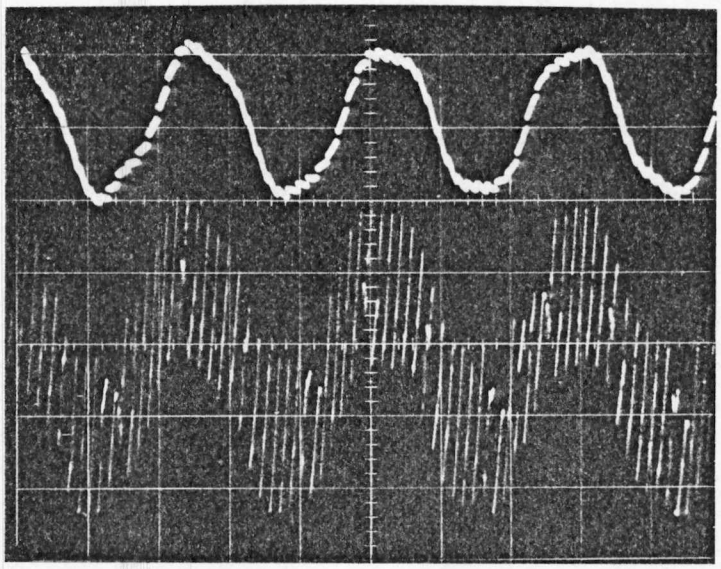


Input Voltage
20 V/ div.
60 Hz

Output Voltage
10 V/ div.
20 Hz

F. Negative-type Output Waveform of a Six-pulse CDFFC

Figure 5-9. (Continued)



Output Voltage
10 V/ div.

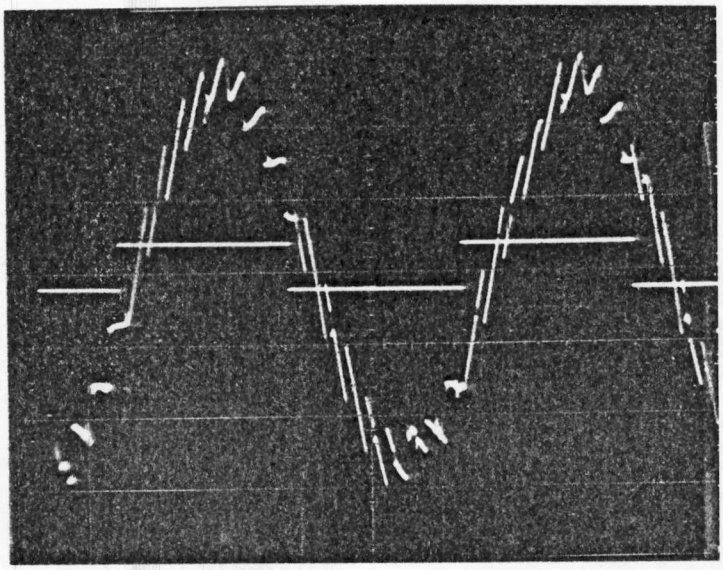
20 Hz; r = 1.0

Output Voltage
5 V/ div.

20 Hz; r = 0.5

G. Output Voltage Waveform of a CDFFC with Different Voltage Ratio r.

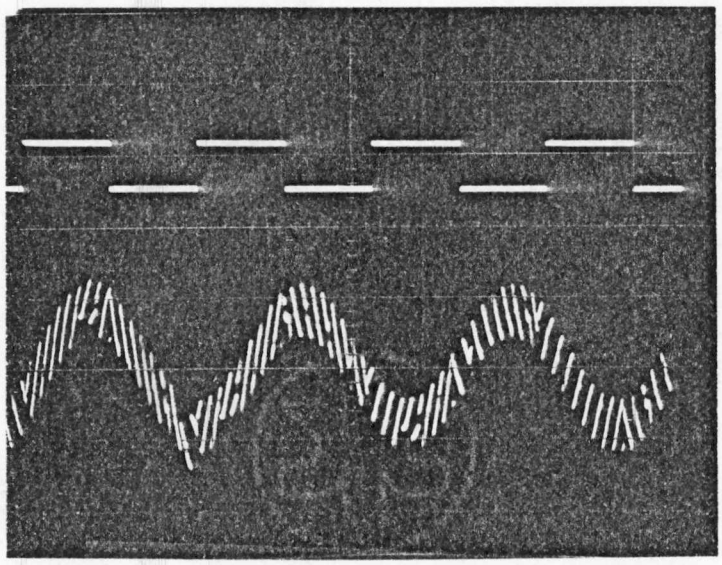
Figure 5-9. (Continued)



Switching Signal and Output Waveform 5 V/ div.

20 Hz

H. Output Waveform of a Six-pulse CDFFC with Leading Input Displacement Angle (see Figure 3-12A)



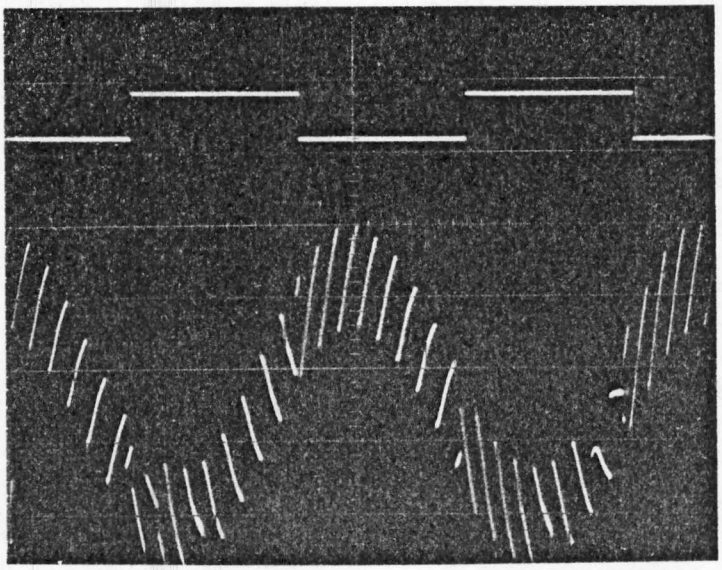
Switching Signal 5 V/ div.

Output Voltage 10 V/ div.

20 Hz

I. Output Waveform of a Six-pulse CDFFC with Out-of-phase Input Displacement Angle (see Figure 3-12B)

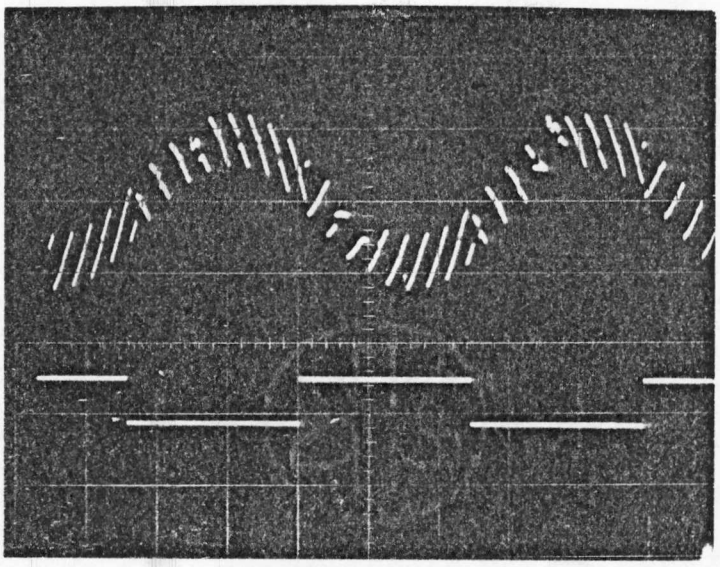
Figure 5-9. (Continued)



Switching Signal
5 V/ div.

Output Voltage
5 V/ div.
20 Hz

J. Output Waveform of a Six-pulse CDFFC with In-phase Input Displacement Angle (see Figure 3-12B)



Output Voltage
10 V/ div.
20 Hz

Switching Signal
5 V/ div.

K. Output Waveform of a Six-pulse CDFFC with Lagging Input Displacement Angle (see Figure 3-12C)

Figure 5-9. (Continued)

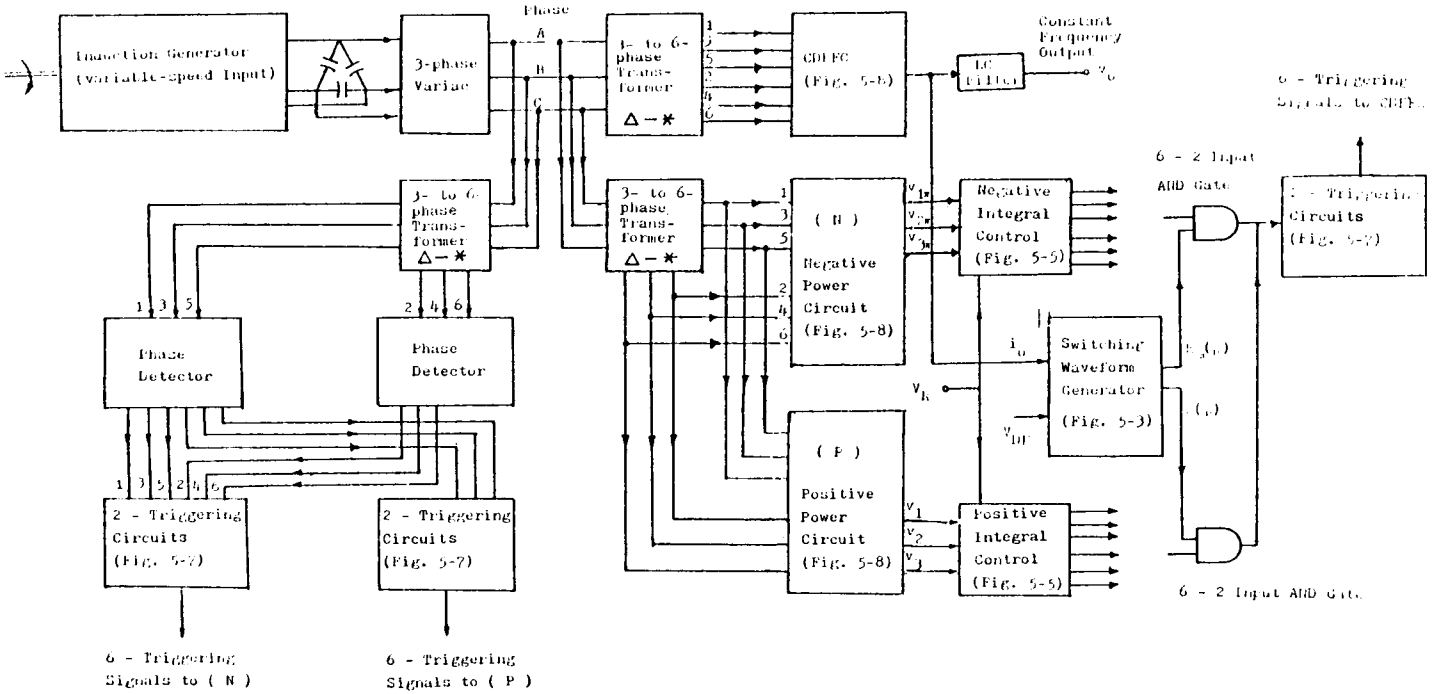


Figure 5-10. Complete schematic diagram for VSCF power-generating system utilizes induction generator and a six-pulse CDFFC.

LIST OF REFERENCES

LIST OF REFERENCES

1. Gyugyi, L., and Pelly, B. R., "Static Power Frequency Changer", John-Wiley and Sons, 1976.

2. Pelly, B. R., "Thyristor Phase-Controlled Converter and Cycloconverter", John Wiley and Sons, 1971.

3. "Power Engineering using Thyristors", Mullard Ltd., Vol. 1, 1970.

4. Mazda, F. F., "Thyristor Control", Newnes-Butterworths, 1973.

5. Gyugyi, L., "Generalized Theory of Static Power Frequency Changer", Ph.d. thesis, Univ. of Salford, 1970.

6. Chirgwin, K. M., and Stratton, L. J., "Variable-speed Constant-frequency Generator System for Aircraft", AIEE Trans. Appl. Ind., 78, pt. II, 304-310, 1959.

7. Jessee, R. D., and Spaven, W. J., "Constant-frequency AC Power using Variable-speed Generator", AIEE Trans. Appl. Ind., 78, pt. II, 411-418, 1959.

8. Chirgwin, K. M., Stratton, L. J., and Toth J. R., "Precise Frequency Power Generation from an Unregulated Shaft", AIEE Trans. Appl. Ind., 79, pt. II, 442-451, 1960.

9. Slabiak, W., and Lawson, L. J., "Precise Control of a Three-phase Squirrel-cage Induction Motor using a Practical Cycloconverter ", IEEE Trans. Appl. Ind. Gen. Appl., Vol. IGA-2, 274-280, July/August, 1966.

10. VanEck, R. A., "Frequency-changer Systems using the Cycloconverter Principle", IEEE Trans. Appl. Ind., 163-168, May 1963.

11. Doxey, B. C., "Theory and Application of the Capacitor-excited Induction Generator", The Engineer, Vol. 216, 893-897, Nov. 1963.

12. Midgley, D., "Machine-rotor Excitation by Stator Electronics", IEE, 1980.

13. Koyakumaru, Y., "An Analysis of Load Characteristics of Self-excited, Single-phase Induction Generator", Electrical Engineering in Japan, Vol. 94, NO. 2, 1974.

14. Doherty, R. E., and Williamson, E. T., "Short-circuit Current of Induction Motors and Generators", AIEE, Vol. XL, Jan. 1921.

15. Yadavalli, S. R., and Jayadev, T. S., "A New Generation Scheme for Large Wind Energy Conversion System", IECEC, Vol. 2, 1961-1965, 1976.

16. Jayadev, T. S., "Induction Generators for Wind Energy Conversion Systems", Report submitted to U. S. ERDA; AER 75-00653, Feb. 1976.

17. Ramakumar, R., "Operation and Control of Wind-electric Systems", Academic Press, Inc., 261-288, 1978.

APPENDIX

APPENDIX A

CONTROLLABLE DISPLACEMENT FACTOR FREQUENCY CHANGER

Table A.1. Dominant terms of the amplitude $A_{6k,2n}$ in Equation (2-36) with frequencies of $6kf_I \pm 2nf_o$ ($k = 1,2$; $n = 0,1,\ldots$).

$2n$	0	2	4	6	8	10	12
$A_{6,2n}$	0.0124	−0.0162	0.0516	0.1069	0.0261	−0.0414	0.0013
$A_{12,2n}$	−0.0016	0.0016	−0.0019	0.0025	−0.0051	0.0210	0.0528

Table A.2. Dominant terms of the amplitude $B_{(3(2k-1)),\,(2n+1)}$ in Equation (2-36) with frequencies of $3(2k-1)f_I \pm (2n+1)f_o$ ($k = 1,2$; $n = 0,1,2...6$).

$2n+1$	1	3	5	7	9	11	13
$B_{3,(2n+1)}$	0.1701	0.2184	0.0404	−0.0051	0.0016	−0.0006	0.0003
$B_{9,(2n+1)}$	−0.0038	0.0045	−0.0080	0.0299	0.0710	0.0191	−0.0032

Table A.3. Numerical values of a and b in the coefficient terms of the harmonic series from Equation (2-45) through (2-50).

r	$a_{2,0}$	$a_{2,2}$	$a_{4,0}$	$a_{4,2}$	$a_{4,4}$	$a_{8,0}$	$a_{8,2}$	$a_{8,4}$	$a_{8,6}$	$a_{8,8}$	$a_{10,0}$	$a_{10,2}$	$a_{10,4}$	$a_{10,6}$	$a_{10,8}$	$a_{10,10}$
1.0	0.000	1.000	0.000	0.000	1.000	0.000	0.000	0.000	0.000	1.000	0.000	0.000	0.000	0.000	0.000	1.000
0.9	0.190	0.810	−0.272	0.616	0.656	−0.043	0.139	−0.334	0.808	0.430	−0.109	0.197	−0.108	−0.146	0.818	0.349
0.8	0.360	0.640	−0.331	0.922	0.410	0.237	−0.466	0.307	0.755	0.168	−0.119	0.302	−0.479	0.585	0.604	0.107
0.7	0.510	0.490	−0.240	1.000	0.240	0.172	−0.478	0.769	0.480	0.058	0.205	−0.355	0.050	0.777	0.294	0.028
0.6	0.640	0.360	−0.051	0.922	0.130	−0.129	0.050	0.823	0.239	0.017	0.227	−0.562	0.660	0.561	0.107	0.006
0.5	0.750	0.250	0.188	0.750	0.063	−0.363	0.656	0.609	0.094	0.004	−0.100	−0.029	0.820	0.278	0.029	0.001
0.4	0.840	0.160	0.437	0.538	0.026	−0.329	0.967	0.334	0.028	0.001	−0.377	0.685	0.591	0.096	0.006	0.000
0.3	0.910	0.090	0.664	0.328	0.008	−0.010	0.876	0.129	0.005	0.000	−0.268	0.977	0.270	0.021	0.001	0.000
0.2	0.960	0.040	0.845	0.154	0.002	0.451	0.520	0.029	0.000	0.000	0.218	0.712	0.067	0.002	0.000	0.000
0.1	0.990	0.010	0.960	0.040	0.000	0.846	0.152	0.002	0.000	0.000	0.765	0.231	0.005	0.000	0.000	0.000

r	$b_{5,1}$	$b_{5,3}$	$b_{5,5}$	$b_{7,1}$	$b_{7,3}$	$b_{7,5}$	$b_{7,7}$	$b_{11,1}$	$b_{11,3}$	$b_{11,5}$	$b_{11,7}$	$b_{11,9}$	$b_{11,11}$	$b_{13,1}$	$b_{13,3}$	$b_{13,5}$	$b_{13,7}$	$b_{13,9}$	$b_{13,11}$	$b_{13,13}$
1.0	0.000	0.000	1.000	0.000	0.000	0.000	1.000	0.000	0.000	0.000	0.000	0.000	1.000	0.000	0.000	0.000	0.000	0.000	0.000	1.000
0.9	−0.530	0.693	0.591	0.276	−0.417	0.785	0.478	−0.300	0.284	−0.208	−0.050	0.810	0.314	0.285	−0.313	0.353	−0.349	0.134	0.775	0.254
0.8	−0.403	0.922	0.328	−0.306	0.103	0.826	0.210	0.012	0.110	−0.384	0.664	0.532	0.086	−0.374	0.356	−0.248	−0.107	0.729	0.402	0.055
0.7	0.036	0.875	0.168	−0.624	0.649	0.600	0.082	0.488	−0.508	0.294	0.716	0.226	0.020	0.058	0.089	−0.401	0.607	0.551	0.131	0.010
0.6	0.538	0.691	0.078	−0.409	0.890	0.348	0.028	0.017	−0.306	0.758	0.434	0.071	0.004	0.498	−0.540	0.317	0.692	0.238	0.030	0.002
0.5	0.938	0.469	0.031	0.164	0.820	0.164	0.008	−0.612	0.419	0.693	0.177	0.016	0.000	−0.133	−0.195	0.766	0.390	0.067	0.005	0.000
0.4	1.142	0.269	0.010	0.771	0.572	0.060	0.002	−0.454	0.863	0.381	0.048	0.002	0.000	−0.674	0.613	0.603	0.130	0.012	0.000	0.000
0.3	1.119	0.123	0.002	1.128	0.298	0.015	0.000	0.406	0.734	0.127	0.008	0.000	0.000	−0.092	0.862	0.246	0.024	0.001	0.000	0.000
0.2	0.883	0.038	0.000	1.086	0.101	0.002	0.000	1.107	0.328	0.021	0.001	0.000	0.000	0.933	0.476	0.045	0.002	0.000	0.000	0.000
0.1	0.485	0.005	0.000	0.659	0.014	0.000	0.000	0.943	0.051	0.001	0.000	0.000	0.000	1.045	0.082	0.002	0.000	0.000	0.000	0.000

A. From Equation (2-45) and (2-47)

Table A.3. (Continued)

r	$a_{1,0}$	$a_{1,2}$	$a_{1,4}$	$a_{1,6}$	$a_{1,8}$	$a_{1,10}$	$a_{1,12}$	$a_{1,14}$	$a_{1,16}$
1.0	0.637	0.424	−0.085	0.036	−0.020	0.013	−0.009	0.007	−0.005
0.9	0.746	0.277	−0.277	0.005	−0.001	0.000	0.000	0.000	0.000
0.8	0.813	0.198	−0.012	0.002	0.000	0.000	0.000	0.000	0.000
0.7	0.863	0.142	−0.006	0.000	0.000	0.000	0.000	0.000	0.000
0.6	0.903	0.100	−0.003	0.000	0.000	0.000	0.000	0.000	0.000
0.5	0.934	0.067	−0.001	0.000	0.000	0.000	0.000	0.000	0.000
0.4	0.959	0.042	0.000	0.000	0.000	0.000	0.000	0.000	0.000
0.3	0.977	0.023	0.000	0.000	0.000	0.000	0.000	0.000	0.000
0.2	0.990	0.010	0.000	0.000	0.000	0.000	0.000	0.000	0.000
0.1	0.997	0.003	0.000	0.000	0.000	0.000	0.000	0.000	0.000

r	$a_{5,0}$	$a_{5,2}$	$a_{5,4}$	$a_{5,6}$	$a_{5,8}$	$a_{5,10}$	$a_{5,12}$	$a_{5,14}$	$a_{5,16}$
1.0	0.127	−0.303	0.707	0.579	−0.163	0.085	−0.053	0.037	−0.028
0.9	−0.014	−0.079	0.921	0.187	−0.019	0.004	−0.001	0.000	0.000
0.8	−0.260	0.460	0.727	0.077	−0.004	0.001	0.000	0.000	0.000
0.7	−0.360	0.840	0.490	0.031	−0.001	0.000	0.000	0.000	0.000
0.6	−0.290	0.987	0.291	0.011	0.000	0.000	0.000	0.000	0.000
0.5	−0.083	0.929	0.150	0.004	0.000	0.000	0.000	0.000	0.000
0.4	0.201	0.733	0.065	0.001	0.000	0.000	0.000	0.000	0.000
0.3	0.502	0.476	0.021	0.000	0.000	0.000	0.000	0.000	0.000
0.2	0.763	0.233	0.004	0.000	0.000	0.000	0.000	0.000	0.000
0.1	0.938	0.061	0.000	0.000	0.000	0.000	0.000	0.000	0.000

r	$a_{7,0}$	$a_{7,2}$	$a_{7,4}$	$a_{7,6}$	$a_{7,8}$	$a_{7,10}$	$a_{7,12}$	$a_{7,14}$	$a_{7,16}$
1.0	−0.091	0.198	−0.270	0.686	0.594	−0.175	0.094	−0.061	0.043
0.9	0.169	−0.322	0.193	0.828	0.142	−0.013	0.002	−0.001	0.000
0.8	0.208	−0.513	0.736	0.526	0.045	−0.002	0.000	0.000	0.000
0.7	−0.043	−0.102	0.857	0.274	0.014	0.000	0.000	0.000	0.000
0.6	−0.304	0.483	0.697	0.120	0.004	0.000	0.000	0.000	0.000
0.5	−0.377	0.890	0.443	0.043	0.001	0.000	0.000	0.000	0.000
0.4	−0.203	0.971	0.220	0.012	0.000	0.000	0.000	0.000	0.000
0.3	0.154	0.764	0.080	0.002	0.000	0.000	0.000	0.000	0.000
0.2	0.563	0.420	0.017	0.000	0.000	0.000	0.000	0.000	0.000
0.1	0.881	0.118	0.001	0.000	0.000	0.000	0.000	0.000	0.000

r	$a_{11,0}$	$a_{11,2}$	$a_{11,4}$	$a_{11,6}$	$a_{11,8}$	$a_{11,10}$	$a_{11,12}$	$a_{11,14}$	$a_{11,16}$
1.0	−0.058	0.120	−0.133	0.165	−0.246	0.667	0.609	−0.187	0.104
0.9	0.075	−0.181	0.277	−0.437	0.547	0.641	0.083	−0.007	0.001
0.8	−0.209	0.430	−0.418	0.169	0.753	0.259	0.016	0.001	0.000
0.7	0.038	0.016	−0.325	0.717	0.472	0.080	0.003	0.000	0.000
0.6	0.278	−0.566	0.371	0.697	0.200	0.019	0.000	0.000	0.000
0.5	0.070	−0.341	0.803	0.405	0.060	0.003	0.000	0.000	0.000
0.4	−0.308	0.438	0.704	0.154	0.012	0.000	0.000	0.000	0.000
0.3	−0.348	0.954	0.357	0.035	0.001	0.000	0.000	0.000	0.000
0.2	0.105	0.797	0.095	0.004	0.000	0.000	0.000	0.000	0.000
0.1	0.719	0.274	0.007	0.000	0.000	0.000	0.000	0.000	0.000

r	$a_{13,0}$	$a_{13,2}$	$a_{13,4}$	$a_{13,6}$	$a_{13,8}$	$a_{13,10}$	$a_{13,12}$	$a_{13,14}$	$a_{13,16}$
1.0	0.049	−0.100	0.108	−0.124	0.158	−0.240	0.662	0.613	−0.190
0.9	0.064	−0.110	0.042	0.103	−0.360	0.646	0.555	0.064	−0.005
0.8	0.044	−0.132	0.271	−0.465	0.444	0.652	0.178	0.010	0.000
0.7	−0.221	0.459	−0.441	0.128	0.723	0.308	0.042	0.001	0.000
0.6	0.078	−0.054	−0.296	0.703	0.466	0.095	0.007	0.000	0.000
0.5	0.279	−0.604	0.473	0.651	0.181	0.020	0.001	0.000	0.000
0.4	−0.061	−0.118	0.815	0.318	0.043	0.003	0.000	0.000	0.000
0.3	−0.394	0.756	0.547	0.085	0.005	0.000	0.000	0.000	0.000
0.2	−0.102	0.923	0.169	0.010	0.000	0.000	0.000	0.000	0.000
0.1	0.619	0.367	0.013	0.000	0.000	0.000	0.000	0.000	0.000

B. From Equation (2-48) to (2-49)

Table A.3. (Continued)

r	$b_{2,1}$	$b_{2,3}$	$b_{2,5}$	$b_{2,7}$	$b_{2,9}$	$b_{2,11}$	$b_{2,13}$	$b_{2,15}$	$b_{2,17}$
1.0	0.849	0.509	−0.121	0.057	−0.033	0.022	−0.015	0.012	−0.009
0.9	1.094	0.273	−0.029	0.006	−0.001	0.000	0.000	0.000	0.000
0.8	1.141	0.169	−0.011	0.001	0.000	0.000	0.000	0.000	0.000
0.7	1.109	0.104	−0.004	0.000	0.000	0.000	0.000	0.000	0.000
0.6	1.023	0.062	−0.002	0.000	0.000	0.000	0.000	0.000	0.000
0.5	0.901	0.034	−0.001	0.000	0.000	0.000	0.000	0.000	0.000
0.4	0.750	0.017	0.000	0.000	0.000	0.000	0.000	0.000	0.000
0.3	0.579	0.007	0.000	0.000	0.000	0.000	0.000	0.000	0.000
0.2	0.394	0.002	0.000	0.000	0.000	0.000	0.000	0.000	0.000
0.1	0.199	0.000	0.000	0.000	0.000	0.000	0.000	0.000	0.000

$b_{4,1}$	$b_{4,3}$	$b_{4,5}$	$b_{4,7}$	$b_{4,9}$	$b_{4,11}$	$b_{4,13}$	$b_{4,15}$	$b_{4,17}$
−0.340	0.728	0.566	−0.154	0.078	−0.049	0.033	−0.024	0.019
−0.249	0.966	0.215	−0.022	0.004	−0.001	0.000	0.000	0.000
0.199	0.845	0.101	−0.006	0.001	0.000	0.000	0.000	0.000
0.638	0.647	0.046	−0.002	0.000	0.000	0.000	0.000	0.000
0.964	0.447	0.020	−0.001	0.000	0.000	0.000	0.000	0.000
1.134	0.276	0.008	0.000	0.000	0.000	0.000	0.000	0.000
1.143	0.148	0.002	0.000	0.000	0.000	0.000	0.000	0.000
1.003	0.065	0.001	0.000	0.000	0.000	0.000	0.000	0.000
0.741	0.020	0.000	0.000	0.000	0.000	0.000	0.000	0.000
0.393	0.002	0.000	0.000	0.000	0.000	0.000	0.000	0.000

r	$b_{8,1}$	$b_{8,3}$	$b_{8,5}$	$b_{8,7}$	$b_{8,9}$	$b_{8,11}$	$b_{8,13}$	$b_{8,15}$	$b_{8,17}$
1.0	−0.162	0.185	−0.261	0.679	0.599	−0.179	0.097	−0.063	0.045
0.9	0.391	−0.397	0.304	0.780	0.124	−0.011	−0.002	0.000	0.000
0.8	0.158	−0.367	0.788	0.444	0.035	−0.002	0.000	0.000	0.000
0.7	−0.442	0.221	0.776	0.203	0.009	0.000	0.000	0.000	0.000
0.6	−0.631	0.736	0.534	0.076	0.002	0.000	0.000	0.000	0.000
0.5	−0.235	0.889	0.281	0.023	0.000	0.000	0.000	0.000	0.000
0.4	0.460	0.716	0.111	0.005	0.000	0.000	0.000	0.000	0.000
0.3	1.025	0.407	0.030	0.001	0.000	0.000	0.000	0.000	0.000
0.2	1.141	0.146	0.004	0.000	0.000	0.000	0.000	0.000	0.000
0.1	0.738	0.020	0.000	0.000	0.000	0.000	0.000	0.000	0.000

$b_{10,1}$	$b_{10,3}$	$b_{10,5}$	$b_{10,7}$	$b_{10,9}$	$b_{10,11}$	$b_{10,13}$	$b_{10,15}$	$b_{10,17}$
0.129	−0.140	0.170	−0.250	0.670	0.606	−0.185	0.102	−0.067
−0.286	0.345	−0.449	0.480	0.686	0.095	−0.008	0.001	0.000
0.362	−0.290	−0.004	0.787	0.311	0.021	0.001	0.000	0.000
0.327	−0.503	0.631	0.571	0.109	0.004	0.000	0.000	0.000
−0.339	0.043	0.788	0.284	0.030	0.001	0.000	0.000	0.000
−0.658	0.680	0.568	0.103	0.006	0.000	0.000	0.000	0.000
−0.197	0.879	0.274	0.026	0.001	0.000	0.000	0.000	0.000
0.648	0.634	0.085	0.004	0.000	0.000	0.000	0.000	0.000
1.151	0.260	0.013	0.000	0.000	0.000	0.000	0.000	0.000
0.881	0.039	0.000	0.000	0.000	0.000	0.000	0.000	0.000

C. From Equation (2-50)

Table A.4. Numerical values of the amplitude of the dominant components in Equation (3-1).

	ρ	$-\frac{\pi}{2}$	$-\frac{\pi}{3}$	$-\frac{\pi}{6}$	0	$+\frac{\pi}{6}$	$+\frac{\pi}{3}$	$+\frac{\pi}{2}$
$3f_1 \pm 2f_0$	$A_{3,0}$	0.000	0.020	0.179	0.318	0.179	0.020	0.000
	$A_{3,+2}$	0.000	0.020	0.167	0.272	0.333	0.486	0.500
	$A_{3,-2}$	0.500	0.486	0.333		0.167	0.020	0.000
	$A_{3,+4}$	0.000	0.019	0.134	0.164	0.274	0.269	0.250
	$A_{3,-4}$	0.250	0.269	0.274		0.134	0.019	0.000
	$A_{3,+6}$ $A_{3,-6}$	0.000	0.017	0.095	0.064	0.095	0.017	0.000
$6f_1 \pm (2f+1)f_0$	$A_{6,+1}$ $A_{6,-1}$	0.000	0.023	0.018	0.006	0.018	0.023	0.000
	$A_{6,+3}$ $A_{6,-3}$	0.000	0.022	0.045	0.055	0.045	0.022	0.000
	$A_{6,+5}$	0.000	0.021	0.058	0.105	0.150	0.181	0.200
	$A_{6,-5}$	0.200	0.181	0.150		0.058	0.021	0.000
	$A_{6,+7}$	0.000	0.019	0.055	0.100	0.136	0.151	0.143
	$A_{6,-7}$	0.143	0.151	0.136		0.055	0.019	0.000
	$A_{6,+9}$ $A_{6,-9}$	0.000	0.016	0.042	0.055	0.042	0.016	0.000

Table A.5. Numerical values of the amplitude of the unwanted components in the output voltage of the CDFFC with sinusoidal mean voltage.

	$3f_i \pm 2nf_o$																	
	$\rho = 0°, 180°$								$\rho = \pm 30°, \pm 150°$									
$2n \rightarrow$	0	2	4	6	8	10	12	14	0	2		4		6	8	10	12	14
$r \downarrow$										■	□	■	□					
1.0	0.318	0.272	0.164	0.064	0.021	0.015	0.009	0.007	0.179	0.333	0.167	0.279	0.134	0.095	0.062	0.044	0.037	0.031
0.9	0.394	0.283	0.137	0.048	0.020	0.013	0.008	0.006	0.264	0.362	0.207	0.237	0.138	0.086	0.058	0.044	0.036	0.030
0.8	0.470	0.276	0.112	0.038	0.018	0.011	0.007	0.005	0.354	0.364	0.229	0.197	0.133	0.079	0.054	0.042	0.034	0.029
0.7	0.538	0.257	0.090	0.031	0.015	0.009	0.006	0.005	0.438	0.348	0.235	0.162	0.122	0.071	0.050	0.038	0.032	0.027
0.6	0.596	0.230	0.071	0.025	0.013	0.008	0.005	0.004	0.516	0.317	0.229	0.131	0.108	0.063	0.044	0.035	0.028	0.024
0.5	0.644	0.199	0.055	0.020	0.011	0.007	0.004	0.003	0.584	0.028	0.212	0.103	0.092	0.054	0.038	0.030	0.025	0.021
0.4	0.632	0.163	0.040	0.015	0.008	0.005	0.004	0.003	0.642	0.227	0.184	0.079	0.074	0.044	0.031	0.025	0.020	0.017
0.3	0.712	0.125	0.028	0.011	0.006	0.004	0.003	0.002	0.689	0.173	0.148	0.057	0.056	0.033	0.024	0.019	0.016	0.013
0.2	0.734	0.084	0.018	0.007	0.004	0.003	0.002	0.001	0.722	0.116	0.104	0.037	0.037	0.023	0.016	0.013	0.011	0.009
0.1	0.746	0.042	0.009	0.004	0.002	0.001	0.001	0.001	0.743	0.057	0.054	0.019	0.019	0.011	0.008	0.007	0.005	0.005

	$3f_i \pm 2nf_o$																	
	$\rho = \pm 60°, \pm 120°$									$\rho = \pm 90°$								
$2n \rightarrow$	0	2		4		6	8	10	12	14	0	2		4		6	8	10	12	14
$r \downarrow$		■	□	■	□							■	□	■	□					
1.0	0.020	0.486	0.020	0.269	0.019	0.017	0.016	0.014	0.012	0.010	0.000	0.500	0.000	0.250	0.000	0.000	0.000	0.000	0.000	0.000
0.9	0.081	0.540	0.063	0.210	0.049	0.038	0.030	0.024	0.020	0.017	0.027	0.579	0.020	0.149	0.015	0.012	0.010	0.008	0.007	0.006
0.8	0.167	0.554	0.110	0.167	0.075	0.054	0.041	0.033	0.028	0.024	0.097	0.613	0.062	0.059	0.043	0.032	0.026	0.021	0.018	0.015
0.7	0.267	0.536	0.151	0.141	0.094	0.065	0.049	0.039	0.033	0.028	0.195	0.604	0.109	0.011	0.071	0.051	0.039	0.032	0.027	0.023
0.6	0.372	0.491	0.180	0.126	0.104	0.070	0.052	0.042	0.035	0.030	0.307	0.561	0.150	0.059	0.091	0.063	0.048	0.039	0.032	0.028
0.5	0.474	0.426	0.193	0.113	0.104	0.069	0.051	0.041	0.034	0.029	0.422	0.490	0.177	0.085	0.101	0.068	0.052	0.041	0.034	0.030
0.4	0.566	0.347	0.189	0.099	0.096	0.062	0.046	0.037	0.031	0.026	0.529	0.399	0.185	0.092	0.099	0.066	0.049	0.039	0.033	0.029
0.3	0.642	0.260	0.167	0.080	0.079	0.051	0.038	0.030	0.025	0.021	0.621	0.298	0.171	0.084	0.086	0.056	0.042	0.033	0.028	0.024
0.2	0.701	0.169	0.127	0.057	0.056	0.036	0.027	0.021	0.018	0.015	0.691	0.193	0.135	0.063	0.063	0.041	0.030	0.024	0.020	0.017
0.1	0.738	0.081	0.071	0.029	0.029	0.019	0.014	0.011	0.009	0.008	0.735	0.092	0.077	0.033	0.033	0.021	0.016	0.013	0.011	0.009

A. With Frequencies $3f_I \pm 2nf_o$

Table A.5. (Continued)

$6f_I \pm (2n+1)f_o$

	$\rho = 0°, 180°$								$\rho = \pm 30°, \pm 150°$											
$(2n+1)\rightarrow$	1	3	5	7	9	11	13	15	1		3		5		7		9	11	13	15
$r\downarrow$									■		■		■		■					
1.0	0.006	0.055	0.105	0.100	0.055	0.026	0.022	0.017	0.018	0.018	0.045	0.045	0.150	0.058	0.136	0.055	0.042	0.027	0.018	0.015
0.9	0.036	0.097	0.117	0.081	0.041	0.026	0.020	0.017	0.024	0.057	0.107	0.079	0.163	0.071	0.096	0.051	0.033	0.022	0.017	0.014
0.8	0.069	0.123	0.111	0.065	0.035	0.023	0.021	0.017	0.042	0.100	0.158	0.096	0.145	0.067	0.064	0.041	0.026	0.019	0.012	0.011
0.7	0.101	0.136	0.098	0.053	0.032	0.023	0.019	0.016	0.097	0.130	0.183	0.095	0.114	0.055	0.041	0.030	0.018	0.013	0.010	0.008
0.6	0.130	0.138	0.084	0.045	0.029	0.022	0.018	0.015	0.162	0.142	0.185	0.081	0.081	0.040	0.024	0.020	0.011	0.008	0.006	0.004
0.5	0.156	0.132	0.071	0.040	0.027	0.021	0.018	0.015	0.221	0.134	0.168	0.062	0.053	0.027	0.014	0.013	0.008	0.005	0.004	0.003
0.4	0.178	0.120	0.060	0.036	0.026	0.021	0.017	0.015	0.266	0.112	0.140	0.049	0.036	0.025	0.015	0.015	0.011	0.008	0.007	0.006
0.3	0.196	0.105	0.052	0.034	0.025	0.020	0.017	0.015	0.288	0.098	0.109	0.052	0.033	0.031	0.021	0.021	0.016	0.013	0.011	0.009
0.2	0.208	0.090	0.047	0.032	0.025	0.020	0.017	0.015	0.286	0.117	0.084	0.063	0.038	0.038	0.026	0.026	0.020	0.017	0.014	0.012
0.1	0.216	0.078	0.044	0.031	0.024	0.020	0.017	0.015	0.262	0.165	0.074	0.071	0.042	0.042	0.030	0.030	0.023	0.019	0.016	0.014

$6f_I \pm (2n+1)f_o$,

	$\rho = \pm 60°, \pm 120°$												$\rho = \pm 90°$											
$(2n+1)\rightarrow$	1		3		5		7		9	11	13	15	1		3		5		7		9	11	13	15
$r\downarrow$	■		■		■		■						■		■		■		■					
1.0	0.023	0.023	0.022	0.022	0.181	0.021	0.151	0.019	0.016	0.014	0.011	0.009	0.000	0.000	0.000	0.000	0.200	0.000	0.143	0.000	0.000	0.000	0.000	0.000
0.9	0.072	0.052	0.097	0.037	0.209	0.025	0.085	0.017	0.012	0.009	0.007	0.005	0.039	0.027	0.059	0.020	0.246	0.016	0.056	0.012	0.010	0.009	0.007	0.006
0.8	0.087	0.045	0.183	0.026	0.188	0.016	0.036	0.011	0.008	0.006	0.004	0.003	0.081	0.043	0.174	0.026	0.200	0.017	0.018	0.012	0.009	0.006	0.008	0.006
0.7	0.065	0.045	0.238	0.036	0.147	0.027	0.017	0.021	0.016	0.013	0.011	0.010	0.067	0.015	0.266	0.002	0.117	0.002	0.015	0.003	0.003	0.003	0.002	0.002
0.6	0.088	0.083	0.247	0.058	0.103	0.039	0.025	0.028	0.022	0.018	0.015	0.013	0.010	0.039	0.298	0.032	0.041	0.025	0.023	0.019	0.015	0.012	0.010	0.010
0.5	0.174	0.112	0.213	0.063	0.066	0.038	0.025	0.026	0.020	0.016	0.013	0.012	0.123	0.088	0.265	0.054	0.007	0.036	0.028	0.027	0.021	0.017	0.015	0.013
0.4	0.260	0.109	0.152	0.047	0.032	0.025	0.016	0.016	0.012	0.009	0.008	0.007	0.235	0.104	0.186	0.051	0.020	0.031	0.022	0.022	0.016	0.014	0.011	0.010
0.3	0.316	0.071	0.084	0.020	0.007	0.008	0.004	0.004	0.002	0.002	0.001	0.001	0.313	0.072	0.090	0.023	0.008	0.011	0.007	0.007	0.005	0.004	0.003	0.003
0.2	0.327	0.047	0.046	0.032	0.021	0.022	0.016	0.016	0.012	0.010	0.009	0.008	0.337	0.005	0.003	0.019	0.015	0.015	0.011	0.011	0.009	0.007	0.006	0.005
0.1	0.291	0.126	0.062	0.061	0.038	0.038	0.027	0.027	0.021	0.017	0.015	0.013	0.301	0.110	0.054	0.057	0.036	0.036	0.026	0.026	0.020	0.016	0.014	0.012

B. With Frequencies $6f_I \pm (2n+1)f_o$

Table A.5. (Continued)

	$12f_I \pm (2n+1)f_o$																					
	$\rho = 0°, 180°$									$\rho = \pm 30°, \pm 150°$												
$(2n+1)\rightarrow$	1	3	5	7	9	11	13	15	17	1		3		5		7		9		11		13		15	17
$r\downarrow$										■	□	■	□	■	□	■	□	■	□	■	□	■	□		
1.0	0.002	0.001	0.007	0.005	0.027	0.050	0.049	0.027	0.011	0.002	0.002	0.003	0.003	0.002	0.002	0.010	0.010	0.020	0.020	0.072	0.027	0.069	0.026	0.020	0.012
0.9	0.011	0.016	0.010	0.031	0.053	0.049	0.030	0.016	0.011	0.017	0.015	0.006	0.007	0.025	0.023	0.014	0.033	0.069	0.033	0.071	0.026	0.034	0.018	0.012	0.008
0.8	0.022	0.021	0.029	0.052	0.053	0.036	0.020	0.013	0.009	0.025	0.011	0.030	0.031	0.017	0.040	0.061	0.036	0.079	0.026	0.045	0.017	0.015	0.010	0.007	0.005
0.7	0.029	0.027	0.050	0.057	0.043	0.025	0.015	0.011	0.008	0.017	0.035	0.042	0.044	0.036	0.038	0.085	0.028	0.062	0.019	0.024	0.012	0.008	0.008	0.006	0.004
0.6	0.035	0.045	0.061	0.051	0.032	0.018	0.012	0.009	0.008	0.039	0.044	0.030	0.043	0.074	0.035	0.080	0.026	0.040	0.018	0.015	0.012	0.009	0.009	0.008	0.006
0.5	0.043	0.061	0.061	0.041	0.023	0.014	0.011	0.009	0.007	0.044	0.049	0.055	0.050	0.085	0.038	0.057	0.026	0.024	0.017	0.013	0.012	0.010	0.010	0.008	0.007
0.4	0.057	0.071	0.056	0.030	0.017	0.012	0.010	0.008	0.007	0.045	0.070	0.088	0.055	0.072	0.036	0.031	0.019	0.013	0.012	0.009	0.009	0.007	0.007	0.006	0.005
0.3	0.075	0.070	0.041	0.022	0.014	0.011	0.009	0.008	0.007	0.090	0.079	0.092	0.042	0.039	0.020	0.012	0.010	0.006	0.006	0.004	0.004	0.003	0.003	0.002	0.002
0.2	0.091	0.059	0.029	0.018	0.013	0.010	0.009	0.007	0.006	0.134	0.060	0.069	0.025	0.018	0.012	0.007	0.007	0.005	0.005	0.004	0.004	0.003	0.003	0.003	0.002
0.1	0.103	0.044	0.023	0.016	0.012	0.010	0.008	0.007	0.006	0.142	0.058	0.041	0.031	0.018	0.018	0.013	0.013	0.010	0.010	0.008	0.008	0.007	0.007	0.006	0.005

C. With Frequencies $12f_I \pm (2n+1)f_o$

Table A.5. (Continued)

$12f_t \pm (2n+1)f_0$

$\rho = \pm 60°, \pm 120$

$(2n+1)\rightarrow$	1		3		5		7		9		11		13		15	17
$r\downarrow$																
1.0	0.001	0.001	0.003	0.003	0.005	0.005	0.007	0.006	0.008	0.008	0.085	0.008	0.078	0.008	0.007	0.006
0.9	0.019	0.018	0.017	0.016	0.008	0.013	0.021	0.010	0.078	0.008	0.090	0.006	0.022	0.005	0.004	0.003
0.8	0.020	0.024	0.017	0.023	0.036	0.019	0.046	0.015	0.102	0.012	0.048	0.009	0.004	0.007	0.006	0.005
0.7	0.043	0.032	0.044	0.022	0.013	0.014	0.103	0.009	0.069	0.006	0.011	0.004	0.003	0.003	0.002	0.002
0.6	0.031	0.029	0.049	0.025	0.074	0.019	0.102	0.015	0.030	0.011	0.007	0.009	0.008	0.007	0.006	0.006
0.5	0.062	0.047	0.041	0.030	0.108	0.019	0.058	0.012	0.009	0.008	0.006	0.006	0.005	0.005	0.004	0.004
0.4	0.064	0.030	0.109	0.017	0.094	0.008	0.014	0.008	0.005	0.006	0.005	0.005	0.004	0.004	0.003	0.003
0.3	0.051	0.050	0.126	0.033	0.051	0.022	0.013	0.016	0.012	0.012	0.010	0.010	0.008	0.008	0.007	0.006
0.2	0.130	0.058	0.076	0.025	0.017	0.013	0.008	0.008	0.006	0.006	0.005	0.005	0.004	0.004	0.004	0.003
0.1	0.161	0.023	0.023	0.016	0.010	0.010	0.008	0.008	0.006	0.006	0.005	0.005	0.004	0.004	0.004	0.003

$12f_t \pm (2n+1)f_0$

$\rho = \pm 90°$

$(2n+1)\rightarrow$	1		3		5		7		9		11		13		15	17
$r\downarrow$																
1.0	0.000	0.000	0.000	0.000	0.000	0.000	0.000	0.000	0.000	0.000	0.091	0.000	0.077	0.000	0.000	0.000
0.9	0.002	0.003	0.002	0.004	0.012	0.004	0.035	0.003	0.087	0.003	0.086	0.003	0.022	0.002	0.002	0.002
0.8	0.018	0.010	0.032	0.005	0.051	0.003	0.050	0.002	0.106	0.001	0.038	0.001	0.005	0.001	0.000	0.000
0.7	0.027	0.022	0.023	0.017	0.017	0.013	0.122	0.010	0.055	0.008	0.019	0.007	0.005	0.006	0.005	0.004
0.6	0.029	0.011	0.066	0.003	0.093	0.000	0.092	0.001	0.026	0.001	0.002	0.001	0.001	0.001	0.001	0.001
0.5	0.035	0.031	0.000	0.023	0.139	0.017	0.033	0.013	0.017	0.010	0.008	0.008	0.007	0.007	0.006	0.005
0.4	0.066	0.028	0.114	0.012	0.091	0.002	0.011	0.004	0.004	0.003	0.002	0.002	0.002	0.002	0.001	0.001
0.3	0.003	0.003	0.155	0.022	0.015	0.016	0.015	0.012	0.010	0.010	0.008	0.008	0.007	0.007	0.006	0.005
0.2	0.117	0.056	0.093	0.027	0.011	0.016	0.012	0.011	0.009	0.009	0.007	0.007	0.006	0.006	0.005	0.005
0.1	0.166	0.000	0.002	0.009	0.007	0.007	0.005	0.005	0.004	0.004	0.003	0.003	0.003	0.003	0.003	0.002

C. (Continued)

Table A.6. Numerical values of the amplitude of the extrabasal components in the input current of the CDFFC with sinusoidal mean voltage.

	$f_I \pm 2nf_o$																													
	$\phi_o = 0°, 180°$						$\phi_o = \pm 30°, \pm 150°$							$\phi_o = \pm 60°, \pm 120°$							$\phi_o = \pm 90°$									
$2n \rightarrow$	2	4	6	8	10	12	2		4	6	8	10	12	2		4	6	8	10	12	2		4	6	8	10	12			
$r\downarrow$																														
1.0	0.42	0.18	0.00	0.04	0.00	0.02	0.72	0.17	0.12	0.06	0.01	0.01	0.01	0.95	0.03	0.03	0.02	0.02	0.01	0.01	1.00	0.00	0.00	0.00	0.00	0.00	0.00			
0.9	0.39	0.12	0.03	0.02	0.01	0.01	0.61	0.19	0.09	0.03	0.01	0.01	0.01	0.80	0.06	0.04	0.02	0.01	0.01	0.01	0.86	0.02	0.01	0.01	0.01	0.00	0.00			
0.8	0.37	0.10	0.03	0.02	0.01	0.01	0.56	0.20	0.08	0.03	0.02	0.01	0.01	0.71	0.09	0.04	0.02	0.01	0.01	0.01	0.77	0.05	0.03	0.02	0.01	0.01	0.00			
0.7	0.36	0.09	0.03	0.02	0.01	0.01	0.52	0.22	0.08	0.03	0.02	0.01	0.01	0.64	0.12	0.05	0.02	0.01	0.01	0.01	0.69	0.09	0.04	0.02	0.01	0.01	0.01			
0.6	0.35	0.08	0.03	0.02	0.01	0.01	0.48	0.23	0.07	0.03	0.02	0.01	0.01	0.58	0.15	0.06	0.03	0.01	0.01	0.01	0.62	0.12	0.05	0.02	0.01	0.01	0.01			
0.5	0.34	0.08	0.03	0.02	0.01	0.01	0.45	0.25	0.07	0.03	0.02	0.01	0.01	0.53	0.18	0.06	0.03	0.01	0.01	0.01	0.56	0.15	0.05	0.02	0.01	0.01	0.01			
0.4	0.34	0.07	0.03	0.02	0.01	0.01	0.42	0.26	0.07	0.03	0.02	0.01	0.01	0.49	0.21	0.06	0.03	0.02	0.01	0.01	0.51	0.19	0.06	0.03	0.01	0.01	0.01			
0.3	0.34	0.07	0.03	0.02	0.01	0.01	0.40	0.28	0.07	0.03	0.02	0.01	0.01	0.44	0.24	0.06	0.03	0.02	0.01	0.01	0.46	0.22	0.06	0.03	0.02	0.01	0.01			
0.2	0.34	0.07	0.03	0.02	0.01	0.01	0.38	0.30	0.07	0.03	0.02	0.01	0.01	0.41	0.27	0.07	0.03	0.02	0.01	0.01	0.42	0.26	0.06	0.03	0.02	0.01	0.01			
0.1	0.33	0.07	0.03	0.02	0.01	0.01	0.35	0.31	0.07	0.03	0.02	0.01	0.01	0.37	0.30	0.07	0.03	0.02	0.01	0.01	0.37	0.30	0.07	0.03	0.02	0.01	0.01			

A. With Frequencies $f_I \pm 2nf_o$

Table A.6. (Continued)

$2f_I \pm (2n+1)f_o$

	$\phi_o = 0°, 180°$						$\phi_o = \pm 30°, \pm 150°$								$\phi_o = \pm 60°, \pm 120°$								$\phi_o = \pm 90°$							
$(2n+1)\rightarrow$	1	[3]	5	7	[9]	11	1		[3]		5	7	[9]	11	1		[3]		5	7	[9]	11	1		[3]		5	7	[9]	11
$r\downarrow$																														
1.0	0.35	0.23	0.09	0.02	0.02	0.01	0.48	0.16	0.33	0.13	0.08	0.03	0.01	0.01	0.51	0.03	0.46	0.03	0.02	0.02	0.02	0.01	0.50	0.00	0.50	0.00	0.00	0.00	0.00	0.00
0.9	0.37	0.17	0.04	0.00	0.00	0.00	0.49	0.21	0.24	0.11	0.04	0.01	0.01	0.00	0.53	0.07	0.35	0.04	0.02	0.01	0.01	0.01	0.53	0.03	0.40	0.02	0.01	0.01	0.01	0.00
0.8	0.38	0.13	0.03	0.00	0.00	0.00	0.49	0.23	0.19	0.09	0.03	0.01	0.01	0.00	0.54	0.11	0.28	0.05	0.02	0.01	0.01	0.01	0.54	0.07	0.32	0.03	0.02	0.01	0.01	0.00
0.7	0.38	0.11	0.02	0.00	0.00	0.00	0.48	0.26	0.15	0.08	0.03	0.01	0.00	0.00	0.53	0.15	0.22	0.06	0.02	0.01	0.01	0.00	0.54	0.11	0.26	0.04	0.02	0.01	0.01	0.00
0.6	0.39	0.09	0.02	0.00	0.00	0.00	0.48	0.28	0.12	0.07	0.02	0.01	0.00	0.00	0.52	0.19	0.18	0.06	0.02	0.01	0.01	0.00	0.54	0.16	0.20	0.05	0.02	0.01	0.01	0.00
0.5	0.39	0.07	0.01	0.00	0.00	0.00	0.46	0.30	0.10	0.06	0.02	0.01	0.00	0.00	0.51	0.23	0.14	0.06	0.02	0.01	0.01	0.00	0.52	0.20	0.15	0.05	0.02	0.01	0.01	0.00
0.4	0.39	0.06	0.01	0.00	0.00	0.00	0.45	0.32	0.07	0.05	0.01	0.00	0.00	0.00	0.49	0.26	0.10	0.05	0.02	0.01	0.00	0.00	0.50	0.24	0.11	0.05	0.02	0.01	0.00	0.00
0.3	0.39	0.04	0.01	0.00	0.00	0.00	0.44	0.34	0.05	0.04	0.01	0.00	0.00	0.00	0.47	0.30	0.07	0.04	0.01	0.01	0.00	0.00	0.48	0.28	0.08	0.04	0.01	0.01	0.00	0.00
0.2	0.39	0.03	0.00	0.00	0.00	0.00	0.43	0.36	0.03	0.03	0.01	0.00	0.00	0.00	0.45	0.33	0.04	0.03	0.01	0.00	0.00	0.00	0.45	0.32	0.05	0.03	0.01	0.00	0.00	0.00
0.1	0.39	0.01	0.00	0.00	0.00	0.00	0.41	0.38	0.02	0.02	0.00	0.00	0.00	0.00	0.42	0.36	0.02	0.02	0.00	0.00	0.00	0.00	0.43	0.36	0.02	0.02	0.00	0.00	0.00	0.00

$4f_I \pm (2n+1)f_o$

	$\phi_o = 0°, 180°$						$\phi_o = \pm 30°, \pm 150°$								$\phi_o = \pm 60°, \pm 120°$								$\phi_o = \pm 90°$							
$(2n+1)\rightarrow$	1	[3]	5	7	[9]	11	1		[3]		5	7	[9]	11	1		[3]		5	7	[9]	11	1		[3]		5	7	[9]	11
$r\downarrow$																														
1.0	0.09	0.14	0.12	0.05	0.01	0.01	0.08	0.08	0.20	0.08	0.18	0.06	0.04	0.02	0.01	0.02	0.02	0.25	0.02	0.23	0.02	0.02	0.01	0.01	0.00	0.00	0.25	0.00	0.25	0.00	0.00	0.00	0.00
0.9	0.14	0.13	0.07	0.02	0.00	0.00	0.16	0.10	0.20	0.06	0.11	0.04	0.02	0.01	0.00	0.09	0.05	0.27	0.03	0.14	0.01	0.01	0.00	0.00	0.04	0.02	0.29	0.01	0.16	0.01	0.00	0.00	0.00
0.8	0.16	0.11	0.05	0.01	0.00	0.00	0.19	0.10	0.18	0.05	0.07	0.03	0.01	0.01	0.00	0.14	0.05	0.25	0.02	0.09	0.01	0.00	0.00	0.00	0.09	0.04	0.28	0.02	0.10	0.01	0.00	0.00	0.00
0.7	0.17	0.10	0.03	0.01	0.00	0.00	0.21	0.09	0.15	0.05	0.05	0.02	0.01	0.00	0.00	0.18	0.05	0.23	0.02	0.06	0.01	0.00	0.00	0.00	0.15	0.04	0.26	0.01	0.05	0.00	0.00	0.00	0.00
0.6	0.18	0.08	0.02	0.01	0.00	0.00	0.23	0.10	0.13	0.05	0.04	0.02	0.01	0.00	0.00	0.21	0.04	0.19	0.02	0.04	0.01	0.00	0.00	0.00	0.20	0.02	0.22	0.00	0.02	0.00	0.00	0.00	0.00
0.5	0.18	0.07	0.02	0.00	0.00	0.00	0.23	0.11	0.10	0.04	0.02	0.02	0.01	0.00	0.00	0.24	0.04	0.15	0.02	0.02	0.01	0.01	0.00	0.00	0.23	0.00	0.18	0.01	0.01	0.01	0.00	0.00	0.00
0.4	0.19	0.05	0.01	0.00	0.00	0.00	0.24	0.12	0.08	0.04	0.02	0.01	0.00	0.00	0.00	0.25	0.06	0.12	0.03	0.01	0.01	0.01	0.00	0.00	0.25	0.04	0.13	0.02	0.00	0.01	0.01	0.00	0.00
0.3	0.19	0.04	0.01	0.00	0.00	0.00	0.23	0.14	0.06	0.03	0.01	0.01	0.00	0.00	0.00	0.25	0.10	0.08	0.03	0.01	0.01	0.00	0.00	0.00	0.25	0.08	0.09	0.03	0.01	0.01	0.01	0.00	0.00
0.2	0.19	0.03	0.00	0.00	0.00	0.00	0.22	0.16	0.04	0.03	0.01	0.01	0.00	0.00	0.00	0.24	0.13	0.05	0.02	0.01	0.01	0.00	0.00	0.00	0.25	0.12	0.06	0.02	0.01	0.01	0.00	0.00	0.00
0.1	0.20	0.01	0.00	0.00	0.00	0.00	0.21	0.18	0.02	0.01	0.00	0.00	0.00	0.00	0.00	0.22	0.17	0.02	0.02	0.00	0.00	0.00	0.00	0.00	0.23	0.16	0.02	0.02	0.00	0.00	0.00	0.00	0.00

B. With Frequencies $2f_I \pm (2n+1)f_o$ and $4f_I \pm 2n+1)fo$

Table A.6. (Continued)

$5f_I \pm 2nf_o$

	$\phi_o = 0°, 180°$						$\phi_o = \pm 30°, \pm 150°$									$\phi_o = \pm 60°, \pm 120°$									$\phi_o = \pm 90°$								
$2n \rightarrow$	[0]	2	4	[6]	8	10	[0]	2		4		[6]	8	10		[0]	2		4		[6]	8	10		[0]	2		4		[6]	8	10	
$r\downarrow$																																	
1.0	0.04	0.07	0.11	0.09	0.05	0.01	0.05	0.05	0.05	0.16	0.06	0.14	0.05	0.04	0.02	0.02	0.02	0.02	0.20	0.02	0.18	0.02	0.01	0.01	0.00	0.00	0.00	0.20	0.00	0.20	0.00	0.00	0.00
0.9	0.09	0.11	0.09	0.05	0.02	0.00	0.08	0.12	0.06	0.15	0.05	0.08	0.03	0.01	0.00	0.05	0.09	0.03	0.21	0.01	0.10	0.01	0.00	0.00	0.02	0.04	0.01	0.23	0.01	0.12	0.00	0.00	0.00
0.8	0.11	0.11	0.07	0.03	0.01	0.00	0.09	0.15	0.07	0.13	0.04	0.05	0.02	0.01	0.00	0.05	0.14	0.02	0.19	0.01	0.06	0.01	0.00	0.00	0.03	0.11	0.01	0.21	0.00	0.06	0.00	0.00	0.00
0.7	0.14	0.11	0.06	0.02	0.01	0.00	0.10	0.16	0.06	0.10	0.03	0.03	0.01	0.00	0.00	0.04	0.17	0.02	0.15	0.01	0.04	0.01	0.00	0.00	0.02	0.16	0.00	0.18	0.00	0.03	0.00	0.00	0.00
0.6	0.15	0.10	0.05	0.02	0.01	0.00	0.12	0.16	0.06	0.08	0.02	0.02	0.01	0.00	0.00	0.05	0.19	0.03	0.12	0.01	0.02	0.01	0.00	0.00	0.00	0.19	0.01	0.14	0.01	0.01	0.01	0.00	0.00
0.5	0.17	0.10	0.04	0.01	0.00	0.00	0.14	0.16	0.06	0.06	0.02	0.01	0.01	0.00	0.00	0.08	0.20	0.03	0.08	0.01	0.01	0.01	0.00	0.00	0.05	0.21	0.02	0.09	0.01	0.00	0.01	0.00	0.00
0.4	0.18	0.09	0.03	0.01	0.00	0.00	0.16	0.15	0.05	0.04	0.01	0.01	0.01	0.00	0.00	0.11	0.19	0.03	0.05	0.01	0.00	0.00	0.00	0.00	0.09	0.20	0.03	0.05	0.01	0.00	0.00	0.00	0.00
0.3	0.19	0.08	0.02	0.01	0.00	0.00	0.18	0.13	0.04	0.03	0.01	0.01	0.01	0.00	0.00	0.15	0.17	0.02	0.02	0.00	0.00	0.00	0.00	0.00	0.13	0.18	0.02	0.02	0.00	0.00	0.00	0.00	0.00
0.2	0.20	0.07	0.02	0.01	0.00	0.00	0.19	0.11	0.04	0.02	0.01	0.01	0.01	0.00	0.00	0.18	0.14	0.02	0.01	0.01	0.00	0.00	0.00	0.00	0.17	0.15	0.00	0.00	0.00	0.00	0.00	0.00	0.00
0.1	0.20	0.07	0.01	0.01	0.00	0.00	0.20	0.09	0.05	0.01	0.01	0.01	0.01	0.00	0.00	0.19	0.10	0.04	0.01	0.01	0.01	0.01	0.00	0.00	0.19	0.11	0.03	0.01	0.01	0.00	0.00	0.00	0.00

C. With Frequencies $5f_I \pm 2nf_o$

Table A.6. (Continued)

$7f_i \pm 2nf_o$

	$\phi_o = 0°, 180°$						$\phi_o = \pm 30°, \pm 150°$									
$2n \rightarrow$	[0]	2	4	[6]	8	10	[0]	2		4		[6]		8		10
$r\downarrow$																
1.0	0.03	0.02	0.05	0.07	0.07	0.03	0.02	0.03	0.03	0.04	0.04	0.11	0.04	0.10	0.04	0.03
0.9	0.05	0.06	0.07	0.06	0.03	0.01	0.05	0.05	0.05	0.09	0.04	0.10	0.03	0.05	0.02	0.01
0.8	0.06	0.07	0.07	0.04	0.02	0.01	0.06	0.07	0.05	0.10	0.03	0.07	0.02	0.03	0.01	0.00
0.7	0.07	0.08	0.06	0.03	0.01	0.00	0.06	0.09	0.04	0.10	0.03	0.05	0.01	0.01	0.01	0.00
0.6	0.09	0.08	0.05	0.02	0.01	0.00	0.07	0.10	0.05	0.09	0.02	0.03	0.01	0.01	0.00	0.00
0.5	0.10	0.08	0.04	0.01	0.00	0.00	0.08	0.11	0.04	0.07	0.02	0.02	0.01	0.00	0.00	0.00
0.4	0.12	0.07	0.03	0.01	0.00	0.00	0.09	0.11	0.04	0.05	0.01	0.01	0.00	0.00	0.00	0.00
0.3	0.13	0.06	0.02	0.01	0.00	0.00	0.11	0.10	0.03	0.03	0.01	0.01	0.00	0.00	0.00	0.00
0.2	0.14	0.06	0.02	0.01	0.00	0.00	0.13	0.09	0.03	0.02	0.01	0.00	0.00	0.00	0.00	0.00
0.1	0.14	0.05	0.01	0.00	0.00	0.00	0.14	0.07	0.03	0.01	0.01	0.00	0.00	0.00	0.00	0.00

$7f_i \pm 2nf_o$

	$\phi_o = \pm 60°, \pm 120°$										$\phi_o = \pm 90°$									
$2n \rightarrow$	[0]	2		4		[6]		8		10	[0]	2		4		[6]		8		10
$r\downarrow$																				
1.0	0.01	0.01	0.01	0.01	0.01	0.14	0.01	0.13	0.01	0.01	0.00	0.00	0.00	0.00	0.00	0.14	0.00	0.14	0.00	0.00
0.9	0.02	0.04	0.02	0.08	0.01	0.14	0.01	0.06	0.01	0.00	0.01	0.02	0.01	0.05	0.00	0.17	0.00	0.06	0.00	0.00
0.8	0.03	0.04	0.02	0.12	0.01	0.11	0.01	0.03	0.00	0.00	0.00	0.02	0.00	0.12	0.00	0.14	0.00	0.03	0.00	0.00
0.7	0.04	0.06	0.02	0.13	0.01	0.08	0.00	0.01	0.00	0.00	0.02	0.01	0.01	0.15	0.01	0.09	0.00	0.01	0.00	0.00
0.6	0.04	0.09	0.02	0.12	0.01	0.05	0.00	0.00	0.00	0.00	0.03	0.07	0.01	0.15	0.00	0.05	0.00	0.00	0.00	0.00
0.5	0.03	0.12	0.02	0.10	0.01	0.02	0.00	0.00	0.00	0.00	0.02	0.11	0.00	0.12	0.00	0.02	0.00	0.00	0.00	0.00
0.4	0.04	0.14	0.02	0.07	0.01	0.01	0.00	0.00	0.00	0.00	0.02	0.14	0.02	0.08	0.01	0.00	0.00	0.00	0.00	0.00
0.3	0.07	0.13	0.02	0.04	0.01	0.00	0.00	0.00	0.00	0.00	0.06	0.14	0.02	0.04	0.01	0.00	0.00	0.00	0.00	0.00
0.2	0.11	0.11	0.01	0.01	0.00	0.00	0.00	0.00	0.00	0.00	0.10	0.12	0.01	0.01	0.00	0.00	0.00	0.00	0.00	0.00
0.1	0.13	0.08	0.02	0.01	0.01	0.00	0.00	0.00	0.00	0.00	0.13	0.09	0.01	0.00	0.00	0.00	0.00	0.00	0.00	0.00

D. With Frequencies $7f_I \pm 2nf_o$

Table A.6. (Continued)

	$11f_I \pm 2nf_o$																										
	$\phi_o = 0°, 180°$									$\phi_o = \pm 30°, \pm 150°$																	
$2n \rightarrow$	[0]	2	4	[6]	8	10	[12]	14	16	[0]	2		4		[6]		8		10		[12]		14	16			
$r\downarrow$																											
1.0	0.01	0.01	0.01	0.01	0.03	0.05	0.04	0.02	0.01	0.01	0.01	0.01	0.01	0.01	0.01	0.01	0.02	0.02	0.07	0.03	0.07	0.02	0.02	0.01			
0.9	0.02	0.03	0.03	0.04	0.04	0.03	0.01	0.00	0.00	0.02	0.02	0.02	0.03	0.02	0.03	0.02	0.06	0.02	0.05	0.01	0.02	0.01	0.00	0.00			
0.8	0.03	0.03	0.04	0.04	0.03	0.02	0.01	0.00	0.00	0.03	0.03	0.03	0.03	0.02	0.05	0.02	0.06	0.01	0.03	0.01	0.01	0.00	0.00	0.00			
0.7	0.04	0.04	0.04	0.03	0.02	0.01	0.00	0.00	0.00	0.03	0.04	0.03	0.04	0.02	0.06	0.01	0.04	0.01	0.02	0.00	0.00	0.00	0.00	0.00			
0.6	0.04	0.04	0.04	0.03	0.01	0.01	0.00	0.00	0.00	0.04	0.04	0.03	0.06	0.02	0.05	0.01	0.03	0.01	0.01	0.00	0.00	0.00	0.00	0.00			
0.5	0.05	0.05	0.04	0.02	0.01	0.00	0.00	0.00	0.00	0.04	0.05	0.03	0.06	0.02	0.04	0.01	0.01	0.00	0.00	0.00	0.00	0.00	0.00	0.00			
0.4	0.06	0.05	0.03	0.01	0.00	0.00	0.00	0.00	0.00	0.04	0.06	0.03	0.05	0.01	0.02	0.01	0.01	0.00	0.00	0.00	0.00	0.00	0.00	0.00			
0.3	0.07	0.05	0.02	0.01	0.00	0.00	0.00	0.00	0.00	0.05	0.07	0.03	0.04	0.01	0.01	0.00	0.00	0.00	0.00	0.00	0.00	0.00	0.00	0.00			
0.2	0.08	0.04	0.01	0.00	0.00	0.00	0.00	0.00	0.00	0.07	0.07	0.02	0.02	0.01	0.00	0.00	0.00	0.00	0.00	0.00	0.00	0.00	0.00	0.00			
0.1	0.09	0.03	0.01	0.00	0.00	0.00	0.00	0.00	0.00	0.08	0.05	0.02	0.01	0.01	0.00	0.00	0.00	0.00	0.00	0.00	0.00	0.00	0.00	0.00			

	$11f_I \pm 2nf_o$																										
	$\phi_o = \pm 60°, \pm 120°$															$\phi_o = \pm 90°$											
$2n \rightarrow$	[0]	2		4		[6]		8		10		[12]		14	16	[0]	2		4		[6]		8		10		[12]		14	16
$r\downarrow$																													
1.0	0.01	0.01	0.01	0.01	0.01	0.01	0.01	0.01	0.01	0.09	0.01	0.09	0.01	0.01	0.01	0.00	0.00	0.00	0.00	0.00	0.00	0.00	0.00	0.00	0.09	0.00	0.09	0.00	0.00	0.00
0.9	0.01	0.02	0.01	0.02	0.01	0.02	0.01	0.07	0.00	0.08	0.00	0.03	0.00	0.00	0.00	0.00	0.00	0.00	0.00	0.00	0.02	0.00	0.06	0.00	0.10	0.00	0.03	0.00	0.00	0.00
0.8	0.01	0.02	0.01	0.03	0.01	0.04	0.01	0.08	0.00	0.05	0.00	0.01	0.00	0.00	0.00	0.00	0.01	0.00	0.02	0.00	0.02	0.00	0.10	0.00	0.05	0.00	0.01	0.00	0.00	0.00
0.7	0.02	0.03	0.01	0.03	0.01	0.07	0.00	0.06	0.00	0.02	0.00	0.00	0.00	0.00	0.00	0.01	0.01	0.01	0.01	0.00	0.08	0.00	0.08	0.00	0.02	0.00	0.00	0.00	0.00	0.00
0.6	0.02	0.03	0.01	0.05	0.01	0.08	0.00	0.04	0.00	0.01	0.00	0.00	0.00	0.00	0.00	0.01	0.02	0.00	0.03	0.00	0.09	0.00	0.04	0.00	0.01	0.00	0.00	0.00	0.00	0.00
0.5	0.02	0.03	0.01	0.08	0.01	0.06	0.00	0.02	0.00	0.00	0.00	0.00	0.00	0.00	0.00	0.01	0.01	0.01	0.08	0.00	0.07	0.00	0.01	0.00	0.00	0.00	0.00	0.00	0.00	0.00
0.4	0.03	0.05	0.01	0.08	0.00	0.03	0.00	0.00	0.00	0.00	0.00	0.00	0.00	0.00	0.00	0.02	0.04	0.01	0.09	0.00	0.03	0.00	0.00	0.00	0.00	0.00	0.00	0.00	0.00	0.00
0.3	0.02	0.08	0.01	0.06	0.01	0.01	0.00	0.00	0.00	0.00	0.00	0.00	0.00	0.00	0.00	0.00	0.08	0.01	0.07	0.00	0.01	0.00	0.00	0.00	0.00	0.00	0.00	0.00	0.00	0.00
0.2	0.05	0.09	0.02	0.03	0.00	0.00	0.00	0.00	0.00	0.00	0.00	0.00	0.00	0.00	0.00	0.03	0.09	0.01	0.03	0.00	0.00	0.00	0.00	0.00	0.00	0.00	0.00	0.00	0.00	0.00
0.1	0.08	0.06	0.01	0.01	0.00	0.00	0.00	0.00	0.00	0.00	0.00	0.00	0.00	0.00	0.00	0.07	0.07	0.00	0.00	0.00	0.00	0.00	0.00	0.00	0.00	0.00	0.00	0.00	0.00	0.00

E. With Frequencies $11f_I \pm 2nf_o$

Table A.6. (Continued)

$13f_I \pm 2nf_o$

	$\phi_o = 0°, 180°$									$\phi_o = \pm 30°, \pm 150°$														
$2n \rightarrow$	0	2	4	6	8	10	12	14	16	0	2	4	6	8	10	12	14	16						
$r\downarrow$																								
1.0	0.01	0.01	0.01	0.01	0.01	0.02	0.04	0.04	0.02	0.01	0.01	0.01	0.01	0.01	0.01	0.01	0.01	0.02	0.02	0.06	0.02	0.06	0.02	0.02
0.9	0.02	0.02	0.02	0.02	0.03	0.03	0.02	0.01	0.00	0.02	0.02	0.02	0.02	0.02	0.02	0.02	0.03	0.02	0.05	0.01	0.04	0.01	0.02	0.00	0.00
0.8	0.02	0.02	0.02	0.03	0.03	0.02	0.01	0.00	0.00	0.02	0.02	0.02	0.03	0.02	0.03	0.02	0.05	0.01	0.04	0.01	0.02	0.00	0.01	0.00	0.00
0.7	0.03	0.03	0.03	0.03	0.02	0.01	0.01	0.00	0.00	0.02	0.03	0.02	0.03	0.02	0.04	0.01	0.04	0.01	0.03	0.00	0.01	0.00	0.00	0.00	0.00
0.6	0.03	0.03	0.03	0.03	0.02	0.01	0.00	0.00	0.00	0.03	0.03	0.02	0.04	0.02	0.05	0.01	0.03	0.01	0.01	0.00	0.00	0.00	0.00	0.00	0.00
0.5	0.03	0.04	0.03	0.02	0.01	0.00	0.00	0.00	0.00	0.03	0.03	0.02	0.05	0.02	0.04	0.01	0.02	0.00	0.01	0.00	0.00	0.00	0.00	0.00	0.00
0.4	0.04	0.04	0.03	0.01	0.01	0.00	0.00	0.00	0.00	0.04	0.05	0.02	0.05	0.01	0.03	0.01	0.01	0.00	0.00	0.00	0.00	0.00	0.00	0.00	0.00
0.3	0.05	0.04	0.02	0.01	0.00	0.00	0.00	0.00	0.00	0.04	0.06	0.02	0.04	0.01	0.01	0.00	0.00	0.00	0.00	0.00	0.00	0.00	0.00	0.00	0.00
0.2	0.07	0.04	0.01	0.00	0.00	0.00	0.00	0.00	0.00	0.06	0.06	0.02	0.02	0.01	0.00	0.00	0.00	0.00	0.00	0.00	0.00	0.00	0.00	0.00	0.00
0.1	0.07	0.03	0.01	0.00	0.00	0.00	0.00	0.00	0.00	0.07	0.05	0.02	0.01	0.00	0.00	0.00	0.00	0.00	0.00	0.00	0.00	0.00	0.00	0.00	0.00

$13f_I \pm 2nf_o$

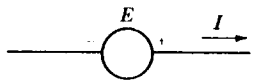
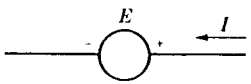
	$\phi_o = \pm 60°, \pm 120°$															$\phi_o = \pm 90°$															
$2n \rightarrow$	0	2	4	6	8	10	12	14	16							0	2	4	6	8	10	12	14	16							
$r\downarrow$																															
1.0	0.00	0.01	0.01	0.01	0.01	0.01	0.01	0.01	0.01	0.01	0.01	0.07	0.01	0.07	0.01	0.01	0.00	0.00	0.00	0.00	0.00	0.00	0.00	0.00	0.00	0.00	0.08	0.00	0.08	0.00	0.00
0.9	0.01	0.01	0.01	0.02	0.01	0.02	0.01	0.02	0.00	0.06	0.00	0.06	0.00	0.02	0.01	0.00	0.00	0.00	0.00	0.00	0.00	0.00	0.00	0.01	0.00	0.07	0.00	0.07	0.00	0.02	0.00	0.00
0.8	0.01	0.02	0.01	0.02	0.01	0.02	0.00	0.05	0.00	0.06	0.00	0.03	0.00	0.00	0.00	0.00	0.00	0.00	0.00	0.01	0.00	0.02	0.00	0.04	0.00	0.08	0.00	0.03	0.00	0.00	0.00	0.00
0.7	0.01	0.02	0.01	0.03	0.01	0.03	0.00	0.06	0.00	0.04	0.00	0.01	0.00	0.00	0.00	0.00	0.01	0.00	0.02	0.00	0.01	0.00	0.08	0.00	0.05	0.00	0.01	0.00	0.00	0.00	0.00
0.6	0.02	0.02	0.01	0.03	0.01	0.06	0.00	0.05	0.00	0.02	0.00	0.00	0.00	0.00	0.00	0.00	0.01	0.00	0.01	0.00	0.06	0.00	0.06	0.00	0.02	0.00	0.00	0.00	0.00	0.00	0.00
0.5	0.01	0.03	0.01	0.05	0.01	0.06	0.00	0.03	0.00	0.00	0.00	0.00	0.00	0.00	0.00	0.00	0.02	0.00	0.04	0.00	0.07	0.00	0.03	0.00	0.01	0.00	0.00	0.00	0.00	0.00	0.00
0.4	0.02	0.03	0.01	0.07	0.00	0.04	0.00	0.01	0.00	0.00	0.00	0.00	0.00	0.00	0.00	0.00	0.00	0.01	0.00	0.07	0.00	0.05	0.00	0.01	0.00	0.00	0.00	0.00	0.00	0.00	0.00
0.3	0.02	0.06	0.01	0.06	0.00	0.02	0.00	0.00	0.00	0.00	0.00	0.00	0.00	0.00	0.00	0.00	0.01	0.05	0.00	0.07	0.00	0.02	0.00	0.00	0.00	0.00	0.00	0.00	0.00	0.00	0.00
0.2	0.03	0.07	0.01	0.03	0.00	0.00	0.00	0.00	0.00	0.00	0.00	0.00	0.00	0.00	0.00	0.00	0.02	0.08	0.01	0.04	0.00	0.00	0.00	0.00	0.00	0.00	0.00	0.00	0.00	0.00	0.00
0.1	0.06	0.06	0.01	0.01	0.00	0.00	0.00	0.00	0.00	0.00	0.00	0.00	0.00	0.00	0.00	0.00	0.06	0.06	0.00	0.01	0.00	0.00	0.00	0.00	0.00	0.00	0.00	0.00	0.00	0.00	0.00

F. With Frequencies $13f_I \pm 2nf_o$

APPENDIX B

INDUCTION GENERATOR

Table B.1. Power relationship between motor and generator.

Circuit diagram	Calculated from EI^*
 Generator action assumed	If P is +, emf supplies power If P is −, emf absorbs power If Q is +, emf supplies reactive power (I lags E) If Q is −, emf absorbs reactive power (I leads E)
 Motor action assumed	If P is +, emf absorbs power If P is −, emf supplies power If Q is +, emf absorbs reactive power (I lags E) If Q is −, emf supplies reactive power (I leads E)

B.2. Expressions for different powers referring to Figure 4-2, the following relationship:

$$\text{Output Power } P_1 = qV_1I_1\cos\phi_1$$
$$= R_2|I_2|^2 + V_1I_1$$

where q=1 for single-phase output; and
q=3 for three-phase output.

$$\text{Rotor Input } P_2 = \left[\frac{R_2(1-S)}{S}\right] I_2^2 + \text{Rotational Losses}$$

$$\text{Efficiency } \eta = \frac{P_{out}}{P_{in}} = \frac{P_1}{P_2}$$

$$\text{Slip } S = N_s - N_1 \quad \text{where } \omega_s = 2\pi f_s = 2\pi N_s/60; \text{ therefore}$$
$$S = \omega_s - \omega \quad \text{where } \omega \text{ is the line frequency.}$$

VITA

Arthur Shek-Kin Kwong was born in Hong Kong, on May 24, 1953. Upon completion of his Primary and Secondary School in Hong Kong and in Canada, he attended three years in The St. Clair College in Canada and received a Diploma of Electrical Technology in 1976. The following September he entered The University of Tennessee, Knoxville and in 1978 he received a Bachelor of Science degree in Electrical Engineering. In the fall of 1978, he entered the Graduate School of The University of Tennessee, Knoxville and received the Master of Science degree in Electrical Engineering in Spring 1981.